FILLING THE GAP IN THE PALEOEARTHQUAKE RECORD BETWEEN THE NEW MADRID AND WABASH VALLEY SEISMIC ZONES

Final Technical Report

Research supported by the U.S. Geological Survey (USGS),
Department of the Interior, under USGS award G12AP20068

Principal Investigator:
Martitia P. Tuttle
M. Tuttle & Associates
P.O. Box 345
Georgetown, ME 04548
Tel: 207-371-2007
E-mail: mptuttle@earthlink.net
URL: http://www.mptuttle.com

Project Period: 1/9/2012-10/31/2016

Program Element III: Research on Earthquake Occurrence, Physics, Effects, Impacts, and Risk
Program Element I: National and Regional Earthquake Hazards Assessments

Key Words: Paleoseismology, Paleoliquefaction, Age Dating

FILLING THE GAP IN THE PALEOEARTHQUAKE RECORD BETWEEN THE NEW MADRID AND WABASH VALLEY SEISMIC ZONES

Martitia Tuttle (PI) and Kathleen Dyer-Williams
M. Tuttle & Associates
P.O. Box 345
Georgetown, ME 04548
Tel: 207-371-2007
E-mail: mptuttle@earthlink.net

ABSTRACT

Earthquake-induced liquefaction features, limited to small and moderate-size sand dikes, were found and studied along three rivers in the region between the New Madrid and Wabash Valley seismic zones. These features were found during systematic surveys along 111 km of selected portions of several rivers. Radiocarbon and optically stimulated luminescence dating were performed on samples collected from deposits intruded by the dikes and from deposits overlying erosional contacts that truncated some of the dikes. In addition, liquefaction potential analysis using geotechnical data from boreholes close to liquefaction sites was performed for scenario events to help evaluate the locations and magnitude of earthquakes responsible for the formation of the dikes.

Along the Cumberland River in northwestern Kentucky, sand dikes were very weathered, exhibiting fines accumulation, prominent iron staining, and iron cementation along dike margins, and likely formed after 7250 yr B.P. These dikes may very well have formed during the **M** 7.3 Vincennes earthquake centered in the Wabash Valley seismic zones between 5900-6300 yr B.P. There was also a second generation of dikes along the Cumberland that was less weathered, crosscut the older dikes, and likely post-dated the Vincennes earthquake. Along the Middle Fork of the Saline River in southeastern Illinois, sand dikes were slightly weathered and formed between 330-1225 yr B.P. These dikes, and possibly other dikes along the main branch of the Saline River, may have formed during the 900-1200 yr B.P. or 350-650 yr B.P. New Madrid paleoearthquakes. Dikes found and studied along Skillet Fork also in southeastern Illinois, were quite weathered, exhibiting iron staining and fines accumulation in the upper part of the dikes, and formed after 2715 yr B.P. There was also a second generation of unweathered dikes, but there was little else besides degree of weathering to help estimate their age. The dikes along Skillet Fork may have formed during the 900-1200 yr B.P. or 350-650 yr B.P. New Madrid paleoearthquakes, or a possible earlier New Madrid event about 2180-3380 yr B.P. The ages and sizes of liquefaction features in northwestern Kentucky, and southeastern Illinois, do not support a proposed alternate magnitude of **M** 6.8 and location southeast of Paducah for the January 23, 1812 New Madrid earthquake.

Although progress has been made in finding additional liquefaction features and constraining the ages of liquefaction features, significant uncertainties remain regarding the sources of earthquakes that induced liquefaction during the Middle and Late Holocene along the Cumberland River, Middle Fork and main branch of the Saline River, and Skillet Fork as well as other rivers in the New Madrid-Wabash Valley region. To reduce those uncertainties, additional

reconnaissance and dating of liquefaction features in the region are needed to further narrow the age estimate of the features and to better correlate them across the region.

INTRODUCTION

Several decades ago, it was proposed that the central US is underlain by a failed late Precambrian-early Paleozoic rift complex or aulocogen (Figure 1; e.g., Ervin and McGinnis, 1975; Braile et al., 1982; Mooney and Andrews, 1984). The rift complex was thought to be composed of the Reelfoot rift extending from the former continental margin of the buried Ouchita Front northeastward to southern Illinois where it split into three arms, the St. Louis arm, the Indiana arm, and the Rough Creek graben. The rift is thought to have influenced geodynamic processes and to have localized the emplacement of plutons and fault activity during the Mesozoic and Cenozoic Eras. Earthquakes in the New Madrid seismic zone were attributed to reactivation of faults of the Reelfoot rift in the contemporary regional stress field (e.g., Braile et al., 1986; Zoback and Zoback, 1989).

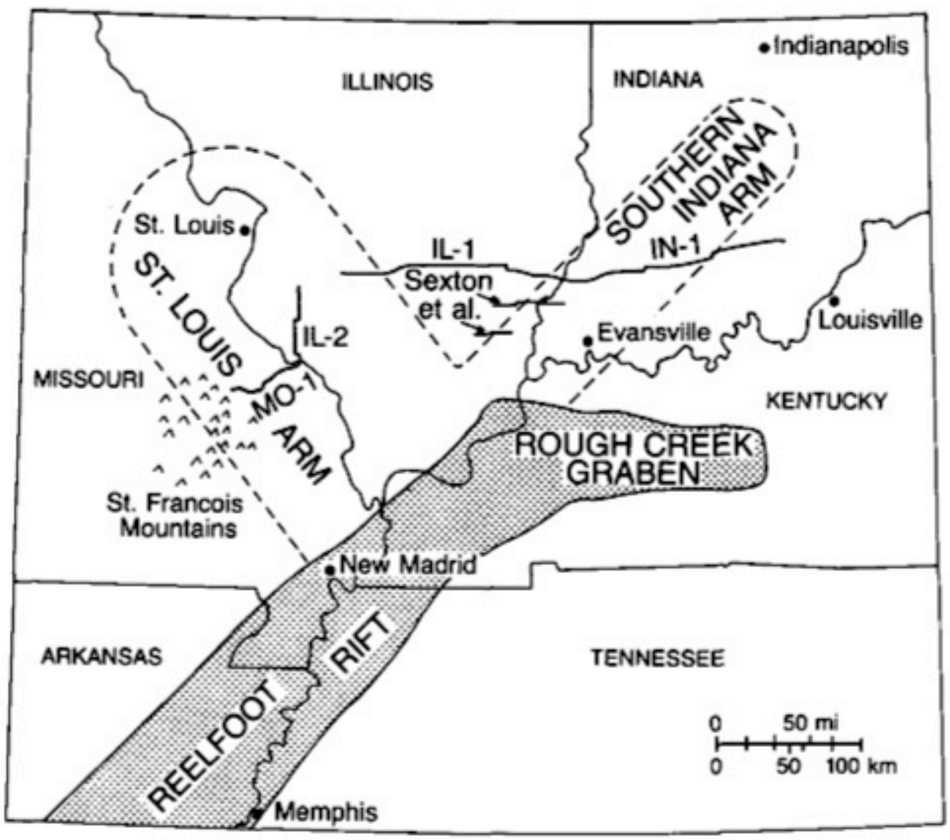

Figure 1. Rift complex underlying the central US composed of Reelfoot rift and Rough Creek graben (from Nelson, 1990; modified from Braile et al., 1982).

The seismotectonic model of the region has evolved and the aulocogen limited to the northeast-trending Reelfoot rift and the east-trending Rough Creek graben (Figure 1; e.g., Nelson, 1990; Nelson et al., 1999; Crone and Wheeler, 2000). The Fluorspar area fault complex (FAC) of western Kentucky and southern Illinois occurs at the intersection of these two major structures (Figure 2). The Wabash Valley fault system located to the northeast of the FAC was recognized through drilling and geophysical imaging. The relationship of the Wabash Valley fault system to the Reelfoot rift and Rough Creek graben is uncertain and earthquakes have been directly linked to only a few faults in the system (e.g., Hildenbrand and Ravat, 1997; McBride et al., 1997; Kim, 2003; and Woolery, 2005). Deformation associated with the Hovey Lake fault, along the Ohio River near its confluence with the Wabash River, extends above the Paleozoic bedrock and into upper Quaternary sediment, suggesting faulting about 37 ka (Woolery, 2005). In a recent study in western Kentucky, a fault (named the Uniontown fault) associated with a prominent scarp on the Ohio River floodplain was identified as a member of the Hovey Lake fault system (Counts et al., 2009; Van Arsdale et al., 2009). The Uniontown fault is thought to have been active between 5.5 and 0.9 ka and to have caused the diversion of the Ohio River from its ancestral course now occupied by the Cache River in southern Illinois to its present course (Counts, 2013).

The Commerce geophysical lineament (CGL), a 400-km-long, 5- to 10-km wide northeast-trending gravity and aeromagnetic anomaly extending from northeastern Arkansas to central Indiana, has been proposed as a major tectonic structure that links the New Madrid seismic zone (NMSZ) and the Wabash Valley seismic zone (WVSZ) and is capable of generating large earthquakes (Figure 2; McBride et al., 1997 and 2002; Baldwin et al., 2002; Harrison and Schultz, 2002; Hildenbrand et al., 2002). Modeling of elastic stress change and re-evaluation of intensity data have been used to argue that a large earthquake in the NMSZ could affect earthquake occurrence in the WVSZ and vice versa and that the January 23, 1812 New Madrid earthquake may have been located near the confluence of the Tennessee and Ohio Rivers (Figure 3; Mueller et al., 2004). Similarly, numerical modeling of stress transfer suggests that faults may have been loaded to the northeast following the 1811-1812 New Madrid earthquakes (Li et al., 2007 and 2009; Merino et al., 2010). In a recent seismotectonic model of the mid-continent, seismicity is viewed as resulting from fault interaction in a complex system. A large earthquake not only would release stress on the fault that ruptured but also change stress on other segments of the fault or other nearby faults, causing seismicity to migrate (Stein et al., 2009). Migration of seismicity across a wider region would help to resolve an apparent inconsistency between a relatively short recurrence time for New Madrid events and low strain rates estimated from geodetic measurements. A possible implication of the model is that current assessments based on quasi-periodic fault behavior may overestimate earthquake hazard in regions of recent large earthquakes and underestimate hazard in regions where seismicity has been recently quiescent (Li et al., 2009; Stein et al., 2009). This project focuses on the region between the NMSZ and the WVSZ and aims to gather additional paleoliquefaction data that will help to better define the liquefaction fields and timing of New Madrid and Wabash Valley paleoearthquakes and to evaluate whether the timing of those paleoearthquakes supports a link between the two seismic zones.

Previous Paleoliquefaction Studies in the Central US

Paleoliquefaction studies provide information about the timing, location, magnitude, and recurrence times of large paleoearthquakes and have helped to develop paleoearthquake chronologies for the New Madrid and Wabash Valley seismic zones and other earthquake sources in the central US. For the NMSZ, 1811-1812-type earthquake sequences including at least one earthquake of $M \geq 7.6$, or New Madrid event, were recognized between 500 ± 150 yr

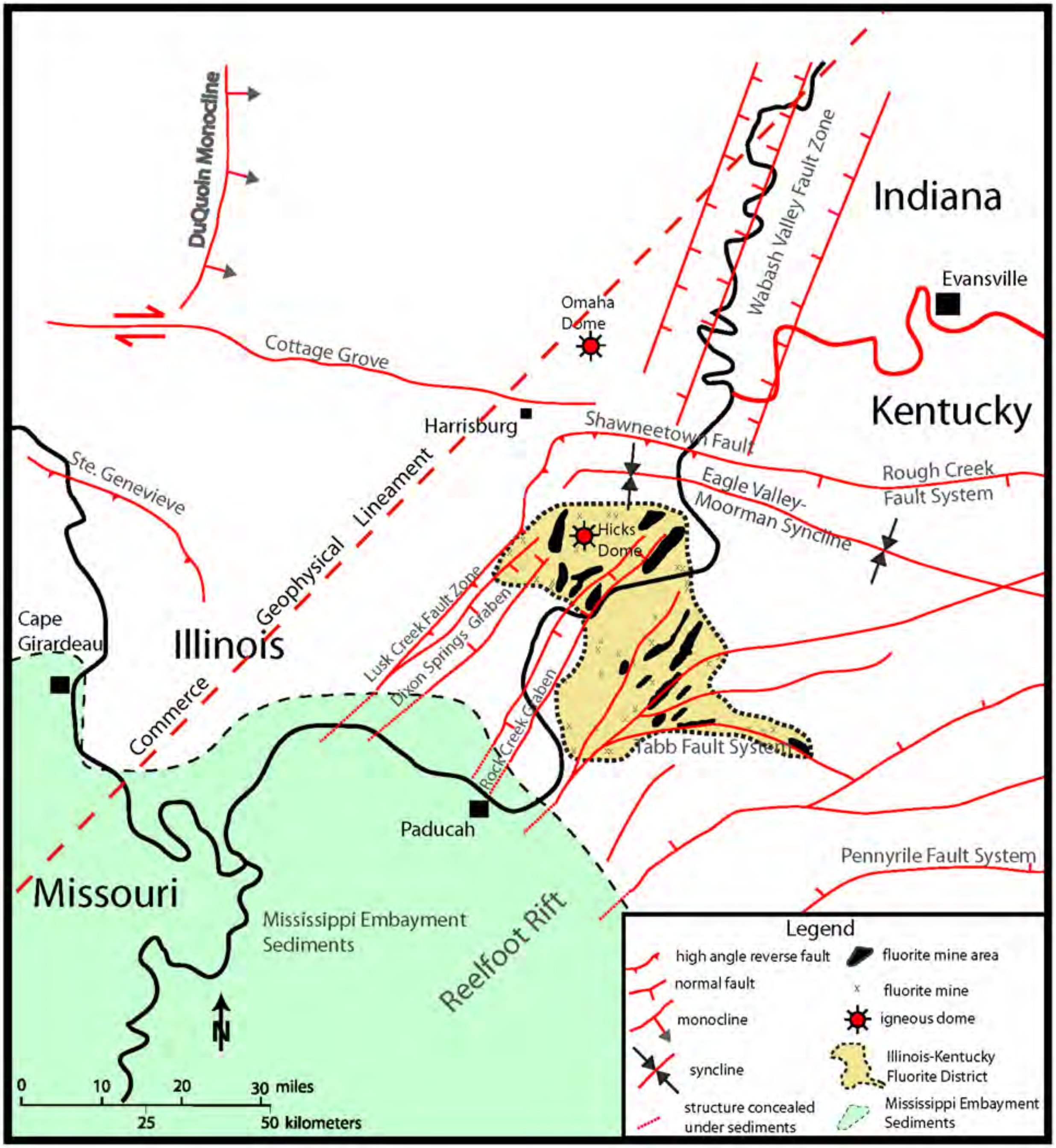

Figure 2. Major tectonic structures in northwestern Kentucky and southern Illinois, including the Commerce Geophysical lineament (Hildenbrand and Ravat, 1997) and faults of the Rough Creek graben and the Reelfoot rift and Wabash Valley fault systems (modified from Denny et al., 2008).

B.P. (A.D. 1450 ± 150 yr), 1050 ± 150 yr B.P. (A.D. 900 ± 150 yr), and possibly between 4300 ± 150 yr B.P. (2350 ± 150 yr B.C.) primarily through the study of sand blows (Figure 3; e.g., Tuttle et al., 2002, and 2005). From these paleoseismic data, a mean recurrence time of 500 years was estimated for New Madrid events during the past 1200 years. For the WVSZ, two paleoearthquakes, a M 7-7.8 event in 6,100 ± 200 yr B.P. (e.g., Hajic et al., 1995; Munson and Munson, 1996; Munson et al., 1997; Pond and Martin, 1997; Olson et al., 2001 and 2005) and a

M 6.3-7.3 event in 12,000 ± 1,000 yr BP (Munson and Munson, 1996; Munson et al., 1997; Pond and Martin, 1997; Olson et al., 2005) were recognized largely through the study of sand dikes (Figure 3). Both Wabash Valley paleoearthquakes were inferred to be located within 40 km of Vincennes, Indiana (e.g., McNulty and Obermeier, 1999).

Liquefaction features have been found in the study region between the NMSZ and the WVSZ during previous studies (Figure 4). Most of the features are sand dikes whose ages are poorly constrained. They include the following (Figure 3): (1) weathered (probably predate 1811-1812 New Madrid earthquakes) sand dikes along Mayfield Creek in western Kentucky, that formed <5880 yr B.P. (Tuttle, 2010); (2) weathered sand dikes along the nearby Tennessee River that formed <4850 yr B.P. and a weathered sand blow and sand dikes along the Clarks River that formed 11,300 yr B.P. ± 200 yr (Tuttle, 2005); (3) sand dikes, sills, and soft-sediment deformation structures along the Cache River in southernmost Illinois, some of which are unweathered and formed since 930 yr B.P. and others that are weathered and formed <4840 yr B.P. (Tuttle et al., 1999; Tuttle and Chester, 2005); (4) sand dikes along the Saline River near Harrisburg, Illinois, thought to have formed during the 1811-1812 New Madrid earthquakes and along Skillet Fork near Waynesville, Illinois, thought to be Late Holocene in age (Hajic et al., 1995); (5) two small dikes along the Ohio River between Paducah and the Wabash River assumed to be historic in age (Obermeier, 1998; not in CEUS paleoliquefaction database and thus not shown on Figure 4).

Paleoliquefaction studies also have identified paleoearthquakes outside the New Madrid and Wabash Valley seismic zones. For example, scattered concentrations of sand dikes in Indiana and Illinois were attributed to large local Middle Holocene earthquakes (e.g., Hajic et al., 1995; Munson and Munson, 1996; McNulty and Obermeier, 1999). More recently, very large weathered sand blows that are Middle to Late Holocene, and possibly Late Pleistocene, in age (4.8, 5.5, 6.8, 9.8 ka and possibly about 19 and 35 ka) discovered near Marianna, Arkansas, are thought to have formed during very large (**M** ≥ 7.2) earthquakes centered at the southern end of the Reelfoot rift (Al-Shukri et al., 2006, 2009, and 2015; Tuttle et al., 2006; Odum et al., 2016).

Paleoliquefaction data plays an important role in assessing earthquake hazard in regions such as the central and eastern U.S. (CEUS) where active faults rarely extend to the ground surface and/or are difficult to recognize. During the CEUS Seismic Source Characterization project, paleoliquefaction data was used in the development of the source models for the New Madrid and Wabash Valley seismic zones (Technical Report, 2012). Similarly, paleoliquefaction data has been incorporated into the National Probabilistic Seismic Hazard Maps (Petersen et al., 2014). Paleoliquefaction data gathered during this project are likely to contribute to future revisions of source models, hazard assessments, and hazard maps of the New Madrid and Wabash Valley seismic zones.

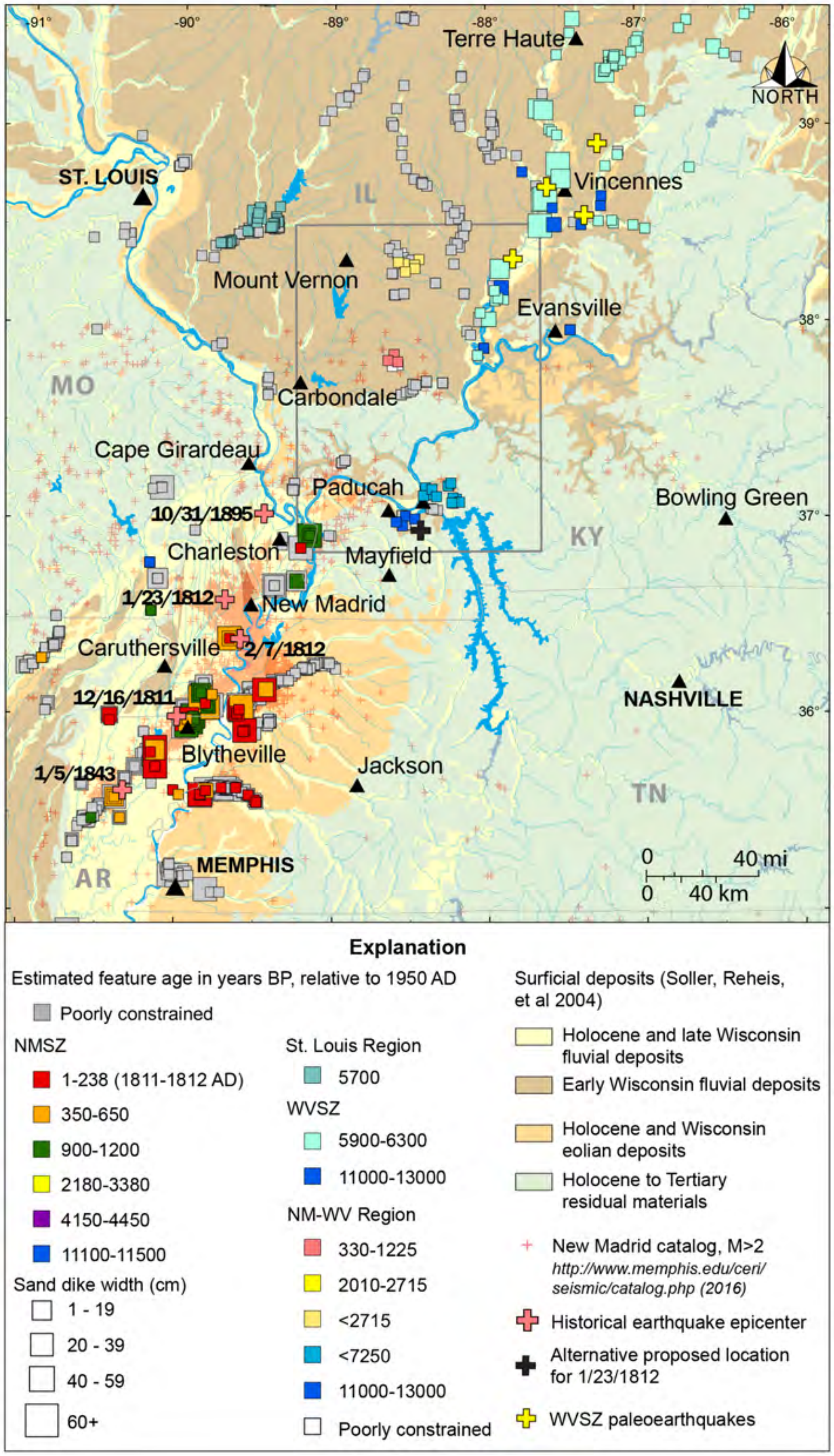

Figure 3. Map showing NMSZ and WVSZ and study region in between, sizes and estimated ages of sand blows and sand dikes from dikes from CEUS paleoliquefaction database and this study, instrumental and historical seismicity. Black cross southeast of Paducah indicates proposed alternate location for January 23, 1812 earthquake (Mueller et al., 2004). Enlargement of outlined subarea shown in Figure 4.

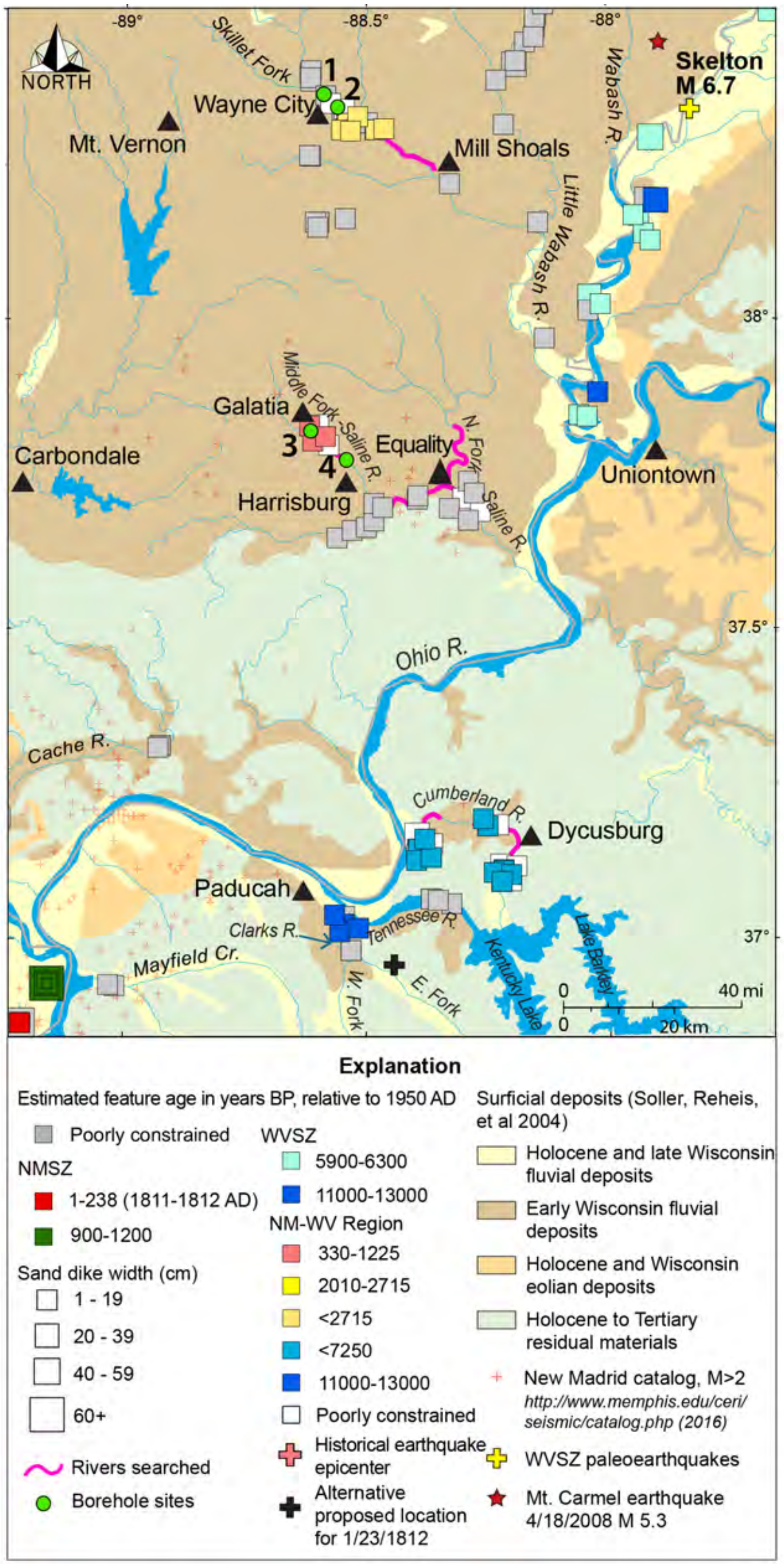

Figure 4. Map showing study region between NMSZ and WVSZ, rivers searched for liquefaction features, sizes and estimated ages of sand blows and sand dikes from CEUS paleoliquefaction database (Tuttle and Hartleb, 2012) and this study, and locations of borehole data used in evaluation of scenario earthquakes.

SEARCH FOR AND DOCUMENTATION OF EARTHQUAKE-INDUCED LIQUEFACTION FEATURES

During the CEUS Seismic Source Characterization Project, a paleoliquefaction database was developed for use in the seismic source models of areas of repeated large magnitude earthquakes (RLMEs), including the NMSZ and WVSZ. During the compilation of liquefaction data compiled for the WVSZ, it became evident that there are many sand dikes in southeastern Illinois whose ages were poorly constrained. Most of the sand dikes in the region were assigned to the Vincennes earthquake (6100 yr B.P.) (Figure 5). However, those on the Saline River were attributed to the 1811-1812 New Madrid earthquakes and several on the Skillet Fork were thought to be Late Holocene in age (Hajic et al., 1995). A recommendation in the technical report that accompanied the paleoliquefaction database was that additional sampling and age analyses be carried out in the WVSZ "to further refine and reduce uncertainties of age estimates and correlation of paleoliquefaction features" (Tuttle and Hartleb, 2012).

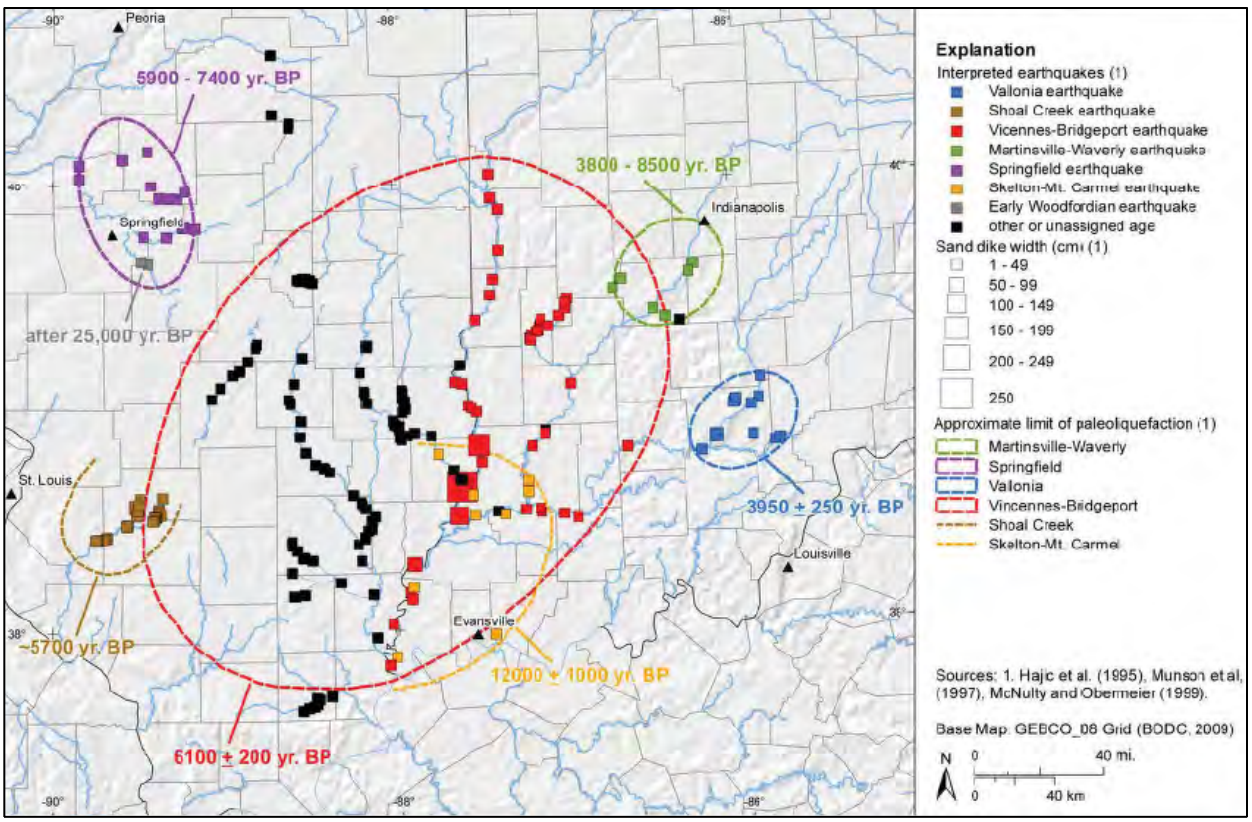

Figure 5. Map of Wabash Valley region of Illinois and Indiana showing age estimates of liquefaction features and paleoearthquake interpretations (from Technical Report, 2012; modified from McNulty and Obermeier, 1999). Ages of sand dikes represented by black squares were mostly poorly constrained, unknown, or unassigned.

There has been some uncertainty about the location of the January 23, 1812 New Madrid earthquake and a suggestion that the event was located southeast of Paducah, Kentucky, near the confluence of the Ohio and Tennessee Rivers (Bakun and Hopper, 2004; Mueller et al., 2004; Hough et al., 2005). Liquefaction features have been found in this area, including a sand blow and related dikes that formed 10834-11304 yr B.P. along Clarks River and sand dikes that formed <4850 yr B.P. along the Tennessee River downriver from Kentucky Lake (Tuttle, 2005).

For this study, the Saline River and two of its tributaries, the Middle and North Forks, as well as the Skillet Fork were selected for survey in southern Illinois (Figure 4). In addition, the Cumberland River very close to the Tennessee River and also downriver from Kentucky Lake was selected for survey in western Kentucky. The search for liquefaction features along these rivers was hampered by heavy rainstorms and prolonged flooding. Not only did the flooding make river surveys pointless due to lack of cutbank exposure but it also resulted in deposition of large quantities of mud on riverbanks for many kilometers. This affected final selection of the river segments searched. More than once, fieldwork had to be canceled or postponed and reconnaissance performed yet again to identify river segments with cutbanks that had not been covered with mud and were well enough exposed to warrant survey. River surveys totaling 111 km were completed in the summer of 2016. Observations made along the rivers and at twenty-five study sites along the five rivers are summarized below and presented in Table 1.

Cumberland River

The Cumberland River was surveyed for earthquake-induced liquefaction features along 20 km downstream from the Kentucky Lake dam from Iuka to west of Pickneyville and for 12 km upstream from its confluence with the Ohio River (Figure 4). The Cumberland River valley is cut into bedrock and is generally 2 km wide except in a few places where it narrows to 1 km. Along the upper portion of the river, bedrock outcropped above the water level near Dycusburg. Here, the river changes direction from northeast to west and is flanked by bedrock on the outside bend of the river. Similarly, along the lower portion of the river, bedrock was exposed in the river's outside bend where it changes direction from west-northwest to south-southeast and again near its mouth as it veers towards the west to join the Ohio River.

There was fairly good exposure of fluvial deposits along the river with numerous cutbanks ranging up to 6 m high. There were two fluvial terrace levels: a 6-m terrace underlain by reddish silt followed by gray layered silt and/or interbedded gray silt, and iron-stained sand, and a 2-m terrace underlain by brown layered silt. The layered silt of the 2-m terrace is likely to be recent fluvial deposits; whereas, the more weathered silt and sand of the 6-m terrace are likely to be Holocene fluvial deposits.

Sand and sandy silt dikes interpreted as earthquake-induced liquefaction features were found at seven sites (CdR2, 3, 6-10; Table 1) along the river. All liquefaction sites are located in the floodplains and away from the valley margins and in Holocene deposits of the 6-m terrace. At all site but one, sand dikes intrude from below and terminate within gray layered silt and/or interbedded gray silt. The exception is site CdR2, where a sand dike extends 5 cm into the base of the overlying reddish silt where it terminates. All of the dikes are either iron stained or cemented suggesting that they are prehistoric in age. There appears to be two generations of dikes based on crosscutting relations and degree of weathering. At CdR8, younger dikes intruded along the margins of older dikes. Most of the dikes are small ranging up to 2.5 cm wide. At three sites near the confluence of the Cumberland with the Ohio, however, sand dikes are noticeably much larger, with the largest dike being 25 cm wide (Figure 6).


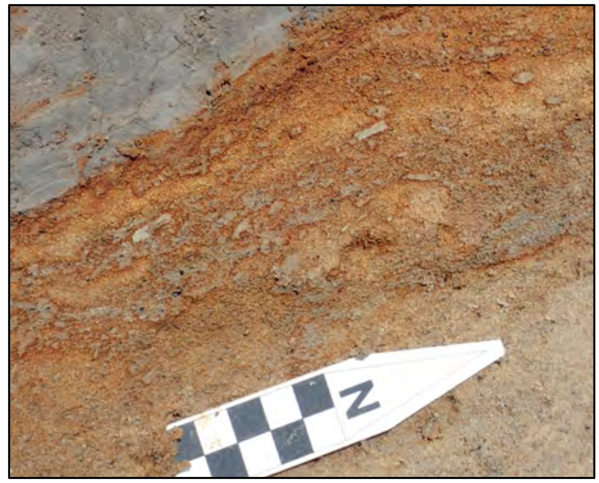

Figure 6. Along the Cumberland River, sand dikes crosscut interbedded gray silt and sand. (Left) Photograph of large iron-cemented sand dike exposed in cutbank near the confluence with the Ohio River; for scale, shovel handle across dike is 50 cm long. (Right) Closeup of margin of sand dike showing iron staining of sand and entrained clasts from intruded host; black and white intervals on scale represent 1 cm.

The dikes at these three sites are subparallel to the river and therefore may be larger due to laterally spreading. The grain-size of the several of the larger sand dikes is slightly coarser, ranging up to medium sand, than the smaller dikes farther upstream. Perhaps subsurface sediment near the mouth of the Cumberland is related to the mighty Ohio and influenced ground failure and the formation of liquefaction features. Borehole data were sought from the Kentucky Department of Transportation for a nearby bridge to assess the characteristics of the subsurface sediment in this area. Unfortunately, no borehole information was available for the bridge.

Three organic samples collected from interbedded gray silt and sand at sites CdR4, CdR8, and CdR9 provide maximum constraining ages for the sand dikes (Table 2). The 2-sigma calibrated dates for samples CdR8-W3 and CdR9-C1 were very similar to one another. Taking the younger of the two, CdR8-W3 provides a maximum constraining age of 7250 yr. B.P. Due to the stratigraphic and weathering similarities of the documented dikes along the river, they likely formed since 7250 yr B.P. Similarly, three OSL samples collected from interbedded gray silt and sand at sites CdR8 and CdR10 provide maximum constraining ages for the dikes ranging from 6585 to 6840 yr B.P. (Table 3) Although the OSL ages are similar in this context, the radiocarbon ages are given preference because they are more reliably accurate. The dikes may be younger than 7250 yr. B.P. but there is no stratigraphic relation to constrain their minimum age. Sample CdR5-C1, collected from the reddish silt and ~1.4 m above the contact with interbedded silt and sand, yielded a calibrated age of 2700-2635, 2615-2590, and 2540-2355 yr B.P. and provides an age estimate for the reddish silt. The result does not provide a minimum age constraint for the dikes because it is not known how far below the ground surface the dikes terminated at the time of the event. The result does not provide a maximum constraining age for the dikes since they pinched out below or near the base of the reddish silt. No dike was observed extending more than 5 cm into the reddish silt.

Table 1. Study Sites in the NM-WV Region.

Site	Longitude °W	Latitude °N	Cutbank Exposure	Exposed Sediment	Liquefaction Feature	Weathering of Feature
Cumberland River						
CdR1	88.18760	37.15177	6 m high; excellent	Reddish silt overlying gray layered silt followed by interbedded silt & sand, some organic-rich	No dikes observed, even though conditions conducive	Not applicable
CdR2	88.21784	37.11241	6 m high; upper 3 m poor due to vegetation, middle 2 m slumpy, lower 1 m excellent	Reddish silt (5 m) overlying brownish gray silt; probe: silt with few sand layers to 1.5 m below water level (BWL)	Several small sand dikes up to 1cm wide across a 5m wide zone intrude brownish gray silt; 1 dike extends 5 cm into reddish silt above	Iron stained within dikes, iron cemented along margins
CdR3	88.21794	37.11185	6 m high; excellent lower	Reddish silt (5 m) overlying gray silt; probe: silt followed by interbedded silt & sand to 1.5 m BWL	Several small sand dikes up to 2.5 cm wide across a 4 m wide zone intrude gray silt; pinch within 0.5 m above water level (AWL)	Iron stained within dikes, iron cemented along margins
CdR4	88.21453	37.10423	4.5 m high; upper 1.5 m poor, lower 3 m good to excellent	Reddish silt (3 m) overlying lower 1.5 m layered silt & interbedded sand; bedrock at water level	None observed	Not applicable
CdR5	88.22072	37.09428	6 m high; excellent	Reddish silt overlying interbedded silt and sand; probe: same as above to 1.5 m BWL	None observed	Not applicable
CdR6	88.22205	37.09391	5-6 m high; upper poor-fair, lower 1 m excellent	Reddish silt overlying gray silt; probe: silt to 1.5 m BWL	Several sand dikes up to 1 cm wide intrude gray silt; dikes pinch within 0.75 m AWL	Dikes iron stained & silty, iron cemented margins

Table 1 Cont'd. Study Sites in the NM-WV Region.

Site	Longitude °W	Latitude °N	Cutbank Exposure	Exposed Sediment	Liquefaction Feature	Weathering of Feature
Cumberland River						
CdR7	88.25054	37.18410	5 m high; upper 2.5 m poor, middle 1.5 m fair, lower 1 m excellent	Reddish silt overlying gray silt with manganese staining; probe: silt to 1.45 m followed by sand to 1.5 m BWL	Several small sandy silt dikes up to 2.5 cm wide and sills up to 1.5 cm wide intrude gray silt; dikes pinch within 1 m AWL	Iron stained within dikes, iron cemented along margins
CdR8	88.39271	37.14651	6 m high; lower 2.5m excellent	Reddish silt, mottled overlying layered gray silt and iron-stained sand followed by gray clayey silt; probe: silt with interbeds of sand	Three silty sand dikes up to 14 cm wide with clay clasts intrude clayey silt and layered gray silt & iron-stained sand; 2 dikes composed of 2 phases with cross-cutting relations; sub-parallel to river	Both phases of compound dikes are iron-stained; older phase is iron cemented; younger phase looser
CdR9	88.39125	37.14631	6 m high; lower 2 m and upper 1.5 m excellent, middle 2.5 partially covered	Reddish silt, overlying layered gray silt and iron-stained sand followed by dark gray clayey silt; probe: silt with interbeds of sand	Two medium to fine sand dikes 5 and 8 cm wide with clay clasts intrude clayey silt and layered silt & sand; subparallel to river	One dike iron cemented; second dike less weathered
CdR10	88.39005	37.14668	3 m high; upper 1.5 m poor, lower 1.5m excellent	Reddish silt overlying layered gray silt and iron stained sand; probe: same as above	Sand dike up to 25 cm wide with clay clasts intrudes layered silt & sand; clasts, erosion and delamination of intruded host	Dike iron-stained, throughout, iron cement-ed near tip and along margins

Table 1 Cont'd. Study Sites in the NM-WV Region.

Site	Longitude °W	Latitude °N	Cutbank Exposure	Exposed Sediment	Liquefaction Feature	Weathering of Feature
Saline River						
SalR1	88.31822	37.72379	4 m high x 60 m long; upper 2.5 m covered with mud, lower 1.5 m good	Reddish brown silt, mottled, overlying iron stained sand, pebbles & molluscs shells followed by clayey silt	None observed	Not applicable
SalR2	88.29055	37.70626	4.5 m high x 60 m long; upper 1.5 m fair, lower 3 m excellent	Reddish brown silt, CaCO3 concretions, overlying iron stained sand, pebbles & molluscs shells followed by clayey silt	Four sand dikes; 2.5, 1.3, 1, 0.5 cm wide; pinch out in silt & base of soil	Upper part of larger dikes iron stained throughout; smaller dikes slightly iron stained
SalR3	88.44772	37.70352	2 m high; upper 0.5m vegetated, lower 1.5m excellent	Reddish brown silt, layered; probe: silt to 1.5 m BWL	None observed	Not applicable
Middle Fork of Saline River						
SalR-MF1	88.60960	37.81717	5 m high x 50 m long; good to excellent	Brownish silt, layered, with sand lamina-tions, overlying reddish silt and sand, mottled red and gray, bioturbated	None observed	Not applicable
SalR-MF2	88.60833	37.81686	1.5 m high x 10 m long; excellent	Brownish silt, layered, overlying silt, upper part iron and manganese staining, mottled red & gray, krotovina; probe: silt to 1m followed by sand to 1.5 m	Two sand dikes; 1.5, 0.5 cm wide; both dikes truncated at contact with overlying brown silt	Upper part of both dikes silty and slightly iron stained

Table 1 Cont'd. Study Sites in the NM-WV Region.

Site	Longitude °W	Latitude °N	Cutbank Exposure	Exposed Sediment	Liquefaction Feature	Weathering of Feature
Middle Fork of Saline River						
SalR-MF3	88.60576	37.81512	5 m high x 15 m long; upper poor lower excellent	Reddish silt and sand, mottled red & gray, bioturbated; krotovina	Two silt-filled cracks that pinch downward; dessication cracks	Not applicable
SalR-MF4	88.59512	37.80907	4.5 m high; upper 2.5 m covered, lower 2 m excellent	Reddish silt and some sand, mottled red and gray, bioturba-ted; probe: silt and sand to 1.4 m followed by sand to 1.5 m	One sand dike, 3.5 cm wide	Upper 80 cm of dike silty and iron stained
Skillet Fork						
StF1	88.57593	38.35735	5 m high x 35 m long; good to excellent	Tan silt, gray & tan silt over-lying red & gray silt with krotovina; probe: silt to 0.7 m followed by sand to 1.5 m	One sand dike, 1 cm wide	Relatively unweathered
StF2	88.5599	38.33632	6 m high; excellent	Tan silt, red and gray silt with krotovina followed by interbedded silt and iron-stained sand, organic-rich silt at WL	None observed	Not applicable
StF3	88.55237	38.33638	6 m high; lower 3m excellent	Gray & tan silt overlying red & gray silt with krotovina	One sand dike, 3 cm wide	Iron stained
StF4	88.55000	38.32885	5 m high; good to excellent	Tan silt, over-lying gray & tan silt with layers of sand follow-ed by red & gray silt with krotovina and organic layer	None observed	Not applicable

Table 1 Cont'd. Study Sites in the NM-WV Region.

Site	Longitude °W	Latitude °N	Cutbank Exposure	Exposed Sediment	Liquefaction Feature	Weathering of Feature
Skillet Fork						
StF5	88.53959	38.31755	5 m high; excellent	Tan silt, overlying reddish brown silt followed by red and gray silt, with krotovina, and iron-stained sand	Three sand dikes, 3.5, 1, 1 cm wide; pinch out in red & gray silt with krotovina; source of dikes at base of cutbank	Dike iron stained throughout; upper part silty
StF6	88.53423	38.31551	3-5m high; lower 1.5m excellent	Interbedded gray silt & peat, underlain by red & gray silt, krotovina, and iron-stained sand; probe: sand to 1.5 m BWL	Two sand dikes, 2 and 0.5 cm wide; smaller dike pinches out in silt, larger dike truncated and overlain by interbedded silt and peat; source of dikes visible	Dikes iron stained throughout
StF7	88.51125	38.31334	Lower 1.5m excellent	Tan silt, overlying layered silt and sand, followed by weathered silt with krotovina	None observed	Not applicable
StF8	88.48040	38.30711	5 m high; upper vegetated, lower 2 m good	Brownish gray silt overlying red & gray silt with krotovina; probe: silt-sandy silt to 110 cm followed by sand to 150 cm	Two sand dikes; 3 and 0.5 cm wide	Larger dike relatively unweathered; smaller dike iron stained

Liquefaction features in the WVSZ formed between 5900-6300 yr B.P. and have been attributed the Vincennes paleoearthquake. It is quite possible, but certainly not required, that the first generation of dikes along the Cumberland River, including the large iron-cemented dikes near the mouth, formed during this event (Table 4). Liquefaction features along nearby the Tennessee River as well as the Cache River in southern Illinois formed <4850 yr B.P. It is also possible that some of the features along the Cumberland River, perhaps the second generation of features, formed during an event that was also responsible for the Tennessee and Cache features. One candidate is the NMSZ event between 4150-4450 yr B.P. that induced liquefaction and led to the formation of sand dikes and blows at the Burkette archeological site near Charleston, Missouri (Tuttle et al., 2005). Another candidate is an event on the Uniontown fault, part of the Hovey Lake fault system, between 0.9-5.5 ka that may have diverted the Ohio River to its present course (Counts, 2013).

Saline River

The Saline River southeast of Harrisburg was surveyed along 22 km from the confluence of the Middle and South Forks past Equality to Route 1 downstream (Figure 4). In these areas, the Middle Fork used to be part of a meandering river but it has been channelized. The area southeast of Harrisburg is fairly flat with an occasional hill. Much of the area is being farmed, including the floodplain of the Saline River. The area near Equality farther east is much hillier, especially south of the river, where the Shawneetown Front Fault Zone forms a prominent ridge called Wildcat Hills. The river flows around the ridge on its north side. East of Equality, the Saline River is joined by the North Fork and the river flows towards the southeast along the northeastern flank of the ridge. In general, the modern floodplain of the Saline River is about 1.5-2 km wide.

Sand dikes had been previously found on the South Fork of the Saline River. During reconnaissance, however, there appeared to be no exposure along the South Fork. The banks were heavily vegetated and recently covered with thick mud from flooding. Mud had been deposited on the banks of the Saline River but there appeared to be some exposure where there had been bank failures and low in the section where the mud had been eroded by the river.

Though limited due to recent deposition of mud (Figure 7), there were occasional cutbank exposures, ranging from 2-8 m high, especially in river bends. There are two terrace levels: a 4-m terrace underlain by reddish brown, mottled, silt overlying iron-stained sand containing pebbles and molluscs shells followed by clayey silt and a 2-m terrace underlain by reddish brown layered silt. The layered silt of the 2-m terrace is likely to be recent fluvial deposits; whereas, the more weathered silt and iron-stained sand of the 4-m terrace are likely to be Holocene fluvial deposits. Occasionally there was a third and higher 8-m terrace that was underlain by orange silt (possibly loess) followed by laminated silt and clay. These might be Late Pleistocene eolian and glacial lacustrine deposits.

Liquefaction features were found at only one site, SalR2, along Saline River (Table 1). At the site, there were four dikes that were composed of very fine to medium sand and that ranged from 0.5 to 2.5 cm wide. Three of the four dikes originated in the iron-stained sand layer containing mollusc shells and the fourth dike originated below water level and crosscut the iron-stained sand. All of the dikes pinched out in the overlying reddish brown, mottled, silt. Two of the dikes extended to the base of the modern soil where they terminated. The upper portions of the two dikes were iron stained throughout. The lower portions of these dikes, and the other two dikes that pinched out lower in the section, were only slightly iron stained. The cutbank was scoured for organic material for dating purposes but none was found. Given their similarity in stratigraphic context and degree of weathering, the dikes at SalR2 are probably similar in age to those found along the Middle Fork of the Saline River described below.

Table 2. Radiocarbon Dating Results for the New Madrid-Wabash Valley Region

River Sample # Lab #	$^{13}C/^{12}C$ Ratio	Radiocarbon Age Yr B.P.[1]	Calibrated Radiocarbon Age Yr B.P.[2]	Calibrated Calendar Date A.D./B.C.[2]	Sample Description
Cumberland River					
CdR4-W1 Beta-445633	-25.3	10070 ± 30	11765-11405	9815-9455 B.C.	Woody material; from silt in inter-bedded silt & sand; ~1m above water level (AWL)
CdR5-C1 Beta-445634	-24.2	2430 ± 30	2700-2635 2615-2590 2540-2355	750-685 B.C. 665-640 B.C. 590-405 B.C.	Charred material; from reddish silt; ~1.4m above inter-bedded silt & sand and ~1.5 m AWL
CdR8-W3 Beta-445635	-26.5	6250 ± 30	7250-7155 7120-7025	5300-5205 B.C. 5170-5075 B.C.	Woody material; from horizontally bedded tree at contact of layered silt & sand/ clayey silt
CdR9-C1 Beta-445636	-27.4	6730 ± 30	7620-7570	5670-5620 B.C.	Charred material; from silt in inter-bedded silt & sand; level with dike tip; ~2m AWL
Saline River					
SalR2-C3 Beta-444670	-24.1	>43500 ± 30	N/A	N/A	Plant material; from weathered silt ~3.3m below terrace surface
Saline River-Middle Fork					
SalR-MF1-W1 Beta-444666	-28.7	400 ± 30	510-430 355-330	A.D. 1440-1520 A.D.1595-1620	Plant material; from brownish layered silt; ~32cm above contact with bioturbated and mottled silt and sand
SalR-MF2-C1 Beta-444667	-24.6	1190 ± 30	1225-1210 1180-1055 1025-1010	A.D. 725-740 A.D. 770-895 A.D. 925-940	Charred material; from krotovina in upper bioturbated & mottled silt & sand
SalR-MF3-C2 Beta-444668	-27.4	3950 ± 30	4515-4485 4445-4385 4370-4355 4330-4300	2565-2535 B.C. 2495-2435 B.C. 2420-2405 B.C. 2380-2350 B.C.	Charred material; from silt layer within weathered silt and sand; ~1.8m below terrace surface

[1] Conventional radiocarbon ages in years B.P. or before present (1950) determined by Beta Analytic, Inc. Errors represent 1 standard deviation statistics or 68% probability.
[2] Calibrated age ranges as determined by Beta Analytic, Inc., using the Pretoria procedure (Talma and Vogel, 1993; Vogel et al., 1993). Ranges represent 2 standard deviation statistics or 95% probability.

Figure 7. Along the Saline River southeast of Harrisburg, large quantities of mud had been deposited on cutbanks during periods of prolonged flooding. Numerous small sand dikes had been found along this river during reconnaissance in the 1990s (Hajic et al., 1995).

Table 2 Cont'd. Radiocarbon Dating for the New Madrid-Wabash Valley Region

River Sample # Lab #	$^{13}C/^{12}C$ Ratio	Radiocarbon Age Yr B.P.[1]	Calibrated Radiocarbon Age Yr B.P.[2]	Calibrated Calendar Date A.D./B.C.[2]	Sample Description
Skillet Fork					
StF4-L1 Beta-445630	-28.4	2460 ± 30	2715-2360	765-410 B.C.	Plant material; from organic layer within red & gray silt, interbeds of sand; ~1.1m AWL
StF6-C1 Beta-445631	-24.2	2140 ± 30	2300-2255 2160-2040 2015-2010	350-305 B.C. 210-90 B.C. 65-60 B.C.	Charred material; from silt/peat contact; above truncated dike
StF8-W1 Beta-445632	-26.5	80 ± 30	265-220 140-25 Post 0	A.D. 1685-1730 A.D. 1810-1925 Post 1950 A.D.	Woody material; horizontally bedded tree at contact of brownish silt/ red & gray silt, krotovina

[1] Conventional radiocarbon ages in years B.P. or before present (1950) determined by Beta Analytic, Inc. Errors represent 1 standard deviation statistics or 68% probability.
[2] Calibrated age ranges as determined by Beta Analytic, Inc., using the Pretoria procedure (Talma and Vogel, 1993; Vogel et al., 1993). Ranges represent 2 standard deviation statistics or 95% probability.

Table 3. OSL Dating for the New Madrid-Wabash Valley Region

Sample Number	Lab Number	Cosmic Dose Rate (mGray/yr)[1]	Dose Rate (mGray/yr)	OSL Age (Yr)[2]	Calendar Age Yr B.P.[3]	Sample Description
Cumberland River						
CdR8-OSL1	BG4298	0.14 ± 0.01	2.37 ± 0.12	6200 ± 385	5755-6585	Silt, interbedded silt and sand cut by sand dikes; ~1.1 m AWL
CdR8-OSL2	BG4299	0.14 ± 0.01	2.41 ± 0.12	6245 ± 395	5790-6580	Clayey silt, 20 cm below OSL1
CdR8-OSL1	BG4300	0.14 ± 0.01	2.04 ± 0.10	6490 ± 410	6020-6840	Silt, interbedded silt and sand cut by sand dike; ~1.4 m AWL
Skillet Fork						
StF6-OSL1	BG4301	0.16 ± 0.01	2.93 ± 0.14	6545 ± 500	6490-7670	Silt, between 2 peat layers, above truncated dike

[1] Cosmic dose rate calculated from parameters in Prescott and Hutton (1994).
[2] Systematic and random errors calculated in a quadrature at one standard deviation. Datum year is A.D. 2010.
[3] Years B.P. or before present (1950).

Middle Fork of Saline River

The Middle Fork of the Saline River was surveyed along 8.5 km from south of Galatia to Route 34 north of Harrisburg and along 2 km upstream from the confluence with the Saline River southeast of Harrisburg (Figure 4). In these areas, the Middle Fork used to be a meandering river but has been channelized.

The area north of Harrisburg, like the area southeast of Harrisburg, is fairly flat with an occasional hill. Upstream from Harrisburg in the vicinity of Galatia, the river is restricted to a 2-km wide floodplain through hillier countryside. Much of the area is being farmed, including the floodplain of the Middle Fork. Because the river had been ditched and straightened, there were long stretches of poor exposure of mostly 4.5-5 m banks. Along these long stetches, there were often 0.5-1 m high cutbanks low in the section due to recent river erosion. There were occasional 4.5-5 m cutbanks usually in small turns of the river within the ditched channel. These cutbanks revealed bioturbated silt and sand with red and gray mottles. At some locations, brownish, layered silt was overlying the bioturbated and mottled silt and sand.

Sand dikes were found at two sites (SalR-MF2 and MF4; Table 1) along the river. At site SalR-MF2, there are two small sand dikes that intrude red and gray bioturbated silt and sand and are truncated by an erosional contact overlain by brownish, layered silt (Figure 8). The dikes are composed of fine sand. The upper parts of the dikes are silty and slightly iron stained. Both dikes crosscut krotovina in the bioturbated and mottled silt and sand unit. A sample of charred material, SalR-MF2-C1, was collected from a krotovina in the upper part of the bioturbated and mottled unit that was crosscut by one of the dikes. The sample yielded a calibrated age with multiple ranges of 1225-1210, 1180-1055, 1025-1010 yr B.P. (Table 2), providing a maximum constraining age for the dikes of 1225 yr B.P. At a nearby site, a sample of plant material, SalR-MF1-W1, was collected from brownish, layered silt about 32 cm above the erosional contact with bioturbated and mottled silt and sand below. This sample yielded a calibrated age of 510-430 and 355-330 yr B.P., providing a minimum constraining age for the dikes of 330 yr B.P. Thus, the dikes at SalR-MF2 likely formed between 330-1225 yr B.P.

At site SalR-MF4, there is one dike up to 3.5 cm wide. The dike intrudes red and gray bioturbated silt and sand but the very upper part of the dike was covered by soil and vegetation. The dike is composed of fine to medium sand with small clasts. The upper 80 cm that was exposed was silty and iron stained. Given its similarity in stratigraphic context and weathering characteristics, the dike at SalR-MF4 likely formed at the same time as the dikes at nearby site SalR-MF2.

The liquefaction features on the Middle Fork appear to be much too young to be attributed to the Vincennes paleoearthquake between 5900-6300 yr B.P. (Table 4). The age of the Middle Fork features overlap two NMSZ paleoearthquakes: the 900-1200 yr. B.P. event and the 350-650 yr B.P. event. It is quite possible, but certainly not required, that one of these events was responsible for the formation of these features. Additional reconnaissance and dating of liquefaction features in the area are needed to narrow the age estimate of the features and to correlate them across the region.

Table 4. Ages of Paleoliquefaction Features in NM-WV Region and the NMSZ & WVSZ Paleoearthquake Chronologies

<table>
<tr><th>NMSZ</th><th>Cumberland River[1]</th><th>Middle Fork of Saline River</th><th>Skillet River</th><th>WVSZ</th></tr>
<tr><td>1811-1812 Eqs
138 yr B.P.</td><td></td><td></td><td></td><td></td></tr>
<tr><td>A.D. 1450
350-650 yr B.P.</td><td></td><td rowspan="2">330-1225 yr B.P.</td><td></td><td></td></tr>
<tr><td>A.D. 900
900-1200 yr B.P.</td><td></td><td></td><td></td></tr>
<tr><td>830 B.C.
2180-3380 yr B.P.</td><td></td><td></td><td>2 generations
< 2715
2010-2715 yr B.P.</td><td></td></tr>
<tr><td>2350 B.C.
4150-4450 yr B.P.</td><td></td><td></td><td></td><td></td></tr>
<tr><td></td><td>2 generations
< 7250</td><td></td><td></td><td>Vincennes Eq
5900-6300 yr B.P.</td></tr>
<tr><td>Western Lowlands
11100-11500 yr B.P.</td><td></td><td></td><td></td><td>Skelton Eq
11000-13000 yr B.P.</td></tr>
</table>

[1] Liquefaction features along nearby Tennessee River in Kentucky, and Cache River in Illinois, formed <4850 yr B.P.; liquefaction features along nearby Clarks River in Kentucky, formed 10834-11304 yr B.P.

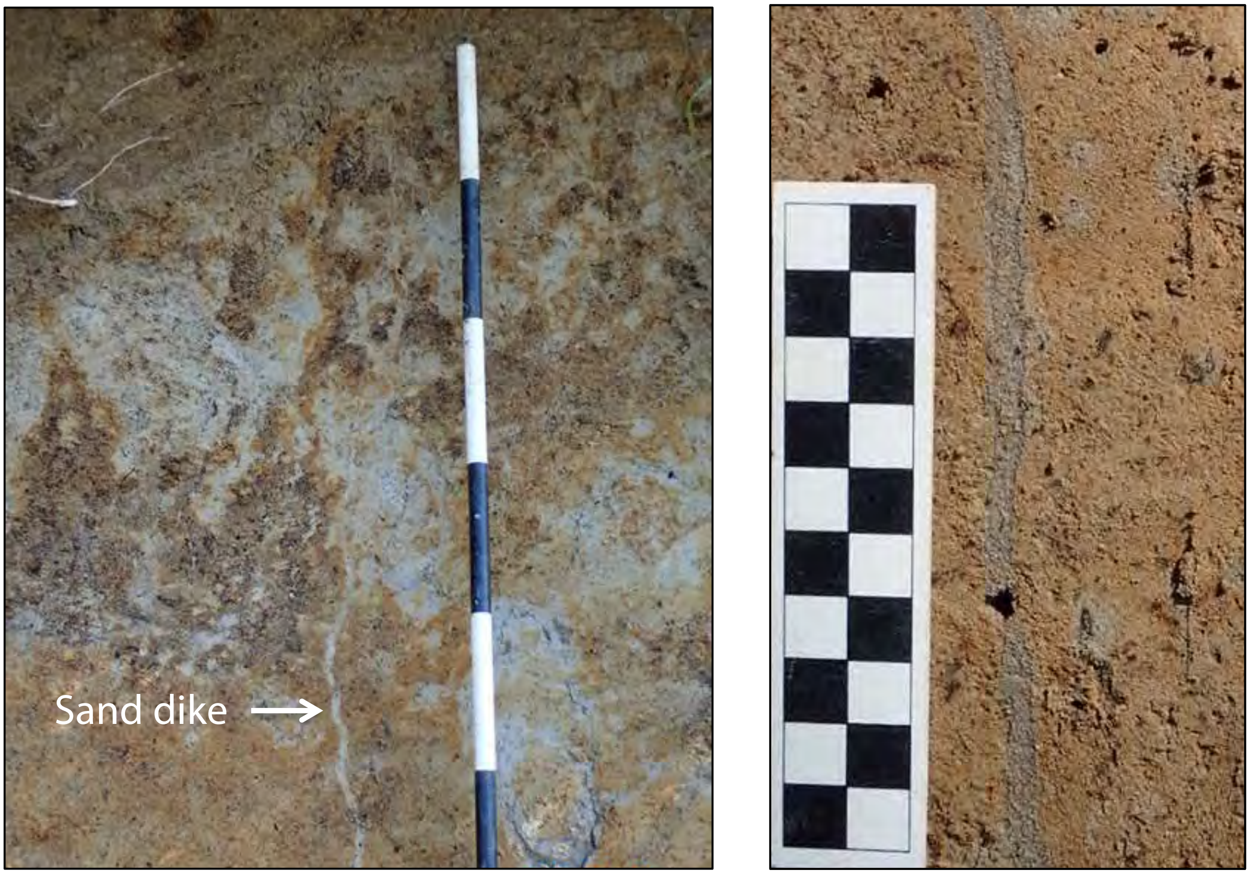

Figure 8. Along the Middle Fork of the Saline River north of Harrisburg, sand dikes crosscut mottled and bioturbated silt and sand and are truncated and overlain by brownish gray layered silt. (Left) Photograph of sand dike exposed in cutbank; on scale, black and white intervals represent 10 cm. (Right) Closeup of sand dike crosscutting iron-stained silty sand; on scale, black and white intervals represent 1 cm.

North Fork of Saline River

Located northeast of Harrisburg, the North Fork of the Saline River was surveyed along 18.5 km from Elba to Route 13 northeast of Equality (Figure 4). In this area, the North Fork is a meandering river though portions of it may have been cleaned out in the past. The North Fork joins the main branch of the Saline River southeast of Equality. The area through which the North Fork flows is similar to that around Harrisburg, flat lying ground that is being farmed and an occasional hill. There are also pit mines in the area.

Like the main branch of the Saline River, the banks of the North Fork had been covered with mud. Also there was a fair amount of slumping of the banks. There were a few rock outcrops, mostly in river bends. There were occasional cutbank exposures, ranging from 2-8 m high, also in river bends. There are two terrace levels: a 4-4.5 m terrace underlain by brown, layered silt overlying red and gray clayey silt and a 2-m terrace underlain by brown layered silt. The layered silt of the 2-m terrace is likely to be recent fluvial deposits; whereas, the more weathered silt and iron-stained sand of the 4-m terrace are likely to be Holocene fluvial deposits. Probing below the 4-m cutbanks, silt was often followed by sand, and at a few sites, by rock. Occasionally there was a third and higher 6 to 8-m terrace that was underlain by rythmites of silt and clay. These are likely to be Late Pleistocene glacial lacustrine deposits.

No sand dikes were found along the North Fork. Although bedrock is shallow in places along the river, there are plenty of locations where sediment conditions are similar to those along the Middle Fork and along the main branch of the Saline where sand dikes formed. Therefore, it seems quite likely that sand dikes occur along the North Fork but were covered by recent deposited mud and slumps.

Skillet Fork

Skillet Fork was surveyed for 28 km from Route 15 north of Wayne City to Mill Shoals (Figure 4). The upper half of the surveyed portion of the river is meandering, except for a few kilometers east of Wayne City that may have been channelized. There are a couple of small rocky falls in the first few kilometers; otherwise, there were only a couple of rock outcrops along the entire length of the surveyed river. Where the river approaches and flows along highway 64, it has been channelized all the way to Mill Shoals and beyond. Between Wayne City and Mill Shoals, the area is of low relief and is being farmed.

Farther down river, the banks of Skillet Fork were covered by mud and had suffered much slumping over the past few years. There were many downed trees in the river. However, exposure was very good along the surveyed portion of the river, even in the channelized portion. There are two terrace levels: a 5 to 6-m terrace and a 2 to 3-m terrace. The 5 to 6-m terrace is underlain by tan silt overlying gray and tan silt with layers of sand followed by red and gray silt with krotovina and iron stained sand near water level to 1.5+ m below the water level at some sites. In a few places, the gray and tan silt unit is missing and in other places red and gray silt is underlain by deformed matrix-supported diamicton. The 2 to 3-m terrace is underlain by gray, layered silt with organic-rich layers.

Sand dikes were found at five sites (StF1, StF3, StF5, StF6, and StF8; Table 1) along the river. All liquefaction sites are located in the 5-m terrace. At all sites, the sand dikes intrude from below and either terminate within red and gray silt with krotovina or are truncated by an erosional contact and overlain by gray, tan, or brown silt (Figure 9). Most of the dikes are either iron stained. Two of the dikes are relatively unweathered. The difference in weathering suggests that there may be two generations of features. All of the dikes are small ranging up to 3.5 cm wide.

A sample of plant material was collected at site StF4 about 1.1 m above the water table from an organic layer within the red and gray silt unit with krotovina. This sample, StF4-L1, yielded a 2-sigma calibrated age of 2715-2360 yr B.P. (Table 2) and provides a maximum constraining age of 2715 yr B.P. for the dikes that intrude this unit. A sample of charred material was collected at site StF6 from the interbedded gray silt and peat unit above a truncated dike (Figure 9). This sample, StF6-C1, gave a 2-sigma calibrated age with multiple ranges of 2300-2255, 2160-2040, and 2015-2010 yr B.P. and provides a minimum constraining age of 2010 yr B.P. for the truncated dike at this site. Also at site StF6, an OSL sample was collected from a gray silt layer

Figure 9. Along Skillet Fork near Wayne City, sand dikes crosscut red and gray silt with krotovina. Some dikes extend through the weathered silt and are truncated and overlain by brown or gray, layered silt. (Left) Photograph of sand dikes at StF6; dikes originate in sand layer at the bottom of the cutbank; one dike extends farther up section where it is truncated and overlain by layered gray silt and peat; shovel and scraper for scale. (Right) Photograph of sand dike at StF5 crosscutting red and gray silt with krotovina; black and white intervals on scale next to dike represent 1 cm.

above the truncated dike. The sample yielded an OSL age of 6490-7670 yr B.P. (Table 3). This age is much older than the radiocarbon age for the same unit and older than the radiocarbon age of the underlying unit. The radiocarbon ages are given preference because they are more reliably accurate. Given their stratigraphic and weathering similarities, most of the dikes documented along Skillet Fork probably formed between 2010-2715 yr B.P. The two relatively unweathered dikes may be younger. Therefore, two earthquakes may have induced liquefaction along this part of the river during the past 2715 yr B.P.

The liquefaction features on Skillet Fork also are too young to be attributed to the Vincennes paleoearthquake between 5900-6300 yr B.P. (Table 4). The age of the Skillet Fork features overlaps the age of a sand blow in the NMSZ that formed between 2180-3380 yr B.P. (Tuttle, 1999; Tuttle and Hartleb, 2012). It is possible that the Skillet Fork features and the New Madrid sand blow formed during the same event. It is also possible that the Skillet Fork sand dikes formed during a local paleoearthquake. Additional reconnaissance and dating of liquefaction features in the area are needed to narrow the age estimate of the features and to correlate them across the region.

EVALUATION OF SCENARIO EARTHQUAKES

In this study, large historical earthquakes thought to be located in the northern part of the NMSZ - the January 23 and February 7 main shocks of the 1812 earthquake sequence - and two large paleoearthquakes thought to be centered in the Wabash Valley seismic zone within 40 km of Vincennes, Indiana - the Vincennes and Skelton earthquakes were used as scenario earthquakes in this evaluation (Table 5; Figure 3). The locations and magnitudes of these events were taken from the CEUS Seismic Source Characterization project (Technical Report, 2012). Moderate events local to the liquefaction sites and a proposed alternate location and magnitude for the January 23, 1812 earthquake (Mueller et al., 2004) also were analyzed.

Table 5. Scenario earthquakes evaluated using liquefaction potential analysis

Source	Event	Magnitude
Local	Local earthquake	5.5
Wabash Valley seismic zone	Vincennes earthquake	7.3
Wabash Valley seismic zone	Skelton earthquake	6.7
New Madrid seismic zone	January 23, 1812	7.0, 7.5
Proposed Alternate Location near Paducah, Kentucky	January 23, 1812	6.8
New Madrid seismic zone	February 7, 1812	7.3, 7.8

Comparison of predicted liquefaction for scenario earthquakes with observed liquefaction in the field, or lack thereof, is used to evaluate, or place limits on, possible source areas and magnitudes of paleoearthquakes. Liquefaction potential analysis was performed for the scenario earthquakes at various moment magnitudes (M 5.5, 6.7, 6.8, 7.0, 7.3, 7.5, and 7.8) and distances (15, 68, 90, 94, 95, 134, 150, 155, 166, 180, 216 and 235 km) between the scenario events and geotechnical sites close to liquefaction sites documented during this study Tables 6 and 7). Geotechnical data used in the analysis included standard penetration test (SPT) data, sediment descriptions, and depths of water table at the time of testing and were gleaned from bridge investigation reports for Skillet Fork and the Middle Fork of the Saline River provided by the Illinois State Department of Transportation. As mentioned above, geotechnical data were sought from the Kentucky State Department of Transportation for a bridge crossing the Cumberland River in the vicinity of liquefaction features but no data were available for the bridge.

Liquefaction Potential Analysis

Liquefaction potential analysis was used to determine if the various scenario earthquakes are likely or not likely to induce liquefaction at the geotechnical sites along rivers where liquefaction features were found during this study. Analysis was performed for those sites and the results considered together to assess which scenario earthquakes may or may not explain the observed distribution of

Table 6. Locations of geotechnical data used in liquefaction potential analysis

Location Borehole (Map ID)	Latitude Dec. Degrees	Longitude Dec. Degrees	Location Description
Skillet Fork 312 (1)	38.36372	-88.58779	Skillet Fork Rt. 600 E, north of Wayne City, IL
Skillet Fork 313 (2)	38.34234	-88.55912	Skillet Fork Rt. 600 N, east of Wayne City, IL
Middle Fork Saline River 310 (3)	37.81913	-88.61462	Middle Fork of the Saline River Ritchie Road bridge, south of Galatia, IL
Middle Fork Saline River 311 (4)	37.77322	-88.54023	Middle Fork of the Saline River Rte. 34 bridge, north of Harrisburg, IL

Table 7. Distances (km) between scenario earthquakes and geotechnical sites used in analysis.

Location Borehole (Map ID)	Local	Vincennes 6100 yr B.P.	Skelton 11000-13000 yr B.P.	New Madrid Jan 23, 1812	New Madrid Feb 7, 1812
Skillet Fork 312 (1)	15	96	68	155, 219	235
Skillet Fork 313 (2)	15	96	68	150	235
Middle Fork Saline River 310 (3)	15	134	94	95, 166	180
Middle Fork Saline River 311 (4)	15	134	94	90	180

liquefaction features. This approach helps to constrain the locations and magnitudes of the paleoearthquakes (e.g., Green et al., 2005; Olson et al., 2005; Tuttle and Hartleb, 2012)
The cyclic-stress method of liquefaction potential analysis, also known as the simplified procedure, was used in this evaluation of scenario earthquakes. This method is well established, remains the standard in engineering practice, and is suitable for many field and tectonic settings (e.g., Seed and Idriss, 1971, 1981, and 1982; Youd et al., 2001; Cetin et al., 2004; Moss et al.,

2006; Robertson, 2004 and 2010; Idriss and Boulanger, 2004, 2008, and 2010; Boulanger and Idriss, 2012).

In the analysis, peak ground accelerations was estimated for scenario earthquakes of moment magnitudes at distances from known or suspected sources by employing regionally appropriate ground motion prediction equations (GMPEs). GMPEs developed for use in the new generation of seismic hazard maps (Atkinson and Boore, 2011; Atkinson et al., 2012; Atkinson and Assatourians, 2012) were used to calculate peak ground accelerations for the scenario earthquakes. After determining the accelerations, cyclic stress ratios (CSR) generated by scenario earthquakes were calculated using the following expression:

$$CSR_{7.5} = \frac{\tau_{ave}}{\sigma'_{vo}} = 0.65\,.\left(\frac{a_{max}}{g}\right).\left(\frac{\sigma_{vo}}{\sigma'_{v0}}\right).r_d\,.\frac{1}{MSF}$$

where a_{max}= peak ground acceleration peak (horizontal) or PGA , (a_{max}/g) is peak ground acceleration divided by gravity, σ_{vo} and $\sigma_{vo\prime}$ are the total and effective vertical overburden stresses, respectively, and r_d is a stress reduction coefficient, and MSF = magnitude scaling factor. The $CSR_{7.5}$ represents the normalized shear stress (τ_{ave}/σ_v) induced in the soil by the earthquake event (i.e, the seismic demand) and commonly referenced to a benchmark case with **M** = 7.5.

Variations in standard penetration test (SPT) procedure were corrected by adjusting the measured blow count (N_m) using the relation:

$$\boldsymbol{N_{1(60)} = C_N\, C_E\, C_B\, C_R\, C_S\, N_m}$$

where $N_{1(60)}$ is normalized blow count corrected for hammer energy (C_E), effective confining stress (C_N), borehole diameter (C_B), rod length (C_R), and sampler configuration (C_S), with N_m being the measured SPT resistance or "blow count" reported in blows/foot (or blows/0.3m).

Following the computations of the cyclic stress ratio and the adjusted and normalized blow count, the liquefaction potential of representative layers at borehole sites was determined by plotting computed cyclic stress ratio (CSR) versus normalized blow count [$(N_1)_{60}$] on charts such as that shown in Figure 10 for **M** 7.5 earthquakes. If the cyclic stress ratio (CSR) is greater than or equal to the cyclic resistance ratio (CRR), the value plots on or above the curve, the soil is likely to liquefy. Conversely, if CSR is less than CRR, the value plots below the curve, and liquefaction is considered unlikely.

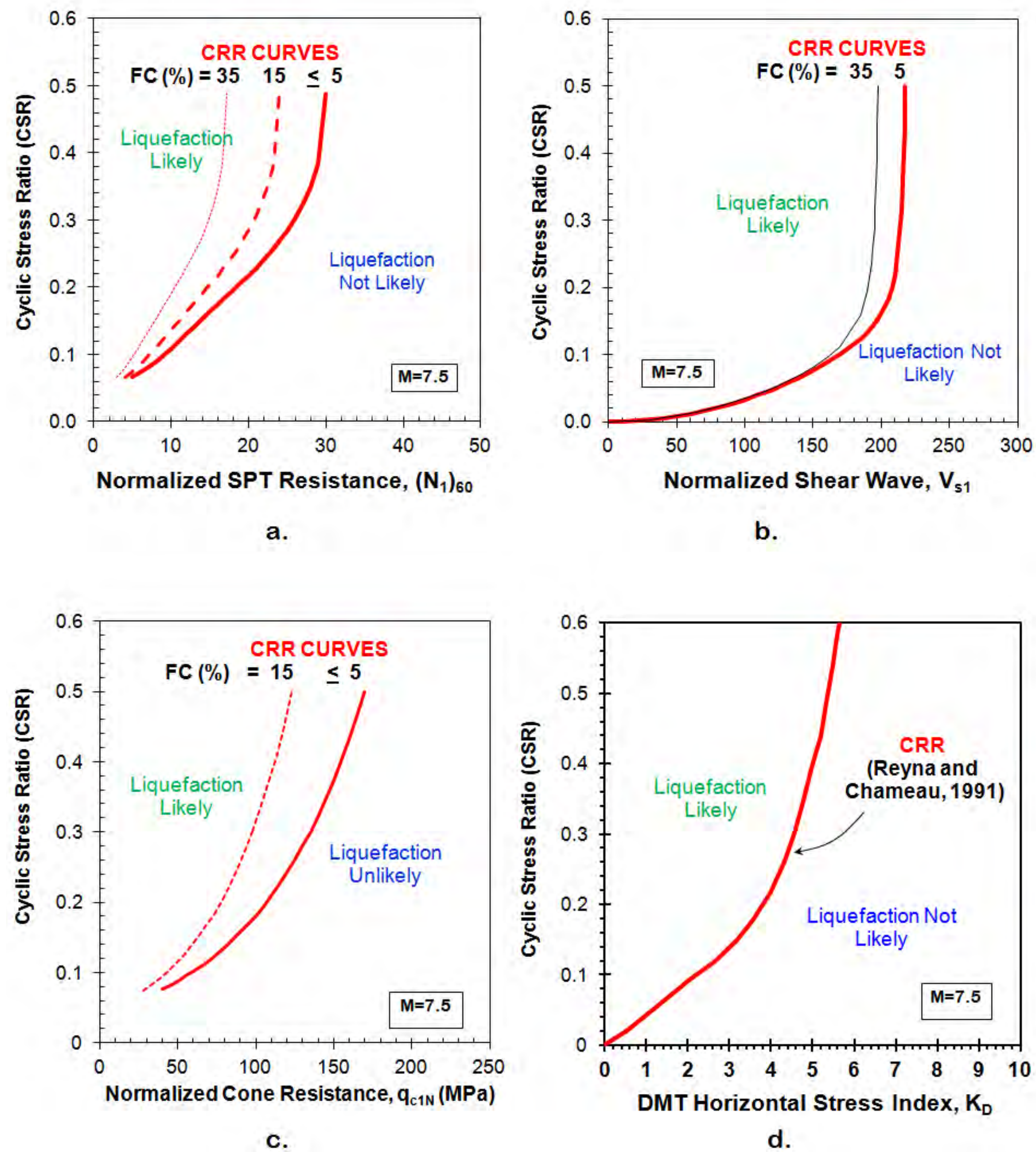

Figure 10. Illustrative sets of cyclic resistance ratio (CRR) curves for M 7.5 earthquakes for four in-situ tests: (a) standard penetration; (b) shear wave velocity; (c) cone penetration; and (d) flat plate dilatometer (after Schneider et al., 1999).

As an approximation to the base curve, for clean sands which are tested in boreholes using the standard penetration test (SPT), the cyclic resistance ratio (CRR) for a **M** 7.5 event proposed by Youd et al. (2001) is given by the relation:

$$CRR_{7.5} = \frac{1}{34-(N_1)_{60-cs}} + \frac{(N_1)_{60}}{135} + \frac{50}{[10\,.\,(N_1)_{60-cs}+45]^2} - \frac{1}{200}$$

for $(N_1)_{60\text{-}cs} < 30$

In this study we use the approximation to the base curve. The CRR for magnitudes other than 7.5 was calculated by multiplying $CRR_{7.5}$ by the appropriate Magnitude Scaling Factor (MSF), which is given by the expression:

$MSF = (M_W/7.5)^{-3.3}$

There are many sources of uncertainty associated with the geotechnical approach to evaluating the locations and magnitudes of paleoearthquakes, including but not limited to the following: (1) identification of the deposits that liquefied during a particular event; (2) measurements of geotechnical properties of the deposits; (3) changes in geotechnical properties due to liquefaction and to post-liquefaction effects related to compaction and weathering; (4) short- and long-term fluctuations in the water table; and (5) regional attenuation of earthquake ground motions (Technical Report, 2012). In order to reflect these uncertainties, the geotechnical data were reviewed and multiple layers representative of the site and likely to be susceptible to liquefaction (e.g., within a depth range of ≤18 m and with blow counts of less than 30) selected for analysis. Water table depths of 3 and 5 m were used in the analysis, reflecting annual average depth range in the region. This seems reasonable because most of the liquefaction features found along the Middle Fork of the Saline River and Skillet Fork during this project are estimated to have formed since 2715 yr B.P. or during the Late Holocene when the water table depth was similar to today. In addition, medium and high GMPEs were used to calculate peak ground accelerations for most of the scenario earthquakes.

The results of the analysis are summarized below. Detailed results are presented in Appendix A. These results help to constrain the locations and magnitudes of paleoearthquakes. Evaluation of additional scenario earthquakes, using high and low GMPEs, and shallower and deeper water table depths, as well as geotechnical data collected at sites of liquefaction would be advantageous and further constrain the interpretations of paleoearthquakes.

Results of Analysis

To help interpret the distribution of observed liquefaction features in the New Madrid-Wabash Valley study region, liquefaction potential analysis was performed for various scenario earthquakes as described above. The results of the analysis are provided in Appendix A and summarized in Table 8 and discussed below.

Water table depth 3 m

Results of analysis using water table depth of 3 m are presented first. Considering a **M** 5.5 earthquake produced by a local source at 15 km distance, the results show that the Skillet Fork site (1) (GT 312) would likely experience liquefaction using either the medium or high GMPE. The Skillet Fork site (2) (GT 113) would experience marginal or some liquefaction during such an event using the medium GMPE and would likely experience liquefaction using the high GMPE. For the Middle Fork of the Saline River, neither site (3) (GT 310) nor site (4) (GT 311) would likely experience liquefaction using medium GMPE. Using the high GMPE, Saline River site (3) would likely experience liquefaction while site (4) would not.

Evaluating the **M** 7.3 Vincennes earthquake as a scenario event, the analysis predicts that the Skillet Fork sites (1) and (2) would likely experience liquefaction using either the medium or high GMPE. Saline River site (3) would experience liquefaction during the event using either the medium or high GMPEs; but liquefaction would be unlikely to occur at site (4) using either GMPE.

Considering the **M** 6.7 Skelton earthquake as a scenario event, the analysis predicts that the Skillet Fork site (1) would experience liquefaction using the medium GMPE while site (2) may only experience marginal liquefaction. Using the high GMPE, the analysis predicts that both sites (1) and (2) would liquefy. For the Saline River, the analysis using the medium GMPE indicates that no liquefaction is likely to be induced at sites (3) and (4); whereas, the analysis using the high GMPE indicates marginal liquefaction at site (3) and no liquefaction at site (4). Evaluating the **M** 7.0 January 23, 1812 earthquake as a scenario event, the analysis using the medium GMPE predicts that the Skillet Fork site (1) and the Saline River site (3) are unlikely to experience liquefaction during an earthquake. If the event were of **M** 7.5, the Saline River site (3) would likely experience liquefaction; whereas, the more distant Skillet Fork site (1) would only experience marginal liquefaction.

Considering the proposed alternate **M** 6.8 January 23, 1812 earthquake in northwestern Kentucky, the analysis using the medium GMPE predicts no liquefaction at the four sites. However, using the high GMPE, liquefaction would be likely to occur at Skillet Fork sites (1) and (2) and Saline River site (3) but not at Saline River site (4).

Evaluating the **M** 7.3 February 7, 1812 earthquake as a scenario event, the analysis using the medium GMPE predicts no liquefaction at Skillet Fork site (1) and Saline River site (3). If the event were of **M** 7.8, the analysis using the medium GMPE predicts no liquefaction at Skillet Fork site (1), marginal liquefaction at Skillet Fork site (2), liquefaction at Saline River site (3), and no liquefaction at Saline River site (4). However, using the high GMPE, the analysis predicts that liquefaction would be likely to occur at all of the four sites.

<u>Water table depth 5 m</u>

Results of analysis using water table depth of 5 m are presented next. Considering a **M** 5.5 earthquake produced by a local source at 15 km distance, the analysis using the medium GMPE suggests that liquefaction would be unlikely to occur at any of the four geotechnical sites. Using the high GMPE, Skillet Fork site (1) and the Saline River site (3) would be likely to experience liquefaction; whereas, the Skillet Fork site (2) would experience marginal liquefaction and Saline River site (4) would likely experience no liquefaction.

Evaluating the **M** 7.3 Vincennes earthquake as a scenario event, the analysis predicts that the Skillet Fork site (1) and Skillet Fork site (2) would likely experience liquefaction using the either the medium or high GMPE. The analysis predicts that liquefaction is unlikely to be induced at Saline River Sites (3) and (4) using the medium GMPE and that liquefaction would be induced at site (3) but not site (4) using the high GMPE.

Table 8. Summary of Evaluation of Scenario Earthquakes

Location (Map ID)	Distance (km)	Results (3m) A_{max} Medium	Results (3m) A_{max} High	Results (5m) A_{max} Medium	Results (5m) A_{max} High	Summ. Results[1]
1. Scenario Event of **M** 5.5 Local Event						
Skillet Fork (1)	15	L	L	N	L	L
Skillet Fork (2)	15	L/N	L	N	L/N	L/N
Saline River (3)	15	N	L	N	L	L
Saline River (4)	15	N	N	N	N	N
2. Scenario Event of **M** 7.3 Vincennes earthquake (Wabash Valley seismic zone)						
Skillet Fork (1)	96	L	L	L	L	L
Skillet Fork (2)	96	L	L	L	L	L
Saline River (3)	134	L	L	N	L	L
Saline River (4)	134	N	N	N	N	N
3. Scenario Event of **M** 6.7 Skelton earthquake (Wabash valley seismic zone)						
Skillet Fork (1)	68	L	L	N	L	L
Skillet Fork (2)	68	L/N	L	N	L	L
Saline River (3)	94	N	L/N	N	L	N
Saline River (4)	94	N	N	N	N	N
4. Scenario Event of **M** 7.0 January 23, 1812 (New Madrid seismic zone)						
Skillet Fork (1)	219	N	NA	NA	NA	N
Saline River (3)	166	N	NA	NA	NA	N
5. Scenario Event of **M** 7.5, January 23, 1812 (New Madrid seismic zone)						
Skillet Fork (1)	219	L/N	NA	NA	NA	L/N
Saline River (3)	166	L	NA	NA	NA	L
6. Scenario Event of **M** 6.8 January 23, 1812 (Alternate Location Northwest Kentucky)						
Skillet Fork (1)	155	N	L	N	N	N
Skillet Fork (2)	150	N	L	N	N	N
Saline River (3)	95	N	L	N	L	L
Saline River (4)	90	N	N	N	N	N
7. Scenario Event of **M** 7.3 February 7, 1812 (New Madrid seismic zone)						
Skillet Fork (1)	235	N	NA	NA	NA	N
Saline River (3)	180	N	NA	NA	NA	N
8. Scenario Event of **M** 7.8 February 7, 1812 (New Madrid seismic zone)						
Skillet Fork (1)	235	N	L	N	L	L
Skillet Fork (2)	235	L/N	L	N	L	L
Saline River (3)	180	L	L	L	L	L
Saline River (4)	180	N/L	L	N	L	L

[1.] L = liquefaction likely for 45% - 100 % of the layers analyzed; L/N = marginal because liquefaction predicted for 24% - 44% of the layers analyzed; N = liquefaction not likely because liquefaction predicted for less than 24% of the layers analyzed (see Appendix A); NA = analysis not performed.

Considering the **M** 6.7 Skelton earthquake as a scenario event, the analysis predicts that none of the sites would experience liquefaction using the medium GMPE. However, using the high GMPE, Skillet Fork sites (1) and (2) and Saline River site (3) would likely liquefy, whereas Saline River site (4) would not.
Considering the proposed alternate **M** 6.8 January 23, 1812 earthquake in northwestern Kentucky, the analysis predicts that none of the sites is likely to liquefy using the medium GMPE. Using the high GMPE, Skillet Fork sites (1) and (2) and Saline River site (4) would not be likely to experience liquefaction, whereas Saline River site (3) would be likely to experience liquefaction.

Evaluating the **M** 7.8 February 7, 1812 earthquake as a scenario event, the analysis using the medium GMPE predicts liquefaction at Saline River site (3) but not at the other three sites; whereas, using the high GMPE liquefaction is likely to be induced at all sites.

Summary

Combing the results for different water table depths and GMPEs, a moderate earthquake of **M** 5.5 located within 15 km could be responsible for liquefaction features along Skillet Fork. In the analysis, the **M** 7.3 Vincennes and **M** 6.7 Skelton events both seem capable of inducing liquefaction along Skillet Fork. However, both these WVSZ paleoearthquakes predate the Skillet Fork liquefaction features thought to have formed <2715 yr B.P. Evaluation of the January 23, 1812 scenario event predicts liquefaction along Skillet Fork if it were of **M** 7.5, as does analysis of the February 7, 1812 earthquake if it were of **M** 7.8. The January 23, 1812 scenario event with the alternative magnitude of **M** 6.8 and location in northwestern Kentucky does not seem capable of inducing liquefaction along Skillet Fork. If similar to the **M** 7.5 January 23, 1812 and **M** 7.8 February 7, 1812 scenario events, the NMSZ paleoearthquakes between 350-650 yr B.P. and 900-1200 yr B.P., and possibly another yet poorly understood NMSZ event between 2180-3380 yr B.P., could have been responsible for liquefaction features along Skillet Fork. The results are similar for the Middle Fork of the Saline River. The only differences are that the **M** 6.7 Skelton scenario event does not induce liquefaction along the Saline River but the scenario event representing the alternate magnitude and location of the January 23, 1812 earthquake does.

CONCLUSION

The relationship between the NMSZ and the WVSZ, and the possible interaction of these two sources of repeated large magnitude earthquakes, is a major unresolved issue that has significant implications for earthquake hazard assessment in the central United States (Figure 3). The Commerce geophysical lineament has been proposed as a major tectonic structure that links the two seismic zones capable of generating large earthquakes. In addition, it has been suggested that the January 23, 1812 New Madrid earthquake was centered outside the NMSZ and in northwestern Kentucky and that the earthquake hazard may have been underestimated in this region where seismicity has been recently quiescent. This project begins to fill a critical data gap in southeastern Illinois and northwestern Kentucky that will eventually help to test these hypotheses.

During this project, 111 km of rivers were searched for earthquake-induced liquefaction features (Figure 4). The search included systematic surveys of selected portions of the Cumberland River in northwestern Kentucky, as well as the Saline River and its Middle and North Forks and the Skillet Fork in southeastern Illinois. It was known from previous paleoliquefaction studies that sand dikes occur along the Saline River and Skillet Fork, though the ages of the dikes were poorly constrained. Apparently, the Cumberland River and Middle and North Forks of the Saline River had not previously been searched. Despite limited cutbank exposure due to deposition of mud and slumping of banks as the result of flooding, sand dikes were found and documented on all these rivers except the North Fork of the Saline (Figure 4).

Most of the liquefaction features found and studied were small, 0.5-3.5 cm wide, sand dikes that were weathered by varying degrees, exhibiting iron staining and fines accumulation. Several of the dikes on the Cumberland River near its confluence with the Ohio River were moderate in size ranging up to 25 cm. The larger size of the features compared to other dikes along the river is likely due to lateral spreading though site conditions close to the Ohio River may also be a factor. The Cumberland River dikes were the most weathered, exhibiting prominent iron staining, iron cementation along dike margins, and silt accumulation in the upper part of the dikes. Two dikes on Skillet Fork were essentially unweathered, suggesting that they were younger than the other dikes. Along the Cumberland River, there were two generations of sand dikes based on crosscutting relations and degree of weathering. Along Skillet Fork, there may have been two generations of dikes, but this interpretation is based on degree of weathering alone and so is more tenuous.

Based on radiocarbon dating of organic material within the deposits intruded by sand dikes, the two generations of liquefaction features along the Cumberland River appear to have formed after 7250 yr B.P. (Table 4). For the dikes along the Middle Fork of the Saline River, maximum and minimum age constraints were determined by dating both deposits intruded by the dikes and deposits overlying an erosional contact that truncated the dikes. Thus, the dikes on the Middle Fork likely formed between 330-1225 yr B.P. Dikes found at one site on the main branch of the Saline River probably formed at the same time based on stratigraphic and weathering similarities. However, the site is too far away to be comfortable with such a correlation with no local age control. For Skillet Fork, maximum and minimum age constraints also were determined for most of the dikes by dating deposits intruded by the dikes and deposits overlying an erosional contact that truncated several dikes. Therefore, most of the more weathered dikes that exhibited iron-staining and silt accumulation formed between 2010-2715 yr B.P. A couple of unweathered dikes along the river may have formed much more recently.

Liquefaction features across the WVSZ formed between 5900-6300 yr B.P. and have been attributed the Vincennes paleoearthquake. It is quite possible, but certainly not required, that the first generation of dikes along the Cumberland River, including the large iron-cemented dikes near the mouth, formed during this event (Figure 4 and Table 4). The second generation of dikes is unlikely to be historical in age given the degree of weathering. They might have formed during the same event responsible for liquefaction features along the Tennessee River nearby as well as the Cache River in southern Illinois that formed <4850 yr B.P. A likely candidate is the NMSZ event between 4150-4450 yr B.P. that was responsible for formation of sand blows near Charleston, Missouri (Tuttle et al., 2005). Another candidate is an event on the Uniontown fault, part of the Hovey Lake fault system, between 0.9-5.5 ka that may have diverted the Ohio River to its present course (Counts, 2013).

The liquefaction features on the Middle Fork of the Saline River and Skillet Fork appear to be too young to be attributed to the Vincennes paleoearthquake between 5900-6300 yr B.P. (Table 4). The age of the Middle Fork dikes overlap two NMSZ paleoearthquakes: the 900-1200 yr B.P. event and the 350-650 yr B.P. event. The age of the Skillet Fork features also overlaps the age of a sand blow in the NMSZ that formed between 2180-3380 yr B.P. It is possible, but not required, that NMSZ events may have been responsible for the formation of these features. The Middle Fork and Skillet Fork features also overlap in age with an event on the Uniontown fault between 0.9-5.5 ka. It is also possible that the sand dikes on both rivers formed during local moderate paleoearthquakes.

Evaluation of scenario earthquakes was performed to further evaluate possible source areas and magnitudes of paleoearthquakes that induced liquefaction along the Middle Fork of the Saline River and Skillet Fork. Geotechnical data used in the analysis were from boreholes close to the liquefaction sites on the two rivers. Unfortunately, no borehole data was available close to liquefaction sites along the Cumberland River. Liquefaction potential analysis confirms that moderate earthquakes of **M** 5.5 located within 15 km could have induced liquefaction along the Middle Fork and Skillet Fork. Although the **M** 7.3 Vincennes event could have induced liquefaction along both rivers, and the **M** 6.7 Skelton event could do the same along Skillet Fork, both WVSZ paleoearthquakes predate the liquefaction features and therefore were not responsible for their formation. The January 23, 1812 and February 7, 1812 scenario events predict liquefaction along both rivers if the events were of **M** 7.5 and **M** 7.8, respectively. This supports the interpretation that the NMSZ paleoearthquakes of 900-1200 yr B.P., 350-650 yr B.P., and possibly 2180-3380 yr B.P. may have been responsible for the sand dikes along Skillet Fork, and that two later paleoearthquakes may have been responsible for the dikes along Middle Fork. Analysis of the January 23, 1812 scenario event with the alternative magnitude of **M** 6.8 and location in northwestern Kentucky does not predict liquefaction along Skillet Fork but it does predict liquefaction along the Middle Fork. Most of the liquefaction features in the vicinity of the proposed alternate location for the January 23, 1812 earthquake are relatively small and do not support the hypothesis that a **M** 6.8 earthquake was centered in this area. In addition, most of the liquefaction features in the area are prehistoric in age and the larger sand dikes along the Cumberland River and the small sand blow on Clarks River appear to be thousands of years old.

During this project, additional liquefaction features have been found, ages of some of the liquefaction features better constrained and compared with timing of NMSZ and WVSZ paleoearthquakes, and scenario earthquakes evaluated to help assess the likely sources and magnitudes of earthquakes responsible for the observed liquefaction features. However, significant uncertainties remain regarding the sources of earthquakes that induced liquefaction during the Middle and Late Holocene along the Cumberland River, Middle Fork of the Saline River, and Skillet Fork and other rivers in the NM-WV region. To reduce those uncertainties, additional reconnaissance and dating of liquefaction features in the region are needed to further narrow the age estimate of the features and to better correlate them across the region.

ACKNOWLEDGMENTS

Numerous researchers have studied paleoliquefaction in the New Madrid and Wabash Valley seismic zone over the past 20 years (see Tuttle and Hartleb, 2012 for summaries and references of paleoliquefaction research performed in both regions). This project builds on that previous work and identifies areas where additional data would help to reduce uncertainties about paleoearthquakes in both seismic zones. We are grateful to Ross Hartleb and Russ Wheeler for discussions and information regarding the Wabash Valley seismic zone, Paul Mayne of Georgia Tech for guidance on liquefaction potential analysis, graduate students Taylor Busch and John Johnson for their assistance with fieldwork, Kathy Tucker for generating GIS-based maps for this project, and Cameron Karrenbauer for tabulating data and editing references. We also thank Dave Miller, Jeff Jones, and Robert Graeff of the Illinois Department of Transportation and Bart Asher of the Kentucky Department of Transportation for providing borehole data and geotechnical reports for bridges in the study region. The views and conclusions presented in this paper are those of the authors and should not be interpreted as necessarily representing the official policies, either expressed or implied, of the U.S. Government.

REFERENCES CITED

Atkinson, G., and D. Boore, 2011, Modification to existing ground-motion prediction Equations in light of new data, Bullletin of the Seismological Sociey of America, v. 101, p. 1121-1135.

Atkinson, G., (with input from) J. Adams, G. Rogers, T. Onur, and K. Assatourians, 2012, White paper on development of ground motion prediction equations for Canadian national seismic hazard maps, www.seismotoolbox.ca (Miscellaneous Resources).

Atkinson, G., (Project Leader), K. Assatourians, 2012, GMPEs for national hazard maps, *www.seismotoolbox.ca* (Miscellaneous resources).

Bakun, W.H., and Hopper, M.G., 2004a, Catalog of significant historical earthquakes in the Central United States, U.S. Geological Survey Open-File Report 2004-1086, 142 p.

Baldwin, J.N., Barron, A.D., and Harris, J.B., 2002, Geophysical and paleoseismic investigation of the Commerce Geophysical Lineament at Holly Ridge, Idalia, Missouri, Final technical report to the US Geological Survey, 36 p.

Boulanger, R.W., and Idriss, I.M., 2012, Probabilistic standard penetration test-based liquefaction: triggering procedure, J. Geotechnical and Geoenvironmental Engineering, v. 138, n. 10, p. 1185-1195.

Braile, L. W., Keller, G. R., Hinze, W. J., and Lidiak, E. G., 1982, An ancient rift complex and its relation to contemporary seismicity in the New Madrid Seismic Zone, Tectonics, v. 1, p. 225-237.

Braile, L.W., Hinze, W.J., Keller, G.R., Lidiak, E.G., and Sexton, J.L., 1986, Tectonic development of the New Madrid rift complex, Mississippi Embayment, North America, Tectonophysics, v. 131, no. 1-2, p. 1−21.

Cetin, K.O., Seed, R.B., Der Kiureghian, A., Tokimatsu, K., Harder, L.F. Jr, Kayen, R.E., and Moss, R.E.S., 2004, SPT-based probabilistic and deterministic assessment of seismic soil liquefaction potential, ASCE Journal of Geotechnical and Environmental Engineering, v. 130, n. 12.

Crone, A.J., and Wheeler, R.L., 2000, Data for Quaternary faults, liquefaction features, and possible tectonic features in the central and eastern United States, east of the Rocky Mountain front, U.S. Geological Survey, Open-file Report 00-260, 332 p.
Counts, R.C., 2013, Late Quaternary landscape evolution and tectonic geomorphology of the Lower Ohio River Valley, USA, Ph.D. dissertation, University of Cincinnati.
Counts, R.C., Van Arsdale, R.B., and Woolery, E.W., 2009, Investigation of Quaternary displacement on the Uniontown fault, western Kentucky [abstract], Geological Society of America Abstracts with Programs, v. 41, no. 1, p. 20.
Denny, F.B., Goldstein, A., Devera, J.A., Lasemi, Z., and Nelson, W.J., 2008, The Illinois-Kentucky Flourite District, Hicks Dome, and Garden of the Gods in southeastern Illinois and northwestern Kentucky, *in* Maria, A.H., and Counts, R.C., eds., From the Cincinnati Arch to the Illinois Basin: Geological Field Excursions along the Ohio River Valley, Geological Society of America Field Guide 12, p. 11-24.
Ervin, C.P., and McGinnis, L.D., 1975, The Reelfoot rift: reactivated precursor of the Mississippi embayment, Geological Society of America Bulletin, v. 86, p. 1287-1295.
Green, R.A., Obermeier, S.F., Olson, S.M., 2005, Engineering geologic and geotechnical analysis of paleoseismic shaking using liquefaction effects: field examples, Engineering Geology, v. 76, p. 263-293.
Hajic, E.R., Wiant, M.D., and Oliver, J.J., 1995, Distribution and dating of prehistoric earthquake liquefaction in southeastern Illinois, central U.S.: Reston, VA, Reston, VA, National Earthquake Hazards Reduction Program, Final Technical Report, (1434-93-G-2359), 34 p.
Harrison, R.W., and Schultz, A., 2002, Tectonic framework of the southwestern margin of the Illinois Basin and its influence on neotectonism and seismicity, Seismological Research Letters, v. 73, p. 698-731.
Hildenbrand, T.G., and D. Ravat, 1997, Geophysical setting of the Wabash Valley fault system, Seismological Research Letters, v. 68, p. 567-585.
Hildenbrand, T.G., McBride, J.H., and D. Ravat, 2002, The Commerce Geophysical lineament and its possible relation to Mesoproterozoic igneous complexes and large earthquakes in the central Illinois basin, Seismological Research Letters, v. 73, p. 640-659.
Hough, S.E., Bilham, R., Mueller, K., Stephenson, W., Williams, R., and Odum, J., 2005, Wagon loads of sand blows in White County, Illinois, Seismological Research Letters, v. 76, no. 3, p. 373-386.
Idriss, I.M., and Boulanger, R.W., 2004, Semi-empirical procedures for evaluating liquefaction potential during earthquakes, Proc., 11th International Conference on Soil Dynamics and Earthquake Engineering, and 3rd International Conference on Earthquake Geotechnical Engineering, D. Doolin et al., eds., Stallion Press, v. 1, p. 32-56.
Idriss, I.M. and Boulanger, R.W., 2008, Soil liquefaction during earthquakes, Earthquake Engineering Research Institute, Monograph 12, EERI MNO-12, 262 p.
Idriss, I.M., and Boulanger, R.W., 2010, SPT-Based liquefaction triggering procedures, Report No. UCDM/CGM – 10/02, Dept. of Civil & Environmental Engineering, University of California at Davis. 259 p.
Kim, W-Y, 2003, The 18 June 2002 Caborn, Indiana, earthquake: Reactivation of ancient rift in the Wabash Valley seismic zone, Bulletin of the Seismological Society of America, v. 93, p. 2201-2211.
Li, Q., Liu, M., Zhang, Q., and Sandoval, E., 2007, Stress evolution and seismicity in the central-

eastern USA: Insights from geodynamic modeling. *In* Continental Intraplate Earthquakes: Science, Hazard, and Policy Issues, ed. S. Stein and S. Mazzotti, Geological Society of America special paper 425, p. 149-166.
Li, Q., Liu, M., and Stein, S., 2009, Spatial-temporal complexity of continental intraplate seismicity: insights from geodynamic modeling and implications for seismic hazard estimation, Bulletin of the Seismological Society of America, v. 99, p. 52-60.
McBride, J.H., Sargent, M.L., Potter, C.J., 1997, Investigating possible earthquake-related structure beneath the southern Illinois Basin from seismic reflection, Seismological Research Letters, v. 68, p. 641-649.
McBride, J.H., Hildenbrand, T.G., Stephenson, W.J., and Potter, C.J., 2002, Interpreting the earthquake source of the Wabash Valley seismic zone (Illinois, Indiana, and Kentucky) from seismic-reflection, gravity, and magnetic-intensity data, Seismological Research Letters, v. 73, p. 660-697.
McNulty, W.E. and Obermeier, S.F., 1999, Liquefaction evidence for at least two strong Holocene paleo-earthquakes in central and southwestern Illinois, USA, Environmental and Engineering Geoscience, v., no. 2, p. 133-146.
Merino, M., Stein, S., Liu, M., and Okal, E., 2010, Comparison of seismicity rates in the New Madrid and Wabash Valley seismic zones, Seismological Research Letters, v. 81, p. 951-954.
Mooney, W., and Andrews, M., 1984, Seismic-refraction studies of the Mississippi Embayment: An overview, in Gori, P.L., and Hays, W.W., eds., Proceedings of the Symposium on the New Madrid seismic zone, U.S. Geological Survey, Open-File Report 84-770, p. 138-167.
Moss, R.E.S., Seed, R.B., Kayen, R.E., Stewart, J.P., and Der Kiureghian, A., 2006, CPT-based probabilistic assessment of seismic soil liquefaction initiation, Pacific Earthquake Engineering Research (PEER) Center Report # 2005/15, April.
Mueller, K., Hough, S.E., and Bilham, R., 2004, Analysing the 1811-1812 New Madrid earthquakes with recent instrumentally recorded aftershocks, Nature, v. 429, p. 284-288.
Munson, P.J. and Munson, C.A., 1996, Paleoliquefaction evidence for recurrent strong earthquakes since 20,000 years BP in the Wabash Valley area of Indiana, report submitted to the U.S. Geological Survey in fulfillment of National Earthquake Hazards Reduction Program Grant No. 14-08-0001-G2117, 137 p.
Munson, P.J., Obermeier, S.F., Munson, C.A., and Hajic, E.R., 1997, Liquefaction evidence for Holocene and Latest Pleistocene seismicity in the southern halves of Indiana and Illinois: A preliminary overview, Seismological Research Letters, v. 68, p. 521-536.
Nelson, W.J., 1990, Comment on "major Proterozoic basement features of the eastern midcontinent of North America revealed by recent COCORP profiling, Geology, v. 18, p. 378.
Nelson, W.J., Denny, B.F., Follmer, L.R., and Masters, J.M., 1999, Quaternary grabens in southernmost Illinois—Deformation near an active intraplate seismic zone, Tectonophysics, v. 305, p. 381-397.
Obermeier, S.F., 1998, Liquefaction evidence for strong earthquakes of Holocene and latest Pleistocene ages in the states of Indiana and Illinois, USA, Engineering Geology, v. 50, p. 227-254.
Odum, J.K., Williams, R.A., Stephenson, W.J., Tuttle, M.P., Al-Shukri, H., 2016, Preliminary assessment of a previously unknown fault zone beneath the Daytona Beach sand blow cluster near Marianna, Arkansas, Seismological Research Letters, v. 87, n. 6, p. 1453-1464.

Olson, S.M., Obermeier, S.F., and Stark, T.D., 2001, Interpretation of penetration resistance for back-analysis at sites of previous liquefaction, Seismological Research Letters, v. 72, no. 1, p. 46-59.

Olson, S.M., Green, R.A., and Obermeier, S.F., 2005, Revised magnitude bound relation for the Wabash Valley seismic zone of the central United States, Seismological Research Letters, v. 76, p. 756-771.

Petersen, M.D., et al., 2014, Documentation for the 2014 Update of the United States National Seismic Hazard Maps, U.S. Geological Survey Open-File Report 2014–1091, 243 p.

Pond, E.C., and Martin, J.R., 1997, Estimated magnitudes and accelerations associated with prehistoric earthquakes in the Wabash Valley region of the central United States, *in* Kolata, D.R., and Hildenbrand, T.G. (editors), Investigations of the Illinois Basin earthquake region, Seismological Research Letters, v. 68, p. 611-623.

Prescott, J.R., and Hutton, J.T., 1994, Cosmic ray contributions to dose rates for luminescence and ESR dating: Large depths and long-term time variations, Radiation Measurements, v. 23, p. 497-500.

Robertson, P. K., 2004, Evaluating soil liquefaction and post-earthquake deformations using the CPT, Geotechnical and Geophysical Site Characterization, v.1 (Proc. ISC-2, Porto), Millpress, Rotterdam, p. 233-252.

Robertson, P.K., 2010, Evaluation of flow liquefaction and liquefied strength using the CPT, Journal of Geotechnical and Geoenvironmental Engineering v. 136, n. 6, p. 842-853.

Schneider, J. A., Mayne, P. W., and Hendren, T. L., 1999, Initial development of an impulse piezovibrocone for liquefaction evaluation, Physics and Mechanics of Soil Liquefaction, Proceedings NSF Workshop, Johns Hopkins Univ., Balkema, Rotterdam p. 341-354.

Seed, H. B. and Idriss, I. M., 1971, Simplified procedure for evaluating soil liquefaction potential. Journal of the Soil Mechanics & Foundations Division (ASCE), v. 97 (SM9), p. 1249-1273.

Seed, H. B., and Idriss, I. M., 1981, Evaluation of liquefaction potential of sand deposits based on observations of performance in previous earthquakes, pre-print 81-544, Session on In-situ Testing to Evaluate Liquefaction Susceptibility, ASCE National Convention, St. Louis, Missouri, October 1981.

Seed, H.B., and Idriss, I.M., 1982, Ground motions and soil liquefaction during earthquakes, Earthquake Engineering Research Institute, Berkley, 134 p.

Al-Shukri, H., Mahdi, H. and Tuttle, M., 2006, Three-dimensional imaging of earthquake-induced liquefaction features with ground penetrating radar near Marianna, Arkansas, Seismological Research Letters, v. 77, p. 505-513.

Al-Shukri, H., Mahdi, H., Al Kadi, O., and Tuttle, M.P., 2009, Spatial and temporal characteristics of paleoseismic features in the southern terminus of the New Madrid seismic zone in eastern Arkansas, Final Technical Report to U.S. Geological Survey Earthquake Hazards Program, Award 1434-07HQGR0069, 24 p.

Al-Shukri, H., Mahdi, H., Tuttle, M.P., Dyer-Williams, K., 2015, Geophysical and paleoseismic investigations of large sand blows along a northwest-oriented lineament near Marianna, Arkansas, Final Technical Report, USGS Grant G12AP20093, 31 p.

Soller, D.R., and Reheis, M.C., 2004, Surficial materials in the conterminous United States, U.S. Geological Survey, Open-file Report 03-275, scale 1:5,000,000, *http://pubs.usgs.gov/of/2003/of03-275/*.

Stein, S., Liu, M., Calais, E., and Li, Q., 2009, Midcontinent earthquakes as a complex system, Seismological Research Letters, v. 80, p. 551-553.

Talma, A.S. and Vogel, J.C., 1993, A simplified approach to calibrating C14 dates, Radiocarbon, v. 35, p. 317-322.
Technical Report, 2012, The Central and Eastern U.S. seismic source characterization for nuclear facilities, U.S. Nuclear Regulatory Commission and Electric Power Research Institute, Palo Alto, CA.
Tuttle, M.P., 2005, Improving the earthquake chronology for the St. Louis region, U.S. Geological Survey, Earthquake Hazards Program, Annual Project Summary (05HQGR0045), 6 p.
Tuttle, M.P., 2010, Search for and study of sand blows at distant sites resulting from prehistoric and historic New Madrid earthquakes: Collaborative Research, M. Tuttle & Associates and Central Region Hazards Team, U.S. Geological Survey, Final Technical Report (02HQGR0097), 48 p.
Tuttle, M., Chester, J., Lafferty, R., Dyer-Williams, K., and Cande, B., 1999, Paleoseismology study northwest of the New Madrid seismic zone, U.S. Nuclear Regulatory Commission, NUREG/CR-5730, 98 p.
Tuttle, M.P., Schweig, E.S., Sims, J.D., Lafferty, R.H., Wolf, L.W., Haynes, M.L., 2002, The earthquake potential of the New Madrid seismic zone, Bulletin of the Seismological Society of America, v. 92, n. 6, p. 2080-2089.
Tuttle, M. and Chester, J.S., 2005, Paleoseismology study in the Cache River valley, southern Illinois, U.S. Geological Survey, Earthquake Hazards Program, Final Technical Report (HQ98GR00015), 14 p.
Tuttle, M.P., Schweig, E., III, Campbell, J., Thomas, P.M., Sims, J.D., and Lafferty, R.H., III, 2005, Evidence for New Madrid earthquakes in A.D. 300 and 2350 B.C., Seismological Research Letters, v. 76, n. 4, p. 489-501.
Tuttle, M.P., Al-Shukri, H, and Mahdi, H., 2006, Very large earthquakes centered southwest of the New Madrid seismic zone 5,000-7,000 years ago, Seismological Research Letters, v. 77, n. 6, p. 664-678.
Tuttle, M.P., and Hartleb, R., 2012, Appendix E. Central and eastern U.S. paleoliquefaction database, uncertainties associated with paleoliquefaction data, and guidance for seismic source characterization, *in* The Central and Eastern U.S. Seismic Source Characterization for Nuclear Facilities, Technical Report, EPRI, Palo Alto, CA, U.S. DOE, and U.S. NRC, 135 p., plus database.
Van Arsdale, R., Counts, R., and Woolery, E., 2009, Quaternary displacement along the Hovey Lake Fault of southern Indiana and western Kentucky, NEHRP Final report submitted to the U.S. Geological Survey, External Award 07-HQ-GR-0052, 11 p.
Vogel, J.C., Fuls, A., Visser, E., and Becker, B., 1993, Pretoria calibration curve for short-lived samples, Radiocarbon, v. 33, p. 73-86.
Woolery, E., 2005, Geophysical and geological evidence of neotectonic deformation along the Hovey Lake fault, lower Wabash Valley fault system, central United States, Bulletin of the Seismological Society of America, v. 95, p. 1193-1201.
Youd, T.L., et al., 2001, Liquefaction resistence of soils: Summary report from the 1996 NCEER and 1998 NCEER/NSF workshops on evaluation of liquefaction resistence of soils, Journal of Geotechnical and Geoenvironmental Engineering, v. 127, n. 10, p. 817-833.
Zoback, M.L., and Zoback, M.D., 1989, Tectonic stress field of the continental United States, in Pakiser, L. C., and Mooney, W. D., eds., Geophysical framework of the continental United States, Geological Society of America Memoir 172, p. 523-539.

BIBLIOGRAPHY OF RELATED PUBLICATIONS

Tuttle, M. P., and Dyer-Williams, K., 2017, Filling the gap in the paleoearthquake record between the New Madrid and Wabash Valley seismic zones, Seismological Research Letters-Eastern Section, *in preparation*.

APPENDIX A EVALUATION OF SCENARIO EARTHQUAKES RESULTS TABLES

A-1a. Evaluation of Local Scenario Earthquakes for Skillet Fork (1) GT 312 GMPEs (Atkinson, 2012) and Water Table Depth of 3 m.

Bridge/ Number	M @ Distance (km)	amax[1]	Boring	Sediment Depth (m)	Blow Count[2]	Cyclic Stress Ratio[3]	Results (NL, L)[4]
RT 600 E	M~5.5 @ 15	0.21	2S	8.2	3	0.20	L
	M~5.5 @ 15	0.21		8.8	2	0.21	L
	M~5.5 @ 15	0.21		9.8	5	0.21	N
	M~5.5 @ 15	0.21		10.4	2	0.21	L
	M~5.5 @ 15	0.21		11.3	2	0.21	L
	M~5.5 @ 15	0.21		11.9	5	0.21	L
	M~5.5 @ 15	0.21		13.4	11	0.20	N
	M~5.5 @ 15	0.21		14.3	6	0.20	N
	M~5.5 @ 15	0.21		15.0	13	0.19	N

A-1b. Evaluation of Local Scenario Earthquakes for Skillet Fork (1) GT 312 Using High GMPEs (Atkinson, 2012) and Water Table Depth of 3 m.

Bridge/ Number	M @ Distance (km)	amax[1]	Boring	Sediment Depth (m)	Blow Count[2]	Cyclic Stress Ratio[3]	Results (NL, L)[4]
Bridge/ Number	M @ Distance (km)	amax[1]	Boring	Sediment Depth (m)	Blow Count[2]	Cyclic Stress Ratio[3]	Results (NL, L)[4]
RT 600 E	M~5.5 @ 15	0.34	2S	8.2	3	0.33	L
	M~5.5 @ 15	0.34		8.8	2	0.33	L
	M~5.5 @ 15	0.34		9.8	5	0.34	L
	M~5.5 @ 15	0.34		10.4	2	0.34	L
	M~5.5 @ 15	0.34		11.3	2	0.34	L
	M~5.5 @ 15	0.34		11.9	5	0.34	L
	M~5.5 @ 15	0.34		13.4	11	0.33	L
	M~5.5 @ 15	0.34		14.3	6	0.32	L
	M~5.5 @ 15	0.34		15.0	13	0.31	N

1. amax = Maximum acceleration at ground surface;

2. Blow Count = Total number of blows required to drive split spoon sampler 0.3 m using standard hammer (63.5 kg) dropping 0.76 m;

3. Cyclic Stress Ratio = Stress causing liquefaction;

4. N= Liquefaction not likely; L = Liquefaction likely

A-2a. Evaluation of Vincennes Scenario Earthquakes for Skillet Fork (1) GT 312 Medium GMPEs (Atkinson, 2012) and Water Table Depth of 3 m.

Bridge/ Number	M @ Distance (km)	amax[1]	Boring	Sediment Depth (m)	Blow Count[2]	Cyclic Stress Ratio[3]	Results (NL, L)[4]
RT 600 E	M~7.3 @ 96	0.15	2S	8.2	3	0.14	L
	M~7.3 @ 96	0.15		8.8	2	0.15	L
	M~7.3 @ 96	0.15		9.8	5	0.15	L
	M~7.3 @ 96	0.15		10.4	2	0.15	L
	M~7.3 @ 96	0.15		11.3	2	0.15	L
	M~7.3 @ 96	0.15		11.9	5	0.15	L
	M~7.3 @ 96	0.15		13.4	11	0.14	L
	M~7.3 @ 96	0.15		14.3	6	0.14	L
	M~7.3 @ 96	0.15		15.0	13	0.14	L

A-2b. Evaluation of Vincennes Scenario Earthquakes for Skillet Fork (1) GT 312 Using High GMPEs (Atkinson, 2012) and Water Table Depth of 3 m.

Bridge/ Number	M @ Distance (km)	amax[1]	Boring	Sediment Depth (m)	Blow Count[2]	Cyclic Stress Ratio[3]	Results (NL, L)[4]
RT 600 E	M~7.3 @ 96	0.32	2S	8.2	3	0.30	L
	M~7.3 @ 96	0.32		8.8	2	0.31	L
	M~7.3 @ 96	0.32		9.8	5	0.31	L
	M~7.3 @ 96	0.32		10.4	2	0.31	L
	M~7.3 @ 96	0.32		11.3	2	0.31	L
	M~7.3 @ 96	0.32		11.9	5	0.31	L
	M~7.3 @ 96	0.32		13.4	11	0.30	L
	M~7.3 @ 96	0.32		14.3	6	0.30	L
	M~7.3 @ 96	0.32		15.0	13	0.29	L

1. amax = Maximum acceleration at ground surface;

2. Blow Count = Total number of blows required to drive split spoon sampler 0.3 m using standard hammer (63.5 kg) dropping 0.76 m;

3. Cyclic Stress Ratio = Stress causing liquefaction;

4. N= Liquefaction not likely; L = Liquefaction likely

A-3a. Evaluation of Skelton 1812 Scenario Earthquakes for Skillet Fork (1) GT 312 GMPEs (Atkinson, 2012) and Water Table Depth of 3 m.

Bridge/ Number	M @ Distance (km)	amax[1]	Boring	Sediment Depth (m)	Blow Count[2]	Cyclic Stress Ratio[3]	Results (NL, L)[4]
RT 600 E	M~6.7 @ 68	0.12	2S	8.2	3	0.12	L
	M~6.7 @ 68	0.12		8.8	2	0.12	L
	M~6.7 @ 68	0.12		9.8	5	0.12	N
	M~6.7 @ 68	0.12		10.4	2	0.12	L
	M~6.7 @ 68	0.12		11.3	2	0.12	L
	M~6.7 @ 68	0.12		11.9	5	0.12	L
	M~6.7 @ 68	0.12		13.4	11	0.12	N
	M~6.7 @ 68	0.12		14.3	6	0.12	N
	M~6.7 @ 68	0.12		15.0	13	0.11	N

A-3b. Evaluation of Skelton Scenario Earthquakes for Skillet Fork (1) GT 312 Using High GMPEs (Atkinson, 2012) and Water Table Depth of 3 m.

Bridge/ Number	M @ Distance (km)	amax[1]	Boring	Sediment Depth (m)	Blow Count[2]	Cyclic Stress Ratio[3]	Results (NL, L)[4]
RT 600 E	M~6.7 @ 68	0.20	2S	8.2	3	0.19	L
	M~6.7 @ 68	0.20		8.8	2	0.19	L
	M~6.7 @ 68	0.20		9.8	5	0.20	L
	M~6.7 @ 68	0.20		10.4	2	0.20	L
	M~6.7 @ 68	0.20		11.3	2	0.20	L
	M~6.7 @ 68	0.20		11.9	5	0.20	L
	M~6.7 @ 68	0.20		13.4	11	0.19	L
	M~6.7 @ 68	0.20		14.3	6	0.19	L
	M~6.7 @ 68	0.20		15.0	13	0.18	L

1. amax = Maximum acceleration at ground surface;
2. Blow Count = Total number of blows required to drive split spoon sampler 0.3 m using standard hammer (63.5 kg) dropping 0.76 m;
3. Cyclic Stress Ratio = Stress causing liquefaction;
4. N= Liquefaction not likely; L = Liquefaction likely

A-4a. Evaluation of January 23, 1812 Scenario Earthquakes for Skillet Fork (1) GT 312 Using Medium GMPEs (Atkinson, 2012) and Water Table Depth of 3 m.

Bridge/ Number	M @ Distance (km)	amax[1]	Boring	Sediment Depth (m)	Blow Count[2]	Cyclic Stress Ratio[3]	Results (NL, L)[4]
RT 600 E	M~6.8 @ 150	0.06	2S	8.2	3	0.06	N
	M~6.8 @ 150	0.06		8.8	2	0.06	N
	M~6.8 @ 150	0.06		9.8	5	0.06	N
	M~6.8 @ 150	0.06		10.4	2	0.06	N
	M~6.8 @ 150	0.06		11.3	2	0.06	N
	M~6.8 @ 150	0.06		11.9	5	0.06	N
	M~6.8 @ 150	0.06		13.4	11	0.06	N
	M~6.8 @ 150	0.06		14.3	6	0.06	N
	M~6.8 @ 150	0.06		15.0	13	0.06	N

A-4b. Evaluation of January 23, 1812 Scenario Earthquakes for Skillet (1) Fork GT 312 Using High GMPEs (Atkinson, 2012) and Water Table Depth of 3 m.

Bridge/ Number	M @ Distance (km)	amax[1]	Boring	Sediment Depth (m)	Blow Count[2]	Cyclic Stress Ratio[3]	Results (NL, L)[4]
RT 600 E	M~6.8 @ 150	0.10	2S	8.2	3	0.10	L
	M~6.8 @ 150	0.10		8.8	2	0.10	L
	M~6.8 @ 150	0.10		9.8	5	0.10	N
	M~6.8 @ 150	0.10		10.4	2	0.10	L
	M~6.8 @ 150	0.10		11.3	2	0.10	L
	M~6.8 @ 150	0.10		11.9	5	0.10	N
	M~6.8 @ 150	0.10		13.4	11	0.10	N
	M~6.8 @ 150	0.10		14.3	6	0.10	N
	M~6.8 @ 150	0.10		15.0	13	0.09	N

1. amax = Maximum acceleration at ground surface;

2. Blow Count = Total number of blows required to drive split spoon sampler 0.3 m using standard hammer (63.5 kg) dropping 0.76 m;

3. Cyclic Stress Ratio = Stress causing liquefaction;

4. N= Liquefaction not likely; L = Liquefaction likely

A-5a. Evaluation of January 23, 1812 Scenario Earthquakes for Skillet Fork (1) GT 312 Using Medium (Atkinson, 2012) and Water Table Depth of 3 m.

Bridge/ Number	M @ Distance (km)	amax[1]	Boring	Sediment Depth (m)	Blow Count[2]	Cyclic Stress Ratio[3]	Results (NL, L)[4]
RT 600 E	M~6.8 @ 155	0.06	2S	8.2	3	0.06	N
	M~6.8 @ 155	0.06		8.8	2	0.06	N
	M~6.8 @ 155	0.06		9.8	5	0.06	N
	M~6.8 @ 155	0.06		10.4	2	0.06	N
	M~6.8 @ 155	0.06		11.3	2	0.06	N
	M~6.8 @ 155	0.06		11.9	5	0.06	N
	M~6.8 @ 155	0.06		13.4	11	0.06	N
	M~6.8 @ 155	0.06		14.3	6	0.06	N
	M~6.8 @ 155	0.06		15.0	13	0.06	N

A-5b. Evaluation of January 23, 1812 Scenario Earthquakes for Skillet Fork (1) GT 312 Using High GMPEs (Atkinson, 2012) and Water Table Depth of 3 m.

Bridge/ Number	M @ Distance (km)	amax[1]	Boring	Sediment Depth (m)	Blow Count[2]	Cyclic Stress Ratio[3]	Results (NL, L)[4]
RT 600 E	M~6.8 @ 155	0.11	2S	8.2	3	0.10	L
	M~6.8 @ 155	0.11		8.8	2	0.10	L
	M~6.8 @ 155	0.11		9.8	5	0.11	N
	M~6.8 @ 155	0.11		10.4	2	0.11	L
	M~6.8 @ 155	0.11		11.3	2	0.11	L
	M~6.8 @ 155	0.11		11.9	5	0.11	L
	M~6.8 @ 155	0.11		13.4	11	0.10	N
	M~6.8 @ 155	0.11		14.3	6	0.10	N
	M~6.8 @ 155	0.11		15.0	13	0.10	N

1. amax = Maximum acceleration at ground surface;

2. Blow Count = Total number of blows required to drive split spoon sampler 0.3 m using standard hammer (63.5 kg) dropping 0.76 m;

3. Cyclic Stress Ratio = Stress causing liquefaction;

4. N= Liquefaction not likely; L = Liquefaction likely

A-6a. Evaluation of February 7, 1812 Scenario Earthquakes for Skillet Fork (1) GT 312 Using Medium GMPEs (Atkinson, 2012) and Water Table Depth of 3 m.

Bridge/ Number	M @ Distance (km)	amax[1]	Boring	Sediment Depth (m)	Blow Count[2]	Cyclic Stress Ratio[3]	Results (NL, L)[4]
RT 600 E	M~7.8 @ 235	0.08	2S	8.2	3	0.08	N
	M~7.8 @ 235	0.08		8.8	2	0.08	N
	M~7.8 @ 235	0.08		9.8	5	0.08	N
	M~7.8 @ 235	0.08		10.4	2	0.08	N
	M~7.8 @ 235	0.08		11.3	2	0.08	N
	M~7.8 @ 235	0.08		11.9	5	0.08	N
	M~7.8 @ 235	0.08		13.4	11	0.08	N
	M~7.8 @ 235	0.08		14.3	6	0.08	N
	M~7.8 @ 235	0.08		15.0	13	0.07	N

A-6b. Evaluation of February 7, 1812 Scenario Earthquakes for Skillet Fork (1) GT 312 Using High GMPEs (Atkinson, 2012) and Water Table Depth of 3 m.

Bridge/ Number	M @ Distance (km)	amax[1]	Boring	Sediment Depth (m)	Blow Count[2]	Cyclic Stress Ratio[3]	Results (NL, L)[4]
RT 600 E	M~7.8 @ 235	0.13	2S	8.2	3	0.12	L
	M~7.8 @ 235	0.13		8.8	2	0.13	L
	M~7.8 @ 235	0.13		9.8	5	0.13	N
	M~7.8 @ 235	0.13		10.4	2	0.13	L
	M~7.8 @ 235	0.13		11.3	2	0.13	L
	M~7.8 @ 235	0.13		11.9	5	0.13	L
	M~7.8 @ 235	0.13		13.4	11	0.12	N
	M~7.8 @ 235	0.13		14.3	6	0.12	L
	M~7.8 @ 235	0.13		15.0	13	0.12	N

1. amax = Maximum acceleration at ground surface;

2. Blow Count = Total number of blows required to drive split spoon sampler 0.3 m using standard hammer (63.5 kg) dropping 0.76 m;

3. Cyclic Stress Ratio = Stress causing liquefaction;

4. N= Liquefaction not likely; L = Liquefaction likely

A-7a. Evaluation of Local Scenario Earthquakes for Skillet Fork GT (1) 312 Using Medium GMPEs (Atkinson, 2012) and Water Table Depth of 5 m.

Bridge/ Number	M @ Distance (km)	amax[1]	Boring	Sediment Depth (m)	Blow Count[2]	Cyclic Stress Ratio[3]	Results (NL, L)[4]
RT 600 E	M~5.5 @ 15	0.21	2S	8.2	3	0.17	N
	M~5.5 @ 15	0.21		8.8	2	0.17	L
	M~5.5 @ 15	0.21		9.8	5	0.17	N
	M~5.5 @ 15	0.21		10.4	2	0.18	N
	M~5.5 @ 15	0.21		11.3	2	0.18	L
	M~5.5 @ 15	0.21		11.9	5	0.18	N
	M~5.5 @ 15	0.21		13.4	11	0.18	N
	M~5.5 @ 15	0.21		14.3	6	0.17	N
	M~5.5 @ 15	0.21		15.0	13	0.17	N

A-7b. Evaluation of Local Scenario Earthquakes for Skillet Fork (1) GT 312 Using High GMPEs (Atkinson, 2012) and Water Table Depth of 5 m.

Bridge/ Number	M @ Distance (km)	amax[1]	Boring	Sediment Depth (m)	Blow Count[2]	Cyclic Stress Ratio[3]	Results (NL, L)[4]
Bridge/ Number	**M @ Distance (km)**	**amax[1]**	**Boring**	**Sediment Depth (m)**	**Blow Count[2]**	**Cyclic Stress Ratio[3]**	**Results (NL, L)[4]**
RT 600 E	M~5.5 @ 15	0.34	2S	8.2	3	0.27	L
	M~5.5 @ 15	0.34		8.8	2	0.28	L
	M~5.5 @ 15	0.34		9.8	5	0.28	L
	M~5.5 @ 15	0.34		10.4	2	0.29	L
	M~5.5 @ 15	0.34		11.3	2	0.29	L
	M~5.5 @ 15	0.34		11.9	5	0.29	L
	M~5.5 @ 15	0.34		13.4	11	0.28	N
	M~5.5 @ 15	0.34		14.3	6	0.28	L
	M~5.5 @ 15	0.34		15.0	13	0.27	N

1. amax = Maximum acceleration at ground surface;

2. Blow Count = Total number of blows required to drive split spoon sampler 0.3 m using standard hammer (63.5 kg) dropping 0.76 m;

3. Cyclic Stress Ratio = Stress causing liquefaction;

4. N= Liquefaction not likely; L = Liquefaction likely

A-8a. Evaluation of Vincennes Scenario Earthquakes for Skillet Fork (1) GT 312 Using Medium GMPEs (Atkinson, 2012) and Water Table Depth of 5 m.

Bridge/ Number	M @ Distance (km)	amax[1]	Boring	Sediment Depth (m)	Blow Count[2]	Cyclic Stress Ratio[3]	Results (NL, L)[4]
RT 600 E	M~7.3 @ 96	0.15	2S	8.2	3	0.12	L
	M~7.3 @ 96	0.15		8.8	2	0.12	L
	M~7.3 @ 96	0.15		9.8	5	0.12	L
	M~7.3 @ 96	0.15		10.4	2	0.12	L
	M~7.3 @ 96	0.15		11.3	2	0.13	L
	M~7.3 @ 96	0.15		11.9	5	0.13	L
	M~7.3 @ 96	0.15		13.4	11	0.12	L
	M~7.3 @ 96	0.15		14.3	6	0.12	L
	M~7.3 @ 96	0.15		15.0	13	0.12	N

A-8b. Evaluation of Vincennes Scenario Earthquakes for Skillet Fork (1) GT 312 Using High GMPEs (Atkinson, 2012) and Water Table Depth of 5 m.

Bridge/ Number	M @ Distance (km)	amax[1]	Boring	Sediment Depth (m)	Blow Count[2]	Cyclic Stress Ratio[3]	Results (NL, L)[4]
	M~7.3 @ 96	0.32		8.8	2	0.25	L
	M~7.3 @ 96	0.32		9.8	5	0.26	L
	M~7.3 @ 96	0.32		10.4	2	0.26	L
	M~7.3 @ 96	0.32		11.3	2	0.27	L
	M~7.3 @ 96	0.32		11.9	5	0.27	L
	M~7.3 @ 96	0.32		13.4	11	0.26	L
	M~7.3 @ 96	0.32		14.3	6	0.26	L
	M~7.3 @ 96	0.32		15.0	13	0.25	L

1. amax = Maximum acceleration at ground surface;

2. Blow Count = Total number of blows required to drive split spoon sampler 0.3 m using standard hammer (63.5 kg) dropping 0.76 m;

3. Cyclic Stress Ratio = Stress causing liquefaction;

4. N= Liquefaction not likely; L = Liquefaction likely

A-9a. Evaluation of Skelton Scenario Earthquakes for Skillet Fork (1) GT 312 Using Medium GMPEs (Atkinson, 2012) and Water Table Depth of 5 m.

Bridge/ Number	M @ Distance (km)	amax[1]	Boring	Sediment Depth (m)	Blow Count[2]	Cyclic Stress Ratio[3]	Results (NL, L)[4]
RT 600 E	M~6.7 @ 68	0.12	2S	8.2	3	0.10	L
	M~6.7 @ 68	0.12		8.8	2	0.10	L
	M~6.7 @ 68	0.12		9.8	5	0.10	N
	M~6.7 @ 68	0.12		10.4	2	0.10	N
	M~6.7 @ 68	0.12		11.3	2	0.10	L
	M~6.7 @ 68	0.12		11.9	5	0.10	N
	M~6.7 @ 68	0.12		13.4	11	0.10	N
	M~6.7 @ 68	0.12		14.3	6	0.10	N
	M~6.7 @ 68	0.12		15.0	13	0.10	N

A-9b. Evaluation of Skelton Scenario Earthquakes for Skillet Fork (1) GT 312 Using High GMPEs (Atkinson, 2012) and Water Table Depth of 5 m.

Bridge/ Number	M @ Distance (km)	amax[1]	Boring	Sediment Depth (m)	Blow Count[2]	Cyclic Stress Ratio[3]	Results (NL, L)[4]
RT 600 E	M~6.7 @ 68	0.20	2S	8.2	3	0.16	L
	M~6.7 @ 68	0.20		8.8	2	0.16	L
	M~6.7 @ 68	0.20		9.8	5	0.16	L
	M~6.7 @ 68	0.20		10.4	2	0.17	L
	M~6.7 @ 68	0.20		11.3	2	0.17	L
	M~6.7 @ 68	0.20		11.9	5	0.17	L
	M~6.7 @ 68	0.20		13.4	11	0.17	L
	M~6.7 @ 68	0.20		14.3	6	0.16	L
	M~6.7 @ 68	0.20		15.0	13	0.16	N

1. amax = Maximum acceleration at ground surface;
2. Blow Count = Total number of blows required to drive split spoon sampler 0.3 m using standard hammer (63.5 kg) dropping 0.76 m;
3. Cyclic Stress Ratio = Stress causing liquefaction;
4. N= Liquefaction not likely; L = Liquefaction likely

A-10a. Evaluation of January 23, 1812 Scenario Earthquakes for Skillet (1) Fork GT 312 Using Medium GMPEs (Atkinson, 2012) and Water Table Depth of 5 m.

Bridge/ Number	M @ Distance (km)	amax[1]	Boring	Sediment Depth (m)	Blow Count[2]	Cyclic Stress Ratio[3]	Results (NL, L)[4]
RT 600 E	M~6.8 @ 150	0.06	2S	8.2	3	0.05	N
	M~6.8 @ 150	0.06		8.8	2	0.05	N
	M~6.8 @ 150	0.06		9.8	5	0.05	N
	M~6.8 @ 150	0.06		10.4	2	0.05	N
	M~6.8 @ 150	0.06		11.3	2	0.05	N
	M~6.8 @ 150	0.06		11.9	5	0.05	N
	M~6.8 @ 150	0.06		13.4	11	0.05	N
	M~6.8 @ 150	0.06		14.3	6	0.05	N
	M~6.8 @ 150	0.06		15.0	13	0.05	N

A-10b. Evaluation of January 23, 1812 Scenario Earthquakes for Skillet Fork (1) GT 312 Using High GMPEs (Atkinson, 2012) and Water Table Depth of 5 m.

Bridge/ Number	M @ Distance (km)	amax[1]	Boring	Sediment Depth (m)	Blow Count[2]	Cyclic Stress Ratio[3]	Results (NL, L)[4]
RT 600 E	M~6.8 @ 150	0.10	2S	8.2	3	0.08	N
	M~6.8 @ 150	0.10		8.8	2	0.08	N
	M~6.8 @ 150	0.10		9.8	5	0.08	N
	M~6.8 @ 150	0.10		10.4	2	0.09	N
	M~6.8 @ 150	0.10		11.3	2	0.09	L
	M~6.8 @ 150	0.10		11.9	5	0.09	N
	M~6.8 @ 150	0.10		13.4	11	0.09	N
	M~6.8 @ 150	0.10		14.3	6	0.08	N
	M~6.8 @ 150	0.10		15.0	13	0.08	N

1. amax = Maximum acceleration at ground surface;
2. Blow Count = Total number of blows required to drive split spoon sampler 0.3 m using standard hammer (63.5 kg) dropping 0.76 m;
3. Cyclic Stress Ratio = Stress causing liquefaction;
4. N= Liquefaction not likely; L = Liquefaction likely

A-11a. Evaluation of January 23, 1812 Scenario Earthquakes for Skillet Fork (1)GT 312 Using Medium GMPEs (Atkinson, 2012) and Water Table Depth of 5 m.

Bridge/ Number	M @ Distance (km)	amax[1]	Boring	Sediment Depth (m)	Blow Count[2]	Cyclic Stress Ratio[3]	Results (NL, L)[4]
RT 600 E	M~6.8 @ 155	0.06	2S	8.2	3	0.05	N
	M~6.8 @ 155	0.06		8.8	2	0.05	N
	M~6.8 @ 155	0.06		9.8	5	0.05	N
	M~6.8 @ 155	0.06		10.4	2	0.05	N
	M~6.8 @ 155	0.06		11.3	2	0.05	N
	M~6.8 @ 155	0.06		11.9	5	0.05	N
	M~6.8 @ 155	0.06		13.4	11	0.05	N
	M~6.8 @ 155	0.06		14.3	6	0.05	N
	M~6.8 @ 155	0.06		15.0	13	0.05	N

A-11b. Evaluation of January 23, 1812 Scenario Earthquakes for Skillet Fork (1) GT 312 Using High GMPEs (Atkinson, 2012) and Water Table Depth of 5 m.

Bridge/ Number	M @ Distance (km)	amax[1]	Boring	Sediment Depth (m)	Blow Count[2]	Cyclic Stress Ratio[3]	Results (NL, L)[4]
RT 600 E	M~6.8 @ 155	0.11	2S	8.2	3	0.08	N
	M~6.8 @ 155	0.11		8.8	2	0.09	L
	M~6.8 @ 155	0.11		9.8	5	0.09	N
	M~6.8 @ 155	0.11		10.4	2	0.09	N
	M~6.8 @ 155	0.11		11.3	2	0.09	L
	M~6.8 @ 155	0.11		11.9	5	0.09	N
	M~6.8 @ 155	0.11		13.4	11	0.09	N
	M~6.8 @ 155	0.11		14.3	6	0.09	N
	M~6.8 @ 155	0.11		15.0	13	0.09	N

1. amax = Maximum acceleration at ground surface;
2. Blow Count = Total number of blows required to drive split spoon sampler 0.3 m using standard hammer (63.5 kg) dropping 0.76 m;
3. Cyclic Stress Ratio = Stress causing liquefaction;
4. N= Liquefaction not likely; L = Liquefaction likely

A-12a. Evaluation of February 7, Scenario Earthquakes for Skillet Fork (1) GT 312 Using Medium GMPEs (Atkinson, 2012) and Water Table Depth of 5 m.

Bridge/ Number	M @ Distance (km)	amax[1]	Boring	Sediment Depth (m)	Blow Count[2]	Cyclic Stress Ratio[3]	Results (NL, L)[4]
RT 600 E	M~7.8 @ 235	0.08	2S	8.2	3	0.06	N
	M~7.8 @ 235	0.08		8.8	2	0.07	N
	M~7.8 @ 235	0.08		9.8	5	0.07	N
	M~7.8 @ 235	0.08		10.4	2	0.07	N
	M~7.8 @ 235	0.08		11.3	2	0.07	N
	M~7.8 @ 235	0.08		11.9	5	0.07	N
	M~7.8 @ 235	0.08		13.4	11	0.07	N
	M~7.8 @ 235	0.08		14.3	6	0.07	N
	M~7.8 @ 235	0.08		15.0	13	0.07	N

A-12b. Evaluation of February 7, Scenario Earthquakes for Skillet Fork (1) GT 312 Using High GMPEs (Atkinson, 2012) and Water Table Depth of 5 m.

Bridge/ Number	M @ Distance (km)	amax[1]	Boring	Sediment Depth (m)	Blow Count[2]	Cyclic Stress Ratio[3]	Results (NL, L)[4]
RT 600 E	M~7.8 @ 235	0.13	2S	8.2	3	0.10	L
	M~7.8 @ 235	0.13		8.8	2	0.10	L
	M~7.8 @ 235	0.13		9.8	5	0.11	N
	M~7.8 @ 235	0.13		10.4	2	0.11	L
	M~7.8 @ 235	0.13		11.3	2	0.11	L
	M~7.8 @ 235	0.13		11.9	5	0.11	L
	M~7.8 @ 235	0.13		13.4	11	0.11	N
	M~7.8 @ 235	0.13		14.3	6	0.11	N
	M~7.8 @ 235	0.13		15.0	13	0.10	N

1. amax = Maximum acceleration at ground surface;

2. Blow Count = Total number of blows required to drive split spoon sampler 0.3 m using standard hammer (63.5 kg) dropping 0.76 m;

3. Cyclic Stress Ratio = Stress causing liquefaction;

4. N= Liquefaction not likely; L = Liquefaction likely

A-13a. Evaluation of Local Scenario Earthquakes for Skillet Fork (2) GT 313 Using Medium GMPEs (Atkinson, (2012) and Water Table Depth of 3 m.

Bridge/ Number	M @ Distance (km)	amax[1]	Boring	Sediment Depth (m)	Blow Count[2]	Cyclic Stress Ratio[3]	Results (NL, L)[4]
RT 600 N	M~5.5 @ 15	0.21	2	7.6	3	0.19	L
	M~5.5 @ 15	0.21		8.2	13	0.20	N
	M~5.5 @ 15	0.21		9.1	10	0.20	N

A-13b. Evaluation of Local Scenario Earthquakes for Skillet Fork (2) GT 313 Using High GMPEs (Atkinson, 2012) and Water Table Depth of 3 m.

Bridge/ Number	M @ Distance (km)	amax[1]	Boring	Sediment Depth (m)	Blow Count[2]	Cyclic Stress Ratio[3]	Results (NL, L)[4]
RT 600 N	M~5.5 @ 15	0.34	2	7.6	3	0.31	L
	M~5.5 @ 15	0.34		8.2	13	0.32	N
	M~5.5 @ 15	0.34		9.1	10	0.32	L

1. amax = Maximum acceleration at ground surface;

2. Blow Count = Total number of blows required to drive split spoon sampler 0.3 m using standard hammer (63.5 kg) dropping 0.76 m;

3. Cyclic Stress Ratio = Stress causing liquefaction;

4. N= Liquefaction not likely; L = Liquefaction likely

A-14a. Evaluation of Vincennes Scenario Earthquakes for Skillet Fork (2) GT 313 Using Medium GMPEs (Atkinson, 2012) and Water Table Depth of 3 m.

Bridge/ Number	M @ Distance (km)	amax[1]	Boring	Sediment Depth (m)	Blow Count[2]	Cyclic Stress Ratio[3]	Results (NL, L)[4]
RT 600 N	M~7.3 @ 96	0.15	2	7.6	3	0.14	L
	M~7.3 @ 96	0.15		8.2	13	0.14	N
	M~7.3 @ 96	0.15		9.1	10	0.14	L

A-14b. Evaluation of Vincennes Scenario Earthquakes for Skillet Fork (2) GT 313 Using High GMPEs (Atkinson, 2012) and Water Table Depth of 3 m.

Bridge/ Number	M @ Distance (km)	amax[1]	Boring	Sediment Depth (m)	Blow Count[2]	Cyclic Stress Ratio[3]	Results (NL, L)[4]
RT 600 N	M~7.3 @ 96	0.32	2	7.6	3	0.29	L
	M~7.3 @ 96	0.32		8.2	13	0.29	L
	M~7.3 @ 96	0.32		9.1	10	0.30	L

1. amax = Maximum acceleration at ground surface;

2. Blow Count = Total number of blows required to drive split spoon sampler 0.3 m using standard hammer (63.5 kg) dropping 0.76 m;

3. Cyclic Stress Ratio = Stress causing liquefaction;

4. N= Liquefaction not likely; L = Liquefaction likely

A-15a. Evaluation of Skelton Scenario Earthquakes for Skillet Fork (2) GT 313 Using Medium GMPEs (Atkinson, 2012) and Water Table Depth of 3 m.

Bridge/ Number	M @ Distance (km)	amax[1]	Boring	Sediment Depth (m)	Blow Count[2]	Cyclic Stress Ratio[3]	Results (NL, L)[4]
RT 600 N	M~6.7 @ 68	0.12	2	7.6	3	0.11	L
	M~6.7 @ 68	0.12		8.2	13	0.11	N
	M~6.7 @ 68	0.12		9.1	10	0.12	N

A-15b. Evaluation of Skelton Scenario Earthquakes for Skillet Fork (2) GT 313 Using High GMPEs (Atkinson, 2012) and Water Table Depth of 3 m.

Bridge/ Number	M @ Distance (km)	amax[1]	Boring	Sediment Depth (m)	Blow Count[2]	Cyclic Stress Ratio[3]	Results (NL, L)[4]
RT 600 N	M~6.7 @ 68	0.20	2	7.6	3	0.18	L
	M~6.7 @ 68	0.20		8.2	13	0.19	N
	M~6.7 @ 68	0.20		9.1	10	0.19	L

1. amax = Maximum acceleration at ground surface;

2. Blow Count = Total number of blows required to drive split spoon sampler 0.3 m using standard hammer (63.5 kg) dropping 0.76 m;

3. Cyclic Stress Ratio = Stress causing liquefaction;

4. N= Liquefaction not likely; L = Liquefaction likely

A-16a. Evaluation of January 23, 1812 Scenario Earthquakes for Skillet Fork (2) GT 313 Using Medium (Atkinson, 2012) and Water Table Depth of 3 m.

Bridge/ Number	M @ Distance (km)	amax[1]	Boring	Sediment Depth (m)	Blow Count[2]	Cyclic Stress Ratio[3]	Results (NL, L)[4]
RT 600 N	M~6.8 @ 150	0.06	2	7.6	3	0.05	N
	M~6.8 @ 150	0.06		8.2	13	0.05	N
	M~6.8 @ 150	0.06		9.1	10	0.05	N

A-16b. Evaluation of January 23, 1812 Scenario Earthquakes for Skillet Fork (2) GT 313 Using High (Atkinson, 2012) and Water Table Depth of 3 m.

Bridge/ Number	M @ Distance (km)	amax[1]	Boring	Sediment Depth (m)	Blow Count[2]	Cyclic Stress Ratio[3]	Results (NL, L)[4]
RT 600 N	M~6.8 @ 150	0.10	2	7.6	3	0.09	L
	M~6.8 @ 150	0.10		8.2	13	0.10	N
	M~6.8 @ 150	0.10		9.1	10	0.10	N

1. amax = Maximum acceleration at ground surface;

2. Blow Count = Total number of blows required to drive split spoon sampler 0.3 m using standard hammer (63.5 kg) dropping 0.76 m;

3. Cyclic Stress Ratio = Stress causing liquefaction;

4. N= Liquefaction not likely; L = Liquefaction likely

A-17a. Evaluation of January 23, 1812 Scenario Earthquakes for Skillet Fork (2) GT 313 Using Medium (Atkinson, 2012) and Water Table Depth of 3 m.

Bridge/ Number	M @ Distance (km)	amax[1]	Boring	Sediment Depth (m)	Blow Count[2]	Cyclic Stress Ratio[3]	Results (NL, L)[4]
RT 600 N	M~6.8 @ 155	0.06	2	7.6	3	0.06	N
	M~6.8 @ 155	0.06		8.2	13	0.06	N
	M~6.8 @ 155	0.06		9.1	10	0.06	N

A-17b. Evaluation of January 23, 1812 Scenario Earthquakes for Skillet Fork (2) GT 313 Using High (Atkinson, 2012) and Water Table Depth of 3 m.

Bridge/ Number	M @ Distance (km)	amax[1]	Boring	Sediment Depth (m)	Blow Count[2]	Cyclic Stress Ratio[3]	Results (NL, L)[4]
RT 600 N	M~6.8 @ 155	0.11	2	7.6	3	0.10	L
	M~6.8 @ 155	0.11		8.2	13	0.10	N
	M~6.8 @ 155	0.11		9.1	10	0.10	N

1. amax = Maximum acceleration at ground surface;

2. Blow Count = Total number of blows required to drive split spoon sampler 0.3 m using standard hammer (63.5 kg) dropping 0.76 m;

3. Cyclic Stress Ratio = Stress causing liquefaction;

4. N= Liquefaction not likely; L = Liquefaction likely

A-18a. Evaluation of February 7, 1812 Scenario Earthquakes for Skillet Fork (2) GT 313 Using Medium GMPEs (Atkinson, 2012) and Water Table Depth of 3 m.

Bridge/ Number	M @ Distance (km)	amax[1]	Boring	Sediment Depth (m)	Blow Count[2]	Cyclic Stress Ratio[3]	Results (NL, L)[4]
RT 600 N	M~7.8 @ 235	0.08	2	7.6	3	0.08	L
	M~7.8 @ 235	0.08		8.2	13	0.08	N
	M~7.8 @ 235	0.08		9.1	10	0.08	N

A-18b. Evaluation of February 7, 1812 Scenario Earthquakes for Skillet Fork (2) GT 313 Using High GMPEs (Atkinson, 2012) and Water Table Depth of 3 m.

Bridge/ Number	M @ Distance (km)	amax[1]	Boring	Sediment Depth (m)	Blow Count[2]	Cyclic Stress Ratio[3]	Results (NL, L)[4]
RT 600 N	M~7.8 @ 235	0.13	2	7.6	3	0.12	L
	M~7.8 @ 235	0.13		8.2	13	0.12	L
	M~7.8 @ 235	0.13		9.1	10	0.12	L

1. amax = Maximum acceleration at ground surface;

2. Blow Count = Total number of blows required to drive split spoon sampler 0.3 m using standard hammer (63.5 kg) dropping 0.76 m;

3. Cyclic Stress Ratio = Stress causing liquefaction;

4. N= Liquefaction not likely; L = Liquefaction likely

A-19a. Evaluation of Local Scenario Earthquakes for Skillet Fork (2) GT 313 Using Medium GMPEs (Atkinson, 2012) and Water Table Depth of 5 m.

Bridge/ Number	M @ Distance (km)	amax[1]	Boring	Sediment Depth (m)	Blow Count[2]	Cyclic Stress Ratio[3]	Results (NL, L)[4]
RT 600 N	M~5.5 @ 15	0.21	2	7.6	3	0.16	N
	M~5.5 @ 15	0.21		8.2	13	0.16	N
	M~5.5 @ 15	0.21		9.1	10	0.17	N

A-19b. Evaluation of Local Scenario Earthquakes for Skillet Fork (2) GT 313 Using High GMPEs (Atkinson, 2012) and Water Table Depth of 5 m.

Bridge/ Number	M @ Distance (km)	amax[1]	Boring	Sediment Depth (m)	Blow Count[2]	Cyclic Stress Ratio[3]	Results (NL, L)[4]
RT 600 N	M~5.5 @ 15	0.34	2	7.6	3	0.26	L
	M~5.5 @ 15	0.34		8.2	13	0.26	N
	M~5.5 @ 15	0.34		9.1	10	0.27	N

1. amax = Maximum acceleration at ground surface;

2. Blow Count = Total number of blows required to drive split spoon sampler 0.3 m using standard hammer (63.5 kg) dropping 0.76 m;

3. Cyclic Stress Ratio = Stress causing liquefaction;

4. N= Liquefaction not likely; L = Liquefaction likely

A-20a. Evaluation of Vincennes Scenario Earthquakes for Skillet Fork (2) GT 313 Using Medium GMPEs (Atkinson, 2012) and Water Table Depth of 5 m.

Bridge/ Number	M @ Distance (km)	amax[1]	Boring	Sediment Depth (m)	Blow Count[2]	Cyclic Stress Ratio[3]	Results (NL, L)[4]
RT 600 N	M~7.3 @ 96	0.15	2	7.6	3	0.11	L
	M~7.3 @ 96	0.15		8.2	13	0.12	N
	M~7.3 @ 96	0.15		9.1	10	0.12	L

A-20b. Evaluation of Vincennes Scenario Earthquakes for Skillet Fork (2) GT 313 Using High GMPEs (Atkinson, 2012) and Water Table Depth of 5 m.

Bridge/ Number	M @ Distance (km)	amax[1]	Boring	Sediment Depth (m)	Blow Count[2]	Cyclic Stress Ratio[3]	Results (NL, L)[4]
RT 600 N	M~7.3 @ 96	0.32	2	7.6	3	0.24	L
	M~7.3 @ 96	0.32		8.2	13	0.24	L
	M~7.3 @ 96	0.32		9.1	10	0.25	L

1. amax = Maximum acceleration at ground surface;

2. Blow Count = Total number of blows required to drive split spoon sampler 0.3 m using standard hammer (63.5 kg) dropping 0.76 m;

3. Cyclic Stress Ratio = Stress causing liquefaction;

4. N = Liquefaction not likely; L = Liquefaction likely

A-21a. Evaluation of Skelton Scenario Earthquakes for Skillet Fork (2) GT 313 Using Medium GMPEs (Atkinson, 2012) and Water Table Depth of 5 m.

Bridge/ Number	M @ Distance (km)	amax[1]	Boring	Sediment Depth (m)	Blow Count[2]	Cyclic Stress Ratio[3]	Results (NL, L)[4]
RT 600 N	M~6.7 @ 68	0.12	2	7.6	3	0.09	N
	M~6.7 @ 68	0.12		8.2	13	0.10	N
	M~6.7 @ 68	0.12		9.1	10	0.10	N

A-21b. Evaluation of Skelton Scenario Earthquakes for Skillet Fork (2) GT 313 Using High GMPEs (Atkinson, 2012) and Water Table Depth of 5 m.

Bridge/ Number	M @ Distance (km)	amax[1]	Boring	Sediment Depth (m)	Blow Count[2]	Cyclic Stress Ratio[3]	Results (NL, L)[4]
RT 600 N	M~6.7 @ 68	0.20	2	7.6	3	0.15	L
	M~6.7 @ 68	0.20		8.2	13	0.15	N
	M~6.7 @ 68	0.20		9.1	10	0.16	L

1. amax = Maximum acceleration at ground surface;

2. Blow Count = Total number of blows required to drive split spoon sampler 0.3 m using standard hammer (63.5 kg) dropping 0.76 m;

3. Cyclic Stress Ratio = Stress causing liquefaction;

4. N= Liquefaction not likely; L = Liquefaction likely

A-22a. Evaluation of January 23, 1812 Scenario Earthquakes for Skillet Fork (2) GT 313 Using Medium (Atkinson, 2012) and Water Table Depth of 5 m.

Bridge/ Number	M @ Distance (km)	amax[1]	Boring	Sediment Depth (m)	Blow Count[2]	Cyclic Stress Ratio[3]	Results (NL, L)[4]
RT 600 N	M~6.8 @ 150	0.06	2	7.6	3	0.05	N
	M~6.8 @ 150	0.06		8.2	13	0.05	N
	M~6.8 @ 150	0.06		9.1	10	0.05	N

A-22b. Evaluation of January 23, 1812 Scenario Earthquakes for Skillet Fork (2) GT 313 Using High (Atkinson, 2012) and Water Table Depth of 5 m.

Bridge/ Number	M @ Distance (km)	amax[1]	Boring	Sediment Depth (m)	Blow Count[2]	Cyclic Stress Ratio[3]	Results (NL, L)[4]
RT 600 N	M~6.8 @ 150	0.10	2	7.6	3	0.08	N
	M~6.8 @ 150	0.10		8.2	13	0.08	N
	M~6.8 @ 150	0.10		9.1	10	0.08	N

1. amax = Maximum acceleration at ground surface;

2. Blow Count = Total number of blows required to drive split spoon sampler 0.3 m using standard hammer (63.5 kg) dropping 0.76 m;

3. Cyclic Stress Ratio = Stress causing liquefaction;

4. N= Liquefaction not likely; L = Liquefaction likely

A-23a. Evaluation of January 23, 1812 Scenario Earthquakes for Skillet Fork (2) GT 313 Using Medium (Atkinson, 2012) and Water Table Depth of 5 m.

Bridge/ Number	M @ Distance (km)	amax[1]	Boring	Sediment Depth (m)	Blow Count[2]	Cyclic Stress Ratio[3]	Results (NL, L)[4]
RT 600 N	M~6.8 @ 155	0.06	2	7.6	3	0.05	N
	M~6.8 @ 155	0.06		8.2	13	0.05	N
	M~6.8 @ 155	0.06		9.1	10	0.05	N

A-23b. Evaluation of January 23, 1812 Scenario Earthquakes for Skillet Fork (2) GT 313 Using High (Atkinson, 2012) and Water Table Depth of 5 m.

Bridge/ Number	M @ Distance (km)	amax[1]	Boring	Sediment Depth (m)	Blow Count[2]	Cyclic Stress Ratio[3]	Results (NL, L)[4]
RT 600 N	M~6.8 @ 155	0.11	2	7.6	3	0.08	N
	M~6.8 @ 155	0.11		8.2	13	0.08	N
	M~6.8 @ 155	0.11		9.1	10	0.09	N

1. amax = Maximum acceleration at ground surface;

2. Blow Count = Total number of blows required to drive split spoon sampler 0.3 m using standard hammer (63.5 kg) dropping 0.76 m;

3. Cyclic Stress Ratio = Stress causing liquefaction;

4. N= Liquefaction not likely; L = Liquefaction likely

A-24a. Evaluation of February 7, 1812 Scenario Earthquakes for Skillet (2) Fork GT 313 Using Medium GMPEs (Atkinson, 2012) and Water Table Depth of 5 m.

Bridge/ Number	M @ Distance (km)	amax[1]	Boring	Sediment Depth (m)	Blow Count[2]	Cyclic Stress Ratio[3]	Results (NL, L)[4]
RT 600 N	M~7.8 @ 235	0.08	2	7.6	3	0.06	L
	M~7.8 @ 235	0.08		8.2	13	0.06	N
	M~7.8 @ 235	0.08		9.1	10	0.07	N

A-24b. Evaluation of February 7, Scenario Earthquakes for Skillet Fork (2) GT 313 Using High GMPEs (Atkinson, 2012) and Water Table Depth of 5 m.

Bridge/ Number	M @ Distance (km)	amax[1]	Boring	Sediment Depth (m)	Blow Count[2]	Cyclic Stress Ratio[3]	Results (NL, L)[4]
RT 600 N	M~7.8 @ 235	0.13	2	7.6	3	0.10	L
	M~7.8 @ 235	0.13		8.2	13	0.10	N
	M~7.8 @ 235	0.13		9.1	10	0.10	L

1. amax = Maximum acceleration at ground surface;

2. Blow Count = Total number of blows required to drive split spoon sampler 0.3 m using standard hammer (63.5 kg) dropping 0.76 m;

3. Cyclic Stress Ratio = Stress causing liquefaction;

4. N= Liquefaction not likely; L = Liquefaction likely

A-25a. Evaluation of Local Scenario Earthquakes for Saline River (3) GT 310 Using Medium GMPEs (Atkinson, 2012) and Water Table Depth of 3 m.

Bridge/ Number	M @ Distance (km)	amax[1]	Boring	Sediment Depth (m)	Blow Count[2]	Cyclic Stress Ratio[3]	Results (N, L)[4]
Richey	M 5.5 @ 15	0.21	1S	3.4	6	0.14	N
Road	M 5.5 @ 15	0.21		4.0	4	0.15	N
	M 5.5 @ 15	0.21		4.9	5	0.17	N
	M 5.5 @ 15	0.21		5.9	3	0.18	N
	M 5.5 @ 15	0.21		6.4	2	0.18	L
	M 5.5 @ 15	0.21		7.0	1		L
	M 5.5 @ 15	0.21		7.9	6	0.19	N
	M 5.5 @ 15	0.21		8.5	4	0.20	N
	M 5.5 @ 15	0.21		9.5	11	0.20	N
	M 5.5 @ 15	0.21		10.1	11	0.20	N

A-25b. Evaluation of Local Scenario Earthquakes for Saline River (3) GT 310 Using High GM (Atkinson, 2012) and Water Table Depth of 3 m.

Bridge/ Number	M @ Distance (km)	amax[1]	Boring	Sediment Depth (m)	Blow Count[2]	Cyclic Stress Ratio[3]	Results (N, L)[4]
Richey	M 5.5 @ 15	0.34	1S	3.4	6	0.23	N
Road	M 5.5 @ 15	0.34		4.0	4	0.25	N
	M 5.5 @ 15	0.34		4.9	5	0.27	L
	M 5.5 @ 15	0.34		5.9	3	0.29	L
	M 5.5 @ 15	0.34		6.4	2	0.30	L
	M 5.5 @ 15	0.34		7.0	1	0.30	L
	M 5.5 @ 15	0.34		7.9	6	0.31	L
	M 5.5 @ 15	0.34		8.5	4	0.32	L
	M 5.5 @ 15	0.34		9.5	11	0.32	N
	M 5.5 @ 15	0.34		10.1	11	0.32	N

1. amax = Maximum acceleration at ground surface;

2. Blow Count = Total number of blows required to drive split spoon sampler 0.3 m using standard hammer (63.5 kg) dropping 0.76 m;

3. Cyclic Stress Ratio = Stress causing liquefaction;

4. N= Liquefaction not likely; L = Liquefaction likely

A-26a. Evaluation of Vincennes Scenario Earthquakes for Saline River (3) GT 310 Using Medium GMPEs (Atkinson, 2012) and Water Table Depth of 3 m.

Bridge/ Number	M @ Distance (km)	amax[1]	Boring	Sediment Depth (m)	Blow Count[2]	Cyclic Stress Ratio[3]	Results (N, L)[4]
Richey	M~7.3 @ 134	0.10	1S	3.4	6	0.06	N
Road	M~7.3 @ 134	0.10		4.0	4	0.07	N
	M~7.3 @ 134	0.10		4.9	5	0.08	N
	M~7.3 @ 134	0.10		5.9	3	0.08	L
	M~7.3 @ 134	0.10		6.4	2	0.08	L
	M~7.3 @ 134	0.10		7.0	1	0.09	L
	M~7.3 @ 134	0.10		7.9	6	0.09	N
	M~7.3 @ 134	0.10		8.5	4	0.09	L
	M~7.3 @ 134	0.10		9.5	11	0.09	N
	M~7.3 @ 134	0.10		10.1	11	0.09	N

A-26b. Evaluation of Vincennes Scenario Earthquakes for Saline River (3) GT 310 Using High GMPEs (Atkinson, 2012) and Water Table Depth of 3 m.

Bridge/ Number	M @ Distance (km)	amax[1]	Boring	Sediment Depth (m)	Blow Count[2]	Cyclic Stress Ratio[3]	Results (N, L)[4]
Richey	M~7.3 @ 134	0.13	1S	3.4	6	0.09	N
Road	M~7.3 @ 134	0.13		4.0	4	0.09	N
	M~7.3 @ 134	0.13		4.9	5	0.10	L
	M~7.3 @ 134	0.13		5.9	3	0.11	L
	M~7.3 @ 134	0.13		6.4	2	0.11	L
	M~7.3 @ 134	0.13		7.0	1	0.11	L
	M~7.3 @ 134	0.13		7.9	6	0.12	L
	M~7.3 @ 134	0.13		8.5	4	0.12	L
	M~7.3 @ 134	0.13		9.5	11	0.12	N
	M~7.3 @ 134	0.13		10.1	11	0.12	N

1. amax = Maximum acceleration at ground surface;

2. Blow Count = Total number of blows required to drive split spoon sampler 0.3 m using standard hammer (63.5 kg) dropping 0.76 m;

3. Cyclic Stress Ratio = Stress causing liquefaction;

4. N= Liquefaction not likely; L = Liquefaction likely

A-27a. Evaluation of Skelton Scenario Earthquakes for Saline River (3) GT 310 Using Medium GMPEs (Atkinson, 2012) and Water Table Depth of 3 m.

Bridge/ Number	M @ Distance (km)	amax[1]	Boring	Sediment Depth (m)	Blow Count[2]	Cyclic Stress Ratio[3]	Results (N, L)[4]
Richey	M~6.7 @ 94	0.10	1S	3.4	6	0.07	N
Road	M~6.7 @ 94	0.10		4.0	4	0.07	N
	M~6.7 @ 94	0.10		4.9	5	0.08	N
	M~6.7 @ 94	0.10		5.9	3	0.08	N
	M~6.7 @ 94	0.10		6.4	2	0.08	N
	M~6.7 @ 94	0.10		7.0	1	0.09	N
	M~6.7 @ 94	0.10		7.9	6	0.09	N
	M~6.7 @ 94	0.10		8.5	4	0.09	N
	M~6.7 @ 94	0.10		9.5	11	0.09	N
	M~6.7 @ 94	0.10		10.1	11	0.09	N

A-27b. Evaluation of Skelton Scenario Earthquakes for Saline River (3) GT 310 Using High GMPEs (Atkinson, 2012) and Water Table Depth 3 m.

Bridge/ Number	M @ Distance (km)	amax[1]	Boring	Sediment Depth (m)	Blow Count[2]	Cyclic Stress Ratio[3]	Results (N, L)[4]
Richey	M~6.7 @ 94	0.14	1S	3.4	6	0.25	N
Road	M~6.7 @ 94	0.14		4.0	4	0.20	N
	M~6.7 @ 94	0.14		4.9	5	0.15	N
	M~6.7 @ 94	0.14		5.9	3	0.12	L
	M~6.7 @ 94	0.14		6.4	2	0.12	L
	M~6.7 @ 94	0.14		7.0	1	0.11	L
	M~6.7 @ 94	0.14		7.9	6	0.16	N
	M~6.7 @ 94	0.14		8.5	4	0.14	L
	M~6.7 @ 94	0.14		9.5	11	0.22	N
	M~6.7 @ 94	0.14		10.1	11	0.22	N

1. amax = Maximum acceleration at ground surface;
2. Blow Count = Total number of blows required to drive split spoon sampler 0.3 m using standard hammer (63.5 kg) dropping 0.76 m;
3. Cyclic Stress Ratio = Stress causing liquefaction;
4. N= Liquefaction not likely; L = Liquefaction likely

A-28a. Evaluation of Jan 23, 1812 Scenario Earthquakes for Saline River (3) GT 310 Using Medium GMPEs (Atkinson, 2012) and Water Table Depth of 3 m.

Bridge/ Number	M @ Distance (km)	amax[1]	Boring	Sediment Depth (m)	Blow Count[2]	Cyclic Stress Ratio[3]	Results (N, L)[4]
Richey	M~6.8 @ 90	0.10	1S	3.4	6	0.07	N
Road	M~6.8 @ 90	0.10		4.0	4	0.07	N
	M~6.8 @ 90	0.10		4.9	5	0.08	N
	M~6.8 @ 90	0.10		5.9	3	0.08	N
	M~6.8 @ 90	0.10		6.4	2	0.08	N
	M~6.8 @ 90	0.10		7.0	1	0.09	L
	M~6.8 @ 90	0.10		7.9	6	0.09	N
	M~6.8 @ 90	0.10		8.5	4	0.09	N
	M~6.8 @ 90	0.10		9.5	11	0.09	N
	M~6.8 @ 90	0.10		10.1	11	0.09	N

A-28b. Evaluation of Jan 23, 1812 Scenario Earthquakes for Saline River (3) River GT 310 Using High GMPEs (Atkinson, 2012) and Water Table Depth of 3 m.

Bridge/ Number	M @ Distance (km)	amax[1]	Boring	Sediment Depth (m)	Blow Count[2]	Cyclic Stress Ratio[3]	Results (N, L)[4]
Richey	M~6.8 @ 90	0.16	1S	3.4	6	0.11	N
Road	M~6.8 @ 90	0.16		4.0	4	0.12	N
	M~6.8 @ 90	0.16		4.9	5	0.13	L
	M~6.8 @ 90	0.16		5.9	3	0.14	L
	M~6.8 @ 90	0.16		6.4	2	0.14	L
	M~6.8 @ 90	0.16		7.0	1	0.15	L
	M~6.8 @ 90	0.16		7.9	6	0.15	L
	M~6.8 @ 90	0.16		8.5	4	0.15	L
	M~6.8 @ 90	0.16		9.5	11	0.16	N
	M~6.8 @ 90	0.16		10.1	11	0.16	N

1. amax = Maximum acceleration at ground surface;

2. Blow Count = Total number of blows required to drive split spoon sampler 0.3 m using standard hammer (63.5 kg) dropping 0.76 m;

3. Cyclic Stress Ratio = Stress causing liquefaction;

4. N= Liquefaction not likely; L = Liquefaction likely

A-29a. Evaluation of Jan 23, 1812 Scenario Earthquakes for Saline River (3) GT 310 Using Medium GMPEs (Atkinson, 2012) and Water Table Depth of 3 m.

Bridge/ Number	M @ Distance (km)	amax[1]	Boring	Sediment Depth (m)	Blow Count[2]	Cyclic Stress Ratio[3]	Results (N, L)[4]
Richey	M~6.8 @ 95	0.09	1S	3.4	6	0.06	N
Road	M~6.8 @ 95	0.09		4.0	4	0.07	N
	M~6.8 @ 95	0.09		4.9	5	0.07	N
	M~6.8 @ 95	0.09		5.9	3	0.08	N
	M~6.8 @ 95	0.09		6.4	2	0.08	N
	M~6.8 @ 95	0.09		7.0	1	0.08	N
	M~6.8 @ 95	0.09		7.9	6	0.08	N
	M~6.8 @ 95	0.09		8.5	4	0.09	N
	M~6.8 @ 95	0.09		9.5	11	0.09	N
	M~6.8 @ 95	0.09		10.1	11	0.09	N

A-29b. Evaluation of Jan 23, 1812 Scenario Earthquakes for Saline River (3) GT 310 Using High GMPEs (Atkinson, 2012) and Water Table Depth of 3 m.

Bridge/ Number	M @ Distance (km)	amax[1]	Boring	Sediment Depth (m)	Blow Count[2]	Cyclic Stress Ratio[3]	Results (N, L)[4]
Richey	M~6.8 @ 95	0.15	1S	3.4	6	0.10	N
Road	M~6.8 @ 95	0.15		4.0	4	0.11	N
	M~6.8 @ 95	0.15		4.9	5	0.12	L
	M~6.8 @ 95	0.15		5.9	3	0.13	L
	M~6.8 @ 95	0.15		6.4	2	0.13	L
	M~6.8 @ 95	0.15		7.0	1	0.14	L
	M~6.8 @ 95	0.15		7.9	6	0.14	L
	M~6.8 @ 95	0.15		8.5	4	0.14	L
	M~6.8 @ 95	0.15		9.5	11	0.15	N
	M~6.8 @ 95	0.15		10.1	11	0.15	N

1. amax = Maximum acceleration at ground surface;
2. Blow Count = Total number of blows required to drive split spoon sampler 0.3 m using standard hammer (63.5 kg) dropping 0.76 m;
3. Cyclic Stress Ratio = Stress causing liquefaction;
4. N= Liquefaction not likely; L = Liquefaction likely

A-30a. Evaluation of February 7, 1812 Scenario Earthquakes for Saline River (3) GT 310 Using Medium GMPEs (Atkinson, 2012) and Water Table Depth of 3 m.

Bridge/ Number	M @ Distance (km)	amax[1]	Boring	Sediment Depth (m)	Blow Count[2]	Cyclic Stress Ratio[3]	Results (N, L)[4]
Richey	M~7.8 @ 180	0.13	1S	3.4	6	0.09	N
Road	M~7.8 @ 180	0.13		4.0	4	0.09	N
	M~7.8 @ 180	0.13		4.9	5	0.10	L
	M~7.8 @ 180	0.13		5.9	3	0.11	L
	M~7.8 @ 180	0.13		6.4	2	0.11	L
	M~7.8 @ 180	0.13		7.0	1	0.11	L
	M~7.8 @ 180	0.13		7.9	6	0.12	L
	M~7.8 @ 180	0.13		8.5	4	0.12	L
	M~7.8 @ 180	0.13		9.5	11	0.12	L
	M~7.8 @ 180	0.13		10.1	11	0.12	L

A-30b. Evaluation of February 7, 1812 Scenario Earthquakes for Saline River (3) GT 310 Using High GMPEs (Atkinson, 2012) and Water Table Depth of 3 m.

Bridge/ Number	M @ Distance (km)	amax[1]	Boring	Sediment Depth (m)	Blow Count[2]	Cyclic Stress Ratio[3]	Results (N, L)[4]
Richey	M~7.8 @ 180	0.18	1S	3.4	6	0.12	N
Road	M~7.8 @ 180	0.18		4.0	4	0.13	L
	M~7.8 @ 180	0.18		4.9	5	0.14	L
	M~7.8 @ 180	0.18		5.9	3	0.15	L
	M~7.8 @ 180	0.18		6.4	2	0.15	L
	M~7.8 @ 180	0.18		7.0	1	0.16	L
	M~7.8 @ 180	0.18		7.9	6	0.16	L
	M~7.8 @ 180	0.18		8.5	4	0.16	L
	M~7.8 @ 180	0.18		9.5	11	0.17	L
	M~7.8 @ 180	0.18		10.1	11	0.17	L

1. amax = Maximum acceleration at ground surface;
2. Blow Count = Total number of blows required to drive split spoon sampler 0.3 m using standard hammer (63.5 kg) dropping 0.76 m;
3. Cyclic Stress Ratio = Stress causing liquefaction;
4. N= Liquefaction not likely; L = Liquefaction likely

A-31a. Evaluation of Local Scenario Earthquakes for Saline River (3) GT 310 Using Medium GMPEs (Atkinson, 2012) and Water Table Depth of 5 m.

Bridge/ Number	M @ Distance (km)	amax[1]	Boring	Sediment Depth (m)	Blow Count[2]	Cyclic Stress Ratio[3]	Results (N, L)[4]
Richey	M 5.5 @ 15	0.21	1S	5.9	3	0.14	N
Road	M 5.5 @ 15	0.21		6.4	2	0.15	N
	M 5.5 @ 15	0.21		7.0	1	0.15	N
	M 5.5 @ 15	0.21		7.9	6	0.16	N
	M 5.5 @ 15	0.21		8.5	4	0.17	N
	M 5.5 @ 15	0.21		9.5	11	0.17	N
	M 5.5 @ 15	0.21		10.1	11	0.17	N

A-31b. Evaluation of Local Scenario Earthquakes for Saline River (3) GT 310 Using High GMPEs (Atkinson, 2012) and Water Table Depth of 3 m.

Bridge/ Number	M @ Distance (km)	amax[1]	Boring	Sediment Depth (m)	Blow Count[2]	Cyclic Stress Ratio[3]	Results (N, L)[4]
Richey	M 5.5 @ 15	0.34	1S	5.9	3	0.23	L
Road	M 5.5 @ 15	0.34		6.4	2	0.24	L
	M 5.5 @ 15	0.34		7.0	1	0.25	L
	M 5.5 @ 15	0.34		7.9	6	0.26	L
	M 5.5 @ 15	0.34		8.5	4	0.27	L
	M 5.5 @ 15	0.34		9.5	11	0.27	N
	M 5.5 @ 15	0.34		10.1	11	0.28	N

1. amax = Maximum acceleration at ground surface;

2. Blow Count = Total number of blows required to drive split spoon sampler 0.3 m using standard hammer (63.5 kg) dropping 0.76 m;

3. Cyclic Stress Ratio = Stress causing liquefaction;

4. N= Liquefaction not likely; L = Liquefaction likely

A-32a. Evaluation of Vincennes Scenario Earthquakes for Saline River (3) GT 310 Using Medium GMPEs (Atkinson, 2012) and Water Table of Depth 5 m.

Bridge/ Number	M @ Distance (km)	amax[1]	Boring	Sediment Depth (m)	Blow Count[2]	Cyclic Stress Ratio[3]	Results (N, L)[4]
Richey	M~7.3 @ 134	0.10	1S	5.9	3	0.07	N
Road	M~7.3 @ 134	0.10		6.4	2	0.07	N
	M~7.3 @ 134	0.10		7.0	1	0.07	L
	M~7.3 @ 134	0.10		7.9	6	0.07	N
	M~7.3 @ 134	0.10		8.5	4	0.08	N
	M~7.3 @ 134	0.10		9.5	11	0.08	N
	M~7.3 @ 134	0.10		10.1	11	0.08	N

A-32b. Evaluation of Vincennes Scenario Earthquakes for Saline River (3) GT 310 Using High GMPEs (Atkinson, 2012) and Water Table of Depth 5 m.

Bridge/ Number	M @ Distance (km)	amax[1]	Boring	Sediment Depth (m)	Blow Count[2]	Cyclic Stress Ratio[3]	Results (N, L)[4]
Richey	M~7.3 @ 134	0.13	1S	5.9	3	0.09	L
Road	M~7.3 @ 134	0.13		6.4	2	0.09	L
	M~7.3 @ 134	0.13		7.0	1	0.09	L
	M~7.3 @ 134	0.13		7.9	6	0.10	L
	M~7.3 @ 134	0.13		8.5	4	0.10	L
	M~7.3 @ 134	0.13		9.5	11	0.10	N
	M~7.3 @ 134	0.13		10.1	11	0.10	N

1. amax = Maximum acceleration at ground surface;

2. Blow Count = Total number of blows required to drive split spoon sampler 0.3 m using standard hammer (63.5 kg) dropping 0.76 m;

3. Cyclic Stress Ratio = Stress causing liquefaction;

4. N= Liquefaction not likely; L = Liquefaction likely

A-33a. Evaluation of Skelton Scenario Earthquakes for Saline River (3) GT 310 Using Medium GMPEs (Atkinson, 2012) and Water Table Depth of 5 m.

Bridge/ Number	M @ Distance (km)	amax[1]	Boring	Sediment Depth (m)	Blow Count[2]	Cyclic Stress Ratio[3]	Results (N, L)[4]
Richey	M~6.7 @ 94	0.10	1S	5.9	3	0.07	N
Road	M~6.7 @ 94	0.10		6.4	2	0.07	N
	M~6.7 @ 94	0.10		7.0	1	0.07	N
	M~6.7 @ 94	0.10		7.9	6	0.07	N
	M~6.7 @ 94	0.10		8.5	4	0.08	N
	M~6.7 @ 94	0.10		9.5	11	0.08	N
	M~6.7 @ 94	0.10		10.1	11	0.08	N

A-33b. Evaluation of Skelton Scenario Earthquakes for Saline River (3) GT 310 Using High GMPEs (Atkinson, 2012) and Water Table Depth of 5 m.

Bridge/ Number	M @ Distance (km)	amax[1]	Boring	Sediment Depth (m)	Blow Count[2]	Cyclic Stress Ratio[3]	Results (N, L)[4]
Richey	M~6.7 @ 94	0.14	1S	5.9	3	0.10	L
Road	M~6.7 @ 94	0.14		6.4	2	0.10	L
	M~6.7 @ 94	0.14		7.0	1	0.11	L
	M~6.7 @ 94	0.14		7.9	6	0.11	N
	M~6.7 @ 94	0.14		8.5	4	0.11	L
	M~6.7 @ 94	0.14		9.5	11	0.12	N
	M~6.7 @ 94	0.14		10.1	11	0.12	N

1. amax = Maximum acceleration at ground surface;

2. Blow Count = Total number of blows required to drive split spoon sampler 0.3 m using standard hammer (63.5 kg) dropping 0.76 m;

3. Cyclic Stress Ratio = Stress causing liquefaction;

4. N= Liquefaction not likely; L = Liquefaction likely

A-34a. Evaluation of Jan 23, 1812 Scenario Earthquakes for Saline River (3) GT 310 Using Medium GMPEs (Atkinson, 2012) and Water Table Depth of 5 m.

Bridge/ Number	M @ Distance (km)	amax[1]	Boring	Sediment Depth (m)	Blow Count[2]	Cyclic Stress Ratio[3]	Results (N, L)[4]
Richey	M~6.8 @ 90	0.10	1S	5.9	3	0.07	N
Road	M~6.8 @ 90	0.10		6.4	2	0.07	N
	M~6.8 @ 90	0.10		7.0	1	0.07	N
	M~6.8 @ 90	0.10		7.9	6	0.07	N
	M~6.8 @ 90	0.10		8.5	4	0.08	N
	M~6.8 @ 90	0.10		9.5	11	0.08	N
	M~6.8 @ 90	0.10		10.1	11	0.08	N

A-34b. Evaluation of Jan 23, 1812 Scenario Earthquakes for Saline River (3) GT 310 Using High GMPEs (Atkinson, 2012) and Water Table Depth of 5 m.

Bridge/ Number	M @ Distance (km)	amax[1]	Boring	Sediment Depth (m)	Blow Count[2]	Cyclic Stress Ratio[3]	Results (N, L)[4]
Richey	M~6.8 @ 90	0.16	1S	5.9	3	0.11	L
Road	M~6.8 @ 90	0.16		6.4	2	0.12	L
	M~6.8 @ 90	0.16		7.0	1	0.12	L
	M~6.8 @ 90	0.16		7.9	6	0.13	L
	M~6.8 @ 90	0.16		8.5	4	0.13	L
	M~6.8 @ 90	0.16		9.5	11	0.13	N
	M~6.8 @ 90	0.16		10.1	11	0.13	N

1. amax = Maximum acceleration at ground surface;

2. Blow Count = Total number of blows required to drive split spoon sampler 0.3 m using standard hammer (63.5 kg) dropping 0.76 m;

3. Cyclic Stress Ratio = Stress causing liquefaction;

4. N= Liquefaction not likely; L = Liquefaction likely

A-35a. Evaluation of Jan 23, 1812 Scenario Earthquakes for Saline River (3) GT 310 Using Medium GMPEs (Atkinson, 2012) and Water Table Depth of 5 m.

Bridge/ Number	M @ Distance (km)	amax[1]	Boring	Sediment Depth (m)	Blow Count[2]	Cyclic Stress Ratio[3]	Results (N, L)[4]
Richey	M~6.8 @ 95	0.09	1S	5.9	3	0.06	N
Road	M~6.8 @ 95	0.09		6.4	2	0.06	N
	M~6.8 @ 95	0.09		7.0	1	0.07	N
	M~6.8 @ 95	0.09		7.9	6	0.07	N
	M~6.8 @ 95	0.09		8.5	4	0.07	N
	M~6.8 @ 95	0.09		9.5	11	0.07	N
	M~6.8 @ 95	0.09		10.1	11	0.07	N

A-35b. Evaluation of Jan 23, 1812 Scenario Earthquakes for Saline River (3) GT 310 Using High GMPEs (Atkinson, 2012) and Water Table Depth of 5 m.

Bridge/ Number	M @ Distance (km)	amax[1]	Boring	Sediment Depth (m)	Blow Count[2]	Cyclic Stress Ratio[3]	Results (N, L)[4]
Richey	M~6.8 @ 95	0.15	1S	5.9	3	0.10	L
Road	M~6.8 @ 95	0.15		6.4	2	0.11	L
	M~6.8 @ 95	0.15		7.0	1	0.11	L
	M~6.8 @ 95	0.15		7.9	6	0.12	N
	M~6.8 @ 95	0.15		8.5	4	0.12	L
	M~6.8 @ 95	0.15		9.5	11	0.12	N
	M~6.8 @ 95	0.15		10.1	11	0.12	N

1. amax = Maximum acceleration at ground surface;
2. Blow Count = Total number of blows required to drive split spoon sampler 0.3 m using standard hammer (63.5 kg) dropping 0.76 m;
3. Cyclic Stress Ratio = Stress causing liquefaction;
4. N= Liquefaction not likely; L = Liquefaction likely

A-36a. Evaluation of February 7, 1812 Scenario Earthquakes for Saline River (3) GT 310 Using Medium GMPEs (Atkinson, 2012) and Water Table Depth of 5 m.

Bridge/ Number	M @ Distance (km)	amax[1]	Boring	Sediment Depth (m)	Blow Count[2]	Cyclic Stress Ratio[3]	Results (N, L)[4]
Richey	M~7.8 @ 180	0.13	1S	5.9	3	0.09	L
Road	M~7.8 @ 180	0.13		6.4	2	0.09	L
	M~7.8 @ 180	0.13		7.0	1	0.09	L
	M~7.8 @ 180	0.13		7.9	6	0.10	L
	M~7.8 @ 180	0.13		8.5	4	0.10	L
	M~7.8 @ 180	0.13		9.5	11	0.10	L
	M~7.8 @ 180	0.13		10.1	11	0.10	L

A-36b. Evaluation of February 7, 1812 Scenario Earthquakes for Saline River (3) GT 310 Using High GMPEs (Atkinson, 2012) and Water Table Depth of 5 m.

Bridge/ Number	M @ Distance (km)	amax[1]	Boring	Sediment Depth (m)	Blow Count[2]	Cyclic Stress Ratio[3]	Results (N, L)[4]
Richey	M~7.8 @ 180	0.18	1S	5.9	3	0.12	L
Road	M~7.8 @ 180	0.18		6.4	2	0.12	L
	M~7.8 @ 180	0.18		7.0	1	0.13	L
	M~7.8 @ 180	0.18		7.9	6	0.13	L
	M~7.8 @ 180	0.18		8.5	4	0.14	L
	M~7.8 @ 180	0.18		9.5	11	0.14	L
	M~7.8 @ 180	0.18		10.1	11	0.14	L

1. amax = Maximum acceleration at ground surface;
2. Blow Count = Total number of blows required to drive split spoon sampler 0.3 m using standard hammer (63.5 kg) dropping 0.76 m;
3. Cyclic Stress Ratio = Stress causing liquefaction;
4. N= Liquefaction not likely; L = Liquefaction likely

A-37a. Evaluation of Local Scenario Earthquakes for Saline River (4) GT 311 Using Medium GMPEs (Atkinson, 2012) and Water Table Depth of 3 m.

Bridge/ Number	M @ Distance (km)	amax[1]	Boring	Sediment Depth (m)	Blow Count[2]	Cyclic Stress Ratio[3]	Results (N, L)[4]
Rt 34	M~5.5 @ 15	0.21	2S	5.5	7	0.17	N
	M~5.5 @ 15	0.21		6.4	8	0.18	N
	M~5.5 @ 15	0.21		7.6	6	0.19	N
	M~5.5 @ 15	0.21		8.5	2	0.20	N
	M~5.5 @ 15	0.21		9.5	4	0.20	N
	M~5.5 @ 15	0.21		10.1	22	0.20	N
	M~5.5 @ 15	0.21		11.0	28	0.20	N
	M~5.5 @ 15	0.21		11.6	26	0.20	N
	M~5.5 @ 15	0.21		12.5	18	0.20	N
	M~5.5 @ 15	0.21		14.0	10	0.19	N

A-37b. Evaluation of Local Scenario Earthquakes for Saline River (4) GT 311 Using High GMPEs (Atkinson, 2012) and Water Table Depth of 3 m.

Bridge/ Number	M @ Distance (km)	amax[1]	Boring	Sediment Depth (m)	Blow Count[2]	Cyclic Stress Ratio[3]	Results (N, L)[4]
Rt 34	M~5.5 @ 15	0.34	2S	5.5	7	0.28	N
	M~5.5 @ 15	0.34		6.4	8	0.30	N
	M~5.5 @ 15	0.34		7.6	6	0.31	N
	M~5.5 @ 15	0.34		8.5	2	0.32	L
	M~5.5 @ 15	0.34		9.5	4	0.32	L
	M~5.5 @ 15	0.34		10.1	22	0.33	N
	M~5.5 @ 15	0.34		11.0	28	0.32	N
	M~5.5 @ 15	0.34		11.6	26	0.32	N
	M~5.5 @ 15	0.34		12.5	18	0.32	N
	M~5.5 @ 15	0.34		14.0	10	0.31	N

1. amax = Maximum acceleration at ground surface;

2. Blow Count = Total number of blows required to drive split spoon sampler 0.3 m using standard hammer (63.5 kg) dropping 0.76 m;

3. Cyclic Stress Ratio = Stress causing liquefaction;

4. N= Liquefaction not likely; L = Liquefaction likely

A-38a. Evaluation of Vincennes Scenario Earthquakes for Saline River (4) GT 311 Using Medium GMPEs (Atkinson, 2012) and Water Table Depth of 3 m.

Bridge/ Number	M @ Distance (km)	amax[1]	Boring	Sediment Depth (m)	Blow Count[2]	Cyclic Stress Ratio[3]	Results (N, L)[4]
Rt 34	M~7.3 @ 134	0.10	2S	5.5	7	0.08	N
	M~7.3 @ 134	0.10		6.4	8	0.08	N
	M~7.3 @ 134	0.10		7.6	6	0.09	N
	M~7.3 @ 134	0.10		8.5	2	0.09	N
	M~7.3 @ 134	0.10		9.5	4	0.09	N
	M~7.3 @ 134	0.10		10.1	22	0.09	N
	M~7.3 @ 134	0.10		11.0	28	0.09	N
	M~7.3 @ 134	0.10		11.6	26	0.09	N
	M~7.3 @ 134	0.10		12.5	18	0.09	N
	M~7.3 @ 134	0.10		14.0	10	0.09	N

A-38b. Evaluation of Vincennes Scenario Earthquakes for Saline River (4) GT 311 Using High GMPEs (Atkinson, 2012) and Water Table Depth of 3 m.

Bridge/ Number	M @ Distance (km)	amax[1]	Boring	Sediment Depth (m)	Blow Count[2]	Cyclic Stress Ratio[3]	Results (N, L)[4]
Rt 34	M~7.3 @ 134	0.13	2S	5.5	7	0.11	N
	M~7.3 @ 134	0.13		6.4	8	0.11	N
	M~7.3 @ 134	0.13		7.6	6	0.12	N
	M~7.3 @ 134	0.13		8.5	2	0.12	L
	M~7.3 @ 134	0.13		9.5	4	0.12	L
	M~7.3 @ 134	0.13		10.1	22	0.12	N
	M~7.3 @ 134	0.13		11.0	28	0.12	N
	M~7.3 @ 134	0.13		11.6	26	0.12	N
	M~7.3 @ 134	0.13		12.5	18	0.12	N
	M~7.3 @ 134	0.13		14.0	10	0.12	N

1. amax = Maximum acceleration at ground surface;

2. Blow Count = Total number of blows required to drive split spoon sampler 0.3 m using standard hammer (63.5 kg) dropping 0.76 m;

3. Cyclic Stress Ratio = Stress causing liquefaction;

4. N= Liquefaction not likely; L = Liquefaction likely

A-39a. Evaluation of Skelton Scenario Earthquakes for Saline River (4) GT 311 Using Medium GMPEs (Atkinson, 2012) and Water Table Depth of 3 m.

Bridge/ Number	M @ Distance (km)	amax[1]	Boring	Sediment Depth (m)	Blow Count[2]	Cyclic Stress Ratio[3]	Results (N, L)[4]
Rt 34	M~6.7 @ 94	0.10	2S	5.5	7	0.08	N
	M~6.7 @ 94	0.10		6.4	8	0.08	N
	M~6.7 @ 94	0.10		7.6	6	0.09	N
	M~6.7 @ 94	0.10		8.5	2	0.09	N
	M~6.7 @ 94	0.10		9.5	4	0.09	N
	M~6.7 @ 94	0.10		10.1	22	0.09	N
	M~6.7 @ 94	0.10		11.0	28	0.09	N
	M~6.7 @ 94	0.10		11.6	26	0.09	N
	M~6.7 @ 94	0.10		12.5	18	0.09	N
	M~6.7 @ 94	0.10		14.0	10	0.09	N

A-39b. Evaluation of Skelton Scenario Earthquakes for Saline River (4) GT 311 Using High GMPEs (Atkinson, 2012) and Water Table Depth of 3 m.

Bridge/ Number	M @ Distance (km)	amax[1]	Boring	Sediment Depth (m)	Blow Count[2]	Cyclic Stress Ratio[3]	Results (N, L)[4]
Rt 34	M~6.7 @ 94	0.14	2S	5.5	7	0.12	N
	M~6.7 @ 94	0.14		6.4	8	0.13	N
	M~6.7 @ 94	0.14		7.6	6	0.13	N
	M~6.7 @ 94	0.14		8.5	2	0.13	L
	M~6.7 @ 94	0.14		9.5	4	0.14	L
	M~6.7 @ 94	0.14		10.1	22	0.14	N
	M~6.7 @ 94	0.14		11.0	28	0.14	N
	M~6.7 @ 94	0.14		11.6	26	0.14	N
	M~6.7 @ 94	0.14		12.5	18	0.13	N
	M~6.7 @ 94	0.144		14.0	10	0.13	N

1. amax = Maximum acceleration at ground surface;

2. Blow Count = Total number of blows required to drive split spoon sampler 0.3 m using standard hammer (63.5 kg) dropping 0.76 m;

3. Cyclic Stress Ratio = Stress causing liquefaction;

4. N= Liquefaction not likely; L = Liquefaction likely

A-40a. Evaluation of January 23, 1812 Scenario Earthquakes for Saline River (4) GT 311 Using Medium GMPEs (Atkinson, 2012) and Water Table Depth of 3 m.

Bridge/ Number	M @ Distance (km)	amax[1]	Boring	Sediment Depth (m)	Blow Count[2]	Cyclic Stress Ratio[3]	Results (N, L)[4]
Rt 34	M~6.8 @ 90	0.10	2S	5.5	7	0.08	N
	M~6.8 @ 90	0.10		6.4	8	0.08	N
	M~6.8 @ 90	0.10		7.6	6	0.09	N
	M~6.8 @ 90	0.10		8.5	2	0.09	N
	M~6.8 @ 90	0.10		9.5	4	0.09	N
	M~6.8 @ 90	0.10		10.1	22	0.09	N
	M~6.8 @ 90	0.10		11.0	28	0.09	N
	M~6.8 @ 90	0.10		11.6	26	0.09	N
	M~6.8 @ 90	0.10		12.5	18	0.09	N
	M~6.8 @ 90	0.10		14.0	10	0.09	N

A-40b. Evaluation of January 23, 1812 Scenario Earthquakes for Saline (4) River GT 311 Using High GMPEs (Atkinson, 2012) and Water Table Depth of 3 m.

Bridge/ Number	M @ Distance (km)	amax[1]	Boring	Sediment Depth (m)	Blow Count[2]	Cyclic Stress Ratio[3]	Results (N, L)[4]
Rt 34	M~6.8 @ 90	0.21	2S	5.5	7	0.17	N
	M~6.8 @ 90	0.21		6.4	8	0.18	N
	M~6.8 @ 90	0.21		7.6	6	0.19	L
	M~6.8 @ 90	0.21		8.5	2	0.19	L
	M~6.8 @ 90	0.21		9.5	4	0.20	L
	M~6.8 @ 90	0.21		10.1	22	0.20	N
	M~6.8 @ 90	0.21		11.0	28	0.20	N
	M~6.8 @ 90	0.21		11.6	26	0.20	N
	M~6.8 @ 90	0.21		12.5	18	0.19	N
	M~6.8 @ 90	0.21		14.0	10	0.19	N

1. amax = Maximum acceleration at ground surface;

2. Blow Count = Total number of blows required to drive split spoon sampler 0.3 m using standard hammer (63.5 kg) dropping 0.76 m;

3. Cyclic Stress Ratio = Stress causing liquefaction;

4. N= Liquefaction not likely; L = Liquefaction likely

A-41a. Evaluation of January 23, 1812 Scenario Earthquakes for Saline River (4) GT 311 Using Medium GMPEs (Atkinson, 2012) and Water Table Depth of 3 m.

Bridge/ Number	M @ Distance (km)	amax[1]	Boring	Sediment Depth (m)	Blow Count[2]	Cyclic Stress Ratio[3]	Results (N, L)[4]
Rt 34	M~6.8 @ 95	0.09	2S	5.5	7	0.08	N
	M~6.8 @ 95	0.09		6.4	8	0.08	N
	M~6.8 @ 95	0.09		7.6	6	0.08	N
	M~6.8 @ 95	0.09		8.5	2	0.09	N
	M~6.8 @ 95	0.09		9.5	4	0.09	N
	M~6.8 @ 95	0.09		10.1	22	0.09	N
	M~6.8 @ 95	0.09		11.0	28	0.09	N
	M~6.8 @ 95	0.09		11.6	26	0.09	N
	M~6.8 @ 95	0.09		12.5	18	0.08	N
	M~6.8 @ 95	0.09		14.0	10	0.08	N

A-41b. Evaluation of January 23, 1812 Scenario Earthquakes for Saline River (4) GT 311 Usin High GMPEs (Atkinson, 2012) and Water Table Depth of 3 m.

Bridge/ Number	M @ Distance (km)	amax[1]	Boring	Sediment Depth (m)	Blow Count[2]	Cyclic Stress Ratio[3]	Results (N, L)[4]
Rt 34	M~6.8 @ 95	0.15	2S	5.5	7	0.13	N
	M~6.8 @ 95	0.15		6.4	8	0.13	N
	M~6.8 @ 95	0.15		7.6	6	0.14	N
	M~6.8 @ 95	0.15		8.5	2	0.14	L
	M~6.8 @ 95	0.15		9.5	4	0.15	L
	M~6.8 @ 95	0.15		10.1	22	0.15	N
	M~6.8 @ 95	0.15		11.0	28	0.15	N
	M~6.8 @ 95	0.15		11.6	26	0.15	N
	M~6.8 @ 95	0.15		12.5	18	0.14	N
	M~6.8 @ 95	0.15		14.0	10	0.14	N

1. amax = Maximum acceleration at ground surface;

2. Blow Count = Total number of blows required to drive split spoon sampler 0.3 m using standard hammer (63.5 kg) dropping 0.76 m;

3. Cyclic Stress Ratio = Stress causing liquefaction;

4. N= Liquefaction not likely; L = Liquefaction likely

A-42a. Evaluation of February 7, 1812 Scenario Earthquakes for Saline River (4) GT 311 Using Medium GMPEs (Atkinson, 2012) and Water Table Depth of 3 m.

Bridge/ Number	M @ Distance (km)	amax[1]	Boring	Sediment Depth (m)	Blow Count[2]	Cyclic Stress Ratio[3]	Results (N, L)[4]
Rt 34	M~7.8 @ 180	0.13	2S	5.5	7	0.11	N
	M~7.8 @ 180	0.13		6.4	8	0.11	N
	M~7.8 @ 180	0.13		7.6	6	0.12	L
	M~7.8 @ 180	0.13		8.5	2	0.12	L
	M~7.8 @ 180	0.13		9.5	4	0.12	L
	M~7.8 @ 180	0.13		10.1	22	0.12	N
	M~7.8 @ 180	0.13		11.0	28	0.12	N
	M~7.8 @ 180	0.13		11.6	26	0.12	N
	M~7.8 @ 180	0.13		12.5	18	0.12	N
	M~7.8 @ 180	0.13		14.0	10	0.12	N

A-42b. Evaluation of February 7, 1812 Scenario Earthquakes for Saline River (4) GT 311 Using High GMPEs (Atkinson, 2012) and Water Table Depth of 3 m.

Bridge/ Number	M @ Distance (km)	amax[1]	Boring	Sediment Depth (m)	Blow Count[2]	Cyclic Stress Ratio[3]	Results (N, L)[4]
Rt 34	M~7.8 @ 180	0.18	2S	5.5	7	0.15	L
	M~7.8 @ 180	0.18		6.4	8	0.15	L
	M~7.8 @ 180	0.18		7.6	6	0.16	L
	M~7.8 @ 180	0.18		8.5	2	0.16	L
	M~7.8 @ 180	0.18		9.5	4	0.17	L
	M~7.8 @ 180	0.18		10.1	22	0.17	N
	M~7.8 @ 180	0.18		11.0	28	0.17	N
	M~7.8 @ 180	0.18		11.6	26	0.17	N
	M~7.8 @ 180	0.18		12.5	18	0.16	N
	M~7.8 @ 180	0.176		14.0	10	0.16	L

1. amax = Maximum acceleration at ground surface;

2. Blow Count = Total number of blows required to drive split spoon sampler 0.3 m using standard hammer (63.5 kg) dropping 0.76 m;

3. Cyclic Stress Ratio = Stress causing liquefaction;

4. N= Liquefaction not likely; L = Liquefaction likely

A-43a. Evaluation of Local Scenario Earthquakes for Saline River (4) GT 311 Using Medium GMPEs (Atkinson, 2012) and Water Table Depth of 5 m.

Bridge/ Number	M @ Distance (km)	amax[1]	Boring	Sediment Depth (m)	Blow Count[2]	Cyclic Stress Ratio[3]	Results (N, L)[4]
Rt 34	M~5.5 @ 15	0.21	2S	5.5	7	0.14	N
	M~5.5 @ 15	0.21		6.4	8	0.15	N
	M~5.5 @ 15	0.21		7.6	6	0.16	N
	M~5.5 @ 15	0.21		8.5	2	0.17	N
	M~5.5 @ 15	0.21		9.5	4	0.17	N
	M~5.5 @ 15	0.21		10.1	22	0.17	N
	M~5.5 @ 15	0.21		11.0	28	0.17	N
	M~5.5 @ 15	0.21		11.6	26	0.17	N
	M~5.5 @ 15	0.21		12.5	18	0.17	N
	M~5.5 @ 15	0.21		14.0	10	0.17	N

A-43b. Evaluation of Local Scenario Earthquakes for Saline River (4) GT 311 Using High GMPEs (Atkinson, 2012) and Water Table Depth of 5 m.

Bridge/ Number	M @ Distance (km)	amax[1]	Boring	Sediment Depth (m)	Blow Count[2]	Cyclic Stress Ratio[3]	Results (N, L)[4]
Rt 34	M~5.5 @ 15	0.34	2S	5.5	7	0.22	N
	M~5.5 @ 15	0.34		6.4	8	0.24	N
	M~5.5 @ 15	0.34		7.6	6	0.26	N
	M~5.5 @ 15	0.34		8.5	2	0.27	L
	M~5.5 @ 15	0.34		9.5	4	0.27	L
	M~5.5 @ 15	0.34		10.1	22	0.28	N
	M~5.5 @ 15	0.34		11.0	28	0.28	N
	M~5.5 @ 15	0.34		11.6	26	0.28	N
	M~5.5 @ 15	0.34		12.5	18	0.28	N
	M~5.5 @ 15	0.34		14.0	10	0.27	N

1. amax = Maximum acceleration at ground surface;
2. Blow Count = Total number of blows required to drive split spoon sampler 0.3 m using standard hammer (63.5 kg) dropping 0.76 m;
3. Cyclic Stress Ratio = Stress causing liquefaction;
4. N= Liquefaction not likely; L = Liquefaction likely

A-44a. Evaluation of Vincennes Scenario Earthquakes for Saline River (4) GT 311 Using Medium GMPEs (Atkinson, 2012) and Water Table Depth of 5 m.

Bridge/ Number	M @ Distance (km)	amax[1]	Boring	Sediment Depth (m)	Blow Count[2]	Cyclic Stress Ratio[3]	Results (N, L)[4]
Rt 34	M~7.3 @ 134	0.10	2S	5.5	7	0.06	N
	M~7.3 @ 134	0.10		6.4	8	0.07	N
	M~7.3 @ 134	0.10		7.6	6	0.07	N
	M~7.3 @ 134	0.10		8.5	2	0.08	N
	M~7.3 @ 134	0.10		9.5	4	0.08	N
	M~7.3 @ 134	0.10		10.1	22	0.08	N
	M~7.3 @ 134	0.10		11.0	28	0.08	N
	M~7.3 @ 134	0.10		11.6	26	0.08	N
	M~7.3 @ 134	0.10		12.5	18	0.08	N
	M~7.3 @ 134	0.10		14.0	10	0.08	N

A-44b. Evaluation of Vincennes Scenario Earthquakes for Saline River (4) GT 311 Using High GMPEs (Atkinson, 2012) and Water Table Depth of 5 m.

Bridge/ Number	M @ Distance (km)	amax[1]	Boring	Sediment Depth (m)	Blow Count[2]	Cyclic Stress Ratio[3]	Results (N, L)[4]
Rt 34	M~7.3 @ 134	0.13	2S	5.5	7	0.08	N
	M~7.3 @ 134	0.13		6.4	8	0.09	N
	M~7.3 @ 134	0.13		7.6	6	0.10	N
	M~7.3 @ 134	0.13		8.5	2	0.10	L
	M~7.3 @ 134	0.13		9.5	4	0.10	L
	M~7.3 @ 134	0.13		10.1	22	0.10	N
	M~7.3 @ 134	0.13		11.0	28	0.10	N
	M~7.3 @ 134	0.13		11.6	26	0.10	N
	M~7.3 @ 134	0.13		12.5	18	0.10	N
	M~7.3 @ 134	0.13		14.0	10	0.10	N

1. amax = Maximum acceleration at ground surface;

2. Blow Count = Total number of blows required to drive split spoon sampler 0.3 m using standard hammer (63.5 kg) dropping 0.76 m;

3. Cyclic Stress Ratio = Stress causing liquefaction;

4. N= Liquefaction not likely; L = Liquefaction likely

A-45a. Evaluation of Skelton Scenario Earthquakes for Saline River (4) GT 311 Using Medium GMPEs (Atkinson, 2012) and Water Table Depth of 5 m.

Bridge/ Number	M @ Distance (km)	amax[1]	Boring	Sediment Depth (m)	Blow Count[2]	Cyclic Stress Ratio[3]	Results (N, L)[4]
Rt 34	M~6.7 @ 94	0.10	2S	5.5	7	0.06	N
	M~6.7 @ 94	0.10		6.4	8	0.07	N
	M~6.7 @ 94	0.10		7.6	6	0.07	N
	M~6.7 @ 94	0.10		8.5	2	0.08	N
	M~6.7 @ 94	0.10		9.5	4	0.08	N
	M~6.7 @ 94	0.10		10.1	22	0.08	N
	M~6.7 @ 94	0.10		11.0	28	0.08	N
	M~6.7 @ 94	0.10		11.6	26	0.08	N
	M~6.7 @ 94	0.10		12.5	18	0.08	N
	M~6.7 @ 94	0.10		14.0	10	0.08	N

A-45b. Evaluation of Skelton Scenario Earthquakes for Saline River (4) GT 311 Using High GMPEs (Atkinson, 2012) and Water Table Depth of 5 m.

Bridge/ Number	M @ Distance (km)	amax[1]	Boring	Sediment Depth (m)	Blow Count[2]	Cyclic Stress Ratio[3]	Results (N, L)[4]
Rt 34	M~6.7 @ 94	0.14	2S	5.5	7	0.09	N
	M~6.7 @ 94	0.14		6.4	8	0.10	N
	M~6.7 @ 94	0.14		7.6	6	0.11	N
	M~6.7 @ 94	0.14		8.5	2	0.11	N
	M~6.7 @ 94	0.14		9.5	4	0.12	N
	M~6.7 @ 94	0.14		10.1	22	0.12	N
	M~6.7 @ 94	0.14		11.0	28	0.12	N
	M~6.7 @ 94	0.14		11.6	26	0.12	N
	M~6.7 @ 94	0.14		12.5	18	0.12	N
	M~6.7 @ 94	0.14		14.0	10	0.11	N

1. amax = Maximum acceleration at ground surface;

2. Blow Count = Total number of blows required to drive split spoon sampler 0.3 m using standard hammer (63.5 kg) dropping 0.76 m;

3. Cyclic Stress Ratio = Stress causing liquefaction;

4. N= Liquefaction not likely; L = Liquefaction likely

A-46a. Evaluation of January 23, 1812 Scenario Earthquakes for Saline River (4) GT 311 Using Medium GMPEs (Atkinson, 2012) and Water Table Depth of 5 m.

Bridge/ Number	M @ Distance (km)	amax[1]	Boring	Sediment Depth (m)	Blow Count[2]	Cyclic Stress Ratio[3]	Results (N, L)[4]
Rt 34	M~6.8 @ 90	0.10	2S	5.5	7	0.06	N
	M~6.8 @ 90	0.10		6.4	8	0.07	N
	M~6.8 @ 90	0.10		7.6	6	0.07	N
	M~6.8 @ 90	0.10		8.5	2	0.08	N
	M~6.8 @ 90	0.10		9.5	4	0.08	N
	M~6.8 @ 90	0.10		10.1	22	0.08	N
	M~6.8 @ 90	0.10		11.0	28	0.08	N
	M~6.8 @ 90	0.10		11.6	26	0.08	N
	M~6.8 @ 90	0.10		12.5	18	0.08	N
	M~6.8 @ 90	0.10		14.0	10	0.08	N

A-46b. Evaluation of January 23, 1812 Scenario Earthquakes for Saline River (4) GT 311 Usin High GMPEs (Atkinson, 2012) and Water Table Depth of 5 m.

Bridge/ Number	M @ Distance (km)	amax[1]	Boring	Sediment Depth (m)	Blow Count[2]	Cyclic Stress Ratio[3]	Results (N, L)[4]
Rt 34	M~6.8 @ 90	0.21	2S	5.5	7	0.14	N
	M~6.8 @ 90	0.21		6.4	8	0.15	N
	M~6.8 @ 90	0.21		7.6	6	0.16	N
	M~6.8 @ 90	0.21		8.5	2	0.16	L
	M~6.8 @ 90	0.21		9.5	4	0.17	L
	M~6.8 @ 90	0.21		10.1	22	0.17	N
	M~6.8 @ 90	0.21		11.0	28	0.17	N
	M~6.8 @ 90	0.21		11.6	26	0.17	N
	M~6.8 @ 90	0.21		12.5	18	0.17	N
	M~6.8 @ 90	0.21		14.0	10	0.17	N

1. amax = Maximum acceleration at ground surface;
2. Blow Count = Total number of blows required to drive split spoon sampler 0.3 m using standard hammer (63.5 kg) dropping 0.76 m;
3. Cyclic Stress Ratio = Stress causing liquefaction;
4. N= Liquefaction not likely; L = Liquefaction likely

A-47a. Evaluation of January 23, 1812 Scenario Earthquakes for Saline River (4) GT 311 Using Medium GMPEs (Atkinson, 2012) and Water Table Depth of 5 m.

Bridge/ Number	M @ Distance (km)	amax[1]	Boring	Sediment Depth (m)	Blow Count[2]	Cyclic Stress Ratio[3]	Results (N, L)[4]
Rt 34	M~6.8 @ 95	0.09	2S	5.5	7	0.06	N
	M~6.8 @ 95	0.09		6.4	8	0.06	N
	M~6.8 @ 95	0.09		7.6	6	0.07	N
	M~6.8 @ 95	0.09		8.5	2	0.07	N
	M~6.8 @ 95	0.09		9.5	4	0.07	N
	M~6.8 @ 95	0.09		10.1	22	0.07	N
	M~6.8 @ 95	0.09		11.0	28	0.07	N
	M~6.8 @ 95	0.09		11.6	26	0.07	N
	M~6.8 @ 95	0.09		12.5	18	0.07	N
	M~6.8 @ 95	0.09		14.0	10	0.07	N

A-47b. Evaluation of January 23, 1812 Scenario Earthquakes for Saline River (4) GT 311 Using High GMPEs (Atkinson, 2012) and Water Table Depth of 5 m.

Bridge/ Number	M @ Distance (km)	amax[1]	Boring	Sediment Depth (m)	Blow Count[2]	Cyclic Stress Ratio[3]	Results (N, L)[4]
Rt 34	M~6.8 @ 95	0.15	2S	5.5	7	0.10	N
	M~6.8 @ 95	0.15		6.4	8	0.11	N
	M~6.8 @ 95	0.15		7.6	6	0.12	N
	M~6.8 @ 95	0.15		8.5	2	0.12	L
	M~6.8 @ 95	0.15		9.5	4	0.12	L
	M~6.8 @ 95	0.15		10.1	22	0.13	N
	M~6.8 @ 95	0.15		11.0	28	0.13	N
	M~6.8 @ 95	0.15		11.6	26	0.13	N
	M~6.8 @ 95	0.15		12.5	18	0.13	N
	M~6.8 @ 95	0.15		14.0	10	0.12	N

1. amax = Maximum acceleration at ground surface;

2. Blow Count = Total number of blows required to drive split spoon sampler 0.3 m using standard hammer (63.5 kg) dropping 0.76 m;

3. Cyclic Stress Ratio = Stress causing liquefaction;

4. N= Liquefaction not likely; L = Liquefaction likely

A-48a. Evaluation of February 7, 1812 Scenario Earthquakes for Saline River (4) GT 311 Using Medium GMPEs (Atkinson, 2012) and Water Table Depth of 5 m.

Bridge/ Number	M @ Distance (km)	amax[1]	Boring	Sediment Depth (m)	Blow Count[2]	Cyclic Stress Ratio[3]	Results (N, L)[4]
	M~7.8 @ 180	0.13	2S	5.5	7	0.08	N
	M~7.8 @ 180	0.13		6.4	8	0.09	N
	M~7.8 @ 180	0.13		7.6	6	0.10	N
	M~7.8 @ 180	0.13		8.5	2	0.10	L
	M~7.8 @ 180	0.13		9.5	4	0.10	L
	M~7.8 @ 180	0.13		10.1	22	0.10	N
	M~7.8 @ 180	0.13		11.0	28	0.10	N
	M~7.8 @ 180	0.13		11.6	26	0.10	N
	M~7.8 @ 180	0.13		12.5	18	0.10	N
	M~7.8 @ 180	0.13		14.0	10	0.10	N

A-48b. Evaluation of February 7, 1812 Scenario Earthquakes for Saline River (4) GT 311 Using High GMPEs (Atkinson, 2012) and Water Table Depth of 5 m.

Bridge/ Number	M @ Distance (km)	amax[1]	Boring	Sediment Depth (m)	Blow Count[2]	Cyclic Stress Ratio[3]	Results (N, L)[4]
Rt 34	M~7.8 @ 180	0.18	2S	5.5	7	0.12	N
	M~7.8 @ 180	0.18		6.4	8	0.12	L
	M~7.8 @ 180	0.18		7.6	6	0.13	L
	M~7.8 @ 180	0.18		8.5	2	0.14	L
	M~7.8 @ 180	0.18		9.5	4	0.14	L
	M~7.8 @ 180	0.18		10.1	22	0.14	N
	M~7.8 @ 180	0.18		11.0	28	0.14	N
	M~7.8 @ 180	0.18		11.6	26	0.14	N
	M~7.8 @ 180	0.18		12.5	18	0.14	N
	M~7.8 @ 180	0.18		14.0	10	0.14	L

1. amax = Maximum acceleration at ground surface;

2. Blow Count = Total number of blows required to drive split spoon sampler 0.3 m using standard hammer (63.5 kg) dropping 0.76 m;

3. Cyclic Stress Ratio = Stress causing liquefaction;

4. N= Liquefaction not likely; L = Liquefaction likely